HEINRICH HEINE
UNIVERSITÄT DÜSSELDORF

MOI II
MOLEKÜLE DER INFEKTION
MANCHOT GRADUIERTENSCHULE

Regulation of autophagy upon vaccinia virus infection

Inaugural-Dissertation

zur Erlangung des Doktorgrades
der Mathematisch-Naturwissenschaftlichen Fakultät

der Heinrich-Heine-Universität Düsseldorf

vorgelegt von

Houda Khatif

aus Düsseldorf

Kaarst, November 2016

aus dem Institut für Virologie
der Heinrich-Heine-Universität Düsseldorf

Gedruckt mit der Genehmigung der
Mathematisch-Naturwissenschaftlichen Fakultät der
Heinrich-Heine-Universität Düsseldorf

Referent: Prof. Dr. Ingo Drexler
Korreferent: Prof. Dr. Dieter Willbold
Tag der mündlichen Prüfung: 17.01.2017

Table of contents

I. List of abbreviations

-/-	knock-out
°C	Celsius
µg	microgram
µl	microlitre
µm	micrometre
3-MA	3-methyladenine
Agn	agonist
AMP	adenosine monophosphate
AMPK	AMP-activated kinase
APCs	antigen presenting cells
AraC	cytosine arabinoside
Atg	autophagy-related gene
ATP	adenosine triphosphate
BMDCs	bone marrow dendritic cells
Cas9	CRISPR-associated protein 9
cDCs	conventional dendritic cells
CEV	cell-associated enveloped virion
cGAMP	cyclic guanosine monophosphate–adenosine monophosphate
cGAS	cyclic GMP-AMP Synthase
CLIP	class II associated Ii peptide
Cop.	Copenhagen
CRISPR	clustered regularly interspaced short palindromic repeats
C-terminus	COOH-terminus
CVA	chorioallantois vaccinia virus Ankara
DC	dendritic cells
DNA	deoxyribonucleic acid
dsDNA	double stranded DNA
dsRed	Discosoma Red
e.g.	exempli gratia, for example
ECL	enhanced chemiluminescent
EEVs	extracellular enveloped virions
eGFP	enhanced green fluorescent protein

ER	endoplasmic reticulum
EVs	enveloped virions
FACS	fluorescence-activated cell sorting
FIP200	200 kDa focal adhesion kinase family-interacting protein
GβL	beta subunit–like protein
GMP	guanosine monophosphate
gRNA	guide RNA
HCMV	human cytomegalovirus
HLA	human leukocyte antigen
hr(s)	hour(s)
HRP	horseradish peroxidase
HSK	herpetic stromal keratitis
HSV-1	human herpes simplex virus 1
i.a.	inter alia
IEVs	intracellular enveloped virions
IFN-I	type I interferon
Ii	invariant chain
IMVs	intracellular enveloped virions
IRF3	Interferon regulatory factor 3
kbp	kilo-base pairs
kDa	kilo-Dalton
LC3	microtubule-associated protein 1 light chain 3
LCMV	lymphocytic choriomeningitis virus
LPS	lipopolysaccharide
M	molar
mA	milliampere
MEF	mouse embryonic fibroblasts
MFI	mean fluorescence intensity
mg	milligram
MHC	major histocompatibility complex
MIIC	MHC class II compartment
min	minute(s)
ml	millilitre
MOI	multiplicity of infection

mRNA	messenger ribonucleic acid
mTOR	mammalian target of rapamycin
MVA	modified vaccinia virus Ankara
MVs	mature virions
MyD88	myeloid differentiation primary-response protein 88
NP	nucleoprotein
ns	not significant
N-terminus	NH_2-terminus
ORF	open reading frame
p.i.	post infection
p.t.	post transfection
PAGE	Polyacrylamide gel electrophoresis
PCR	polymerase chain reaction
pDNA	plasmid DNA
PE	phosphatidylethanolamine
PI3K	phosphatidylinositol 3-kinase
PI3P	phosphatidylinositol-3-phosphate
PRAS40	proline-rich Akt/PKB substrate 40 kDa
PRRs	pathogen recognition receptors
PUVA	psoralen and ultraviolet A radiation
qRT-PCR	quantitative reverse transcriptase polymerase chain reaction
Rapa.	rapamycin
Raptor	regulatory associated protein of mTOR
RNA	ribonucleic acid
SDS	sodium dodecyl sulfate
sec	seconds
SIIN	SIINFEKL
STING	stimulator of IFN genes
TAP	transporter associated with antigen processing
TBK1	TANK-binding kinase 1
TLRs	Toll like receptors
TRIF	TIR domain-containing adaptor protein inducing interferon β
U	units
ULK1	unc-51 like autophagy activating kinase 1

Untr.	untreated
UV	ultraviolet
V	volt
VACV	vaccinia virus
WIPI2	WD repeat domain phosphoinositide-interacting protein 2
WR	Western Reserve
wt	wild type
xg	relative centrifugal force

II. Zusammenfassung

Vaccina Viren (VACV) sind doppelsträngige DNA Viren, die zu den Pockenviren gehören, und sich ausschließlich im Cytoplasma replizieren, in sogenannten „viral factories“. VACV werden unter anderem zur Entwicklung wichtiger Impfstoffe verwendet. Dafür eignet sich der attenuierte und replikationsdefiziente Stamm das Modifizierte Vaccinia-Virus Ankara (MVA) sehr gut, welcher auch in der Forschung als viraler Vektor eingesetzt wird. MVA ist durch zahlreiche Passagen des Ausgangsvirus Chorioallantois Vaccinia Virus Ankara auf Hühnerembryofibroblasten entstanden, in deren Verlauf sechs große Regionen im ursprünglichen Genom deletiert wurden, die unter anderem für die immunmodulatorischen Eigenschaften wie z.B. Immunevasion der Viren entscheidend sind. Diese Regionen dienen als Insertionsstellen zur Einführung fremder DNA z.B. zur Expression von Antigenen [1]. Ein umfassendes Verständnis der Wirkmechanismen dieser Viren im Umgang mit dem Wirt und der nach Infektion ausgelösten Immunantwort sollte die Identifikation neuer Zielstrukturen für immuntherapeutische Ansätze unterstützen.

Während einer Infektion werden Pathogene, die in den Körper bzw. in eine Zelle eindringen, durch das Immunsystem erkannt und eine spezifische Immunantwort zu deren Bekämpfung ausgelöst. Bei der adaptiven Immunantwort spielen $CD4^+$ T-Zellen eine entscheidende Rolle. Diese sind in der Lage fremde Antigene, die von MHC (Haupthistokompatibilitätskomplex) Klasse II Rezeptoren auf der Zelloberfläche präsentiert werden, zu erkennen. Peptide endogenen Ursprungs werden über Autophagie generiert [2, 3]. In einigen Vorarbeiten konnten wir zeigen, dass bei einer MVA Infektion von dendritischen Zellen (BMDCs) Autophagie induziert wird und über verstärkte MHC Klasse II Antigenpräsentation eine effiziente Aktivierung von $CD4^+$ T-Zellen stattfindet [4]. Eine Infektion durch den Wildtypstamm Western Reserve (WR) führte hingegen zu einer starken initialen Beeinträchtigung von Autophagie. Somit war das Ziel dieses Projektes zu untersuchen, wie Autophagie von VACV beeinflusst wird. Zum einen war es uns wichtig herauszufinden, wie MVA Autophagie induziert, und zum anderen, welche virale und zelluläre Faktoren für die WR-vermittelte Inhibition von Autophagie verantwortlich sind.

Die Induktion bzw. Inhibition von Autophagie wurde anhand der LC3-Lipidierung unter anderem im Immunoblot nachgewiesen. Nach MVA Infektion wurde im Vergleich zu den WR-infizierten Zellen eine starke Zunahme des LC3-II Proteins beobachtet, darstellend für eine Induktion von Autophagie.

Die Expression vaccinia-viraler Gene findet in einer frühen, intermediären und späten Phase statt. Es stellte sich heraus, dass die Inhibition von Autophagie durch ein früh exprimiertes Gen vermittelt wird. Zusätzlich konnten wir zeigen, dass Virusadsorption nicht ausreichend ist, sondern ein effizientes Eindringen des Virus in die Zelle vorausgesetzt wird. Unter Berücksichtigung dieser Ergebnisse wurden 20 VACV-Gene selektiert, welche in MVA nicht vorhanden oder funktionell sind und mittels der CRISPR-Cas9 Methode WR-Deletionsmutanten für jedes einzelne Gen erzeugt. Diese Mutanten wurden auf den Verlust des inhibitorischen Effekts von VACV auf die Induktion von Autophagie in einem in dieser Arbeit etablierten Testverfahren mittels Durchflusszytometrie hin untersucht. Leider konnten wir mit den bislang getesteten Mutanten keine signifikanten Ergebnisse erzielen. Dies schließt jedoch nicht aus, dass die Deletion zweier oder mehrerer Gene gleichzeitig benötigt wird, um eine Aktivierung von Autophagie hervorzurufen.

Auf molekularer Ebene konnten wir feststellen, dass die Induktion bzw. Inhibition von Autophagie, die jeweils durch MVA bzw. WR herbeigeführt wird, mit STING (Stimulator of Interferon Genes) zusammenzuhängt. Nach Erkennung doppelsträngiger DNA durch cGAS (cGAMP Synthetase) wird cGAMP (zyklisches GMP-AMP) produziert und das Adaptorprotein STING aktivert. Dies führt letztendlich zur Produktion von Typ I Interferon. In MVA infizierten STING knockout BMDCs konnte keine Hochregulation von Autophagie beobachtet werden. Zudem fand in Zellen mit normaler STING Expression ein vollständiger Abbau des Moleküls in kürzester Zeit nach MVA Infektion statt, was bei WR infizierten Zellen nicht der Fall war. Dies kann als Hinweis gewertet werden, dass STING in dem MVA-vermittelten Autophagie-induzierenden Signalweg eine wichtige Rolle spielt. Demzufolge war es von großem Interesse herauszufinden, wie und warum dieser Abbau bzw. die Hemmung des Abbaus stattfindet. Des Weiteren wurde der Autophagiesignalweg, der nach MVA Infektion in der Zelle angeschaltet wird und der von dem kanonischen Weg abweicht, näher untersucht.

III. Summary

Vaccinia virus (VACV) is a double-stranded DNA virus that belongs to the poxvirus family, and replicates exclusively in the cytoplasm in so called viral factories. VACV are i.a. employed to establish specific vaccines. An attenuated form of VACV, the replication-deficient modified vaccinia virus Ankara (MVA), is commonly and preferentially used as a viral vector. MVA was generated through extensive passaging of the parental strain chorioallantois vaccinia virus Ankara in chicken embryo fibroblasts. Hence, the MVA genome bears six major deletions that affect genes encoding for host range and immune evasion factors, and which are used to introduce foreign antigens. Gaining deeper knowledge about how these viruses interact with the host and the immune system, should grant the opportunity to identify new targets for immunotherapeutic approaches.

During an infection, invading pathogens are recognized by the immune system and a specific immune response is initiated. In regard of the adaptive immunity, $CD4^+$ T-cells are able to recognize MHC (major histocompatibility complex) class II antigens that are presented at the cell surface. Thus, autophagy has been demonstrated to be required as an antigen provider for production of MHC class II peptides if derived from an endogenous source. In previous experiments, we were able to demonstrate MVA infection of dendritic cells (BMDCs) to cause a strong $CD4^+$ T-cell activation after recognition of endogenous viral antigens. However, infection with the wild type strain Western Reserve (WR) significantly inhibited autophagy. Therefore, we aimed to characterize the impact of VACV infection on autophagy, and to identify the viral and cellular interaction partners that are responsible for the strain-specific activating or inhibiting effects, respectively.

Autophagy induction or inhibition was tracked by analysing LC3-lipidation mainly through immunoblotting. Upon MVA infection, we observed an increase in LC3-II protein synthesis contrary to WR-infected cells, demonstrating an induction of autophagy by MVA. VACV gene expression occurs in an early, intermediate and late phase. Autophagy inhibition turned out to be an early gene mediated process, which required not only cellular adsorption but efficient virus entry. Hence, according to these observations, we selected 20 VACV genes being deleted or inactive in MVA and generated WR deletion mutants using the CRISPR-Cas9 method. We screened the deletion mutants for autophagy induction via a newly established assay based on flow cytometry. So far, we were not able to identify the inhibitory candidate gene. Still, it is possible that deletion of more than one gene is required to efficiently overcome the inhibitory effect.

Further results reflected VACV autophagy interference to likely depend on Stimulator of Interferon Genes (STING). STING is a cellular adaptor molecule, which gets activated via the second messenger cGAMP (cyclic GMP-AMP), which is produced after double stranded DNA stimulation of cGAS (cGAMP synthase). STING activation will finally lead to expression of type I interferons. Interestingly, in MVA-infected STING knockout BMDCs autophagy was not triggered anymore. Additionally, STING was immediately degraded upon MVA infection in cells with regular STING expression, contrary to WR-infected cells. These outcomes emphasize the relevance of STING for MVA-mediated induction of autophagy. Thus, it was crucial to understand, how and why STING is degraded. Moreover, we tried to further characterize the autophagy pathway, which is activated after MVA infection and which strongly differs from the canonical pathway.

1. Introduction

1.1. Biology of vaccinia virus (VACV)

1.1.1. Origin and relevance of VACV

Poxviruses are double-stranded DNA viruses that replicate exclusively in the cytoplasm. Members of the *poxviridae* dispose some of the largest virus genomes ranging from 130 to 360 kbps [5], comprising up to 260 different open-reading frames [6, 7]. Poxviruses are subdivided into two families, namely the *entemopoxviriniae* that infect insects and the *chordopoxviriniae* that are infectious for vertebrates and includes the orthopoxviruses [5]. Among the orthopoxviruses, vaccinia viruses (VACV) including modified vaccinia virus Ankara (MVA) are the most extensively studied strains.

VACV became known through its role as an active agent used for vaccination against smallpox disease, firstly reported by Edward Jenner in 1976 [8]. After eradication of variola in 1980 [9], VACV is still employed as a tool of scientific research and development of new vaccines [10]. It is used as a vector for expression of recombinant genes. To overcome the strong virulence of VACV, an attenuated form, the modified vaccinia virus Ankara (MVA), originally derived from chorioallantois vaccinia virus Ankara (CVA), was generated. Due to extensive passaging (over 500 passages) of CVA in primary chicken embryo fibroblasts, the virus lost about 15% of its genome and bears six major deletions [1], that affect genes coding for host range and immune evasion factors [11]. Related to its immunogenicity and safety, MVA is commonly used as a vaccine against several infectious diseases [12]. Although MVA is able to infect cells, it does not have the capacity to produce infectious progeny and therefore is incapable to replicate in mammalian cells [13].

1.1.2. Cell-entry and replication of VACV

Unlike to other virus families, the entry mechanisms of poxviruses remain not completely understood and can vary depending on the strain and cell type [14, 15]. Additionally, virus entry depends also on the infectious form of VACV, distinguishing here between mature virions (MVs) and enveloped virions (EVs) [7]. Intracellular MVs (IMVs), the most abundant form of VACV, dispose only one membrane and are localized within the host cell until lysis. The intracellular enveloped virions (IEVs) belong to wrapped MVs, which exhibit an additional membrane gathered from the trans-Golgi network or early endosomes. IEVs are transported to the cell periphery via microtubules, where the outer virion membrane fuses with the plasma membrane to release particles surrounded by two layers, either in form of free extracellular enveloped virions (EEVs)

or as cell-associated enveloped virions (CEVs) in order to infect other cells [16]. Contrary to VACV, MVA is mainly present in form of immature virions or in non-permissive cells as abnormal virions, due to missing regulatory genes, which causes abortive virion assembly lacking replicative genomes [17, 18].

Regarding virus penetration, MVs require binding to cellular glycosaminoglycans [19, 20] or directly to liposomes for cell attachment [20, 21] and are released through cell lysis to mediate host-to-host transmission [7, 16]. For EVs that are released by cellular exocytosis to infect neighbouring cells or tissues [22, 23], no cellular binding factors have been described so far [24]. Virus internalization succeeds either directly at the plasma membrane or through cellular endocytosis in macropinocytic vesicles [25, 26]. Fusion is mediated by an "Entry Fusion Complex" that comprises in total eleven proteins for virus attachment, membrane fusion and delivery of the core into the host cell [27].

Next, the DNA is released within the host and replicates in so called viral factories, which are a hallmark of poxvirus replication [28, 29]. This is possible, because poxviruses carry their own enzymes for mRNA and DNA synthesis. Hence, the VACV gene transcription is subdivided into 3 classes with subsequent activity (early, intermediate and late) [30]. Early genes are mainly responsible for DNA replication and transcription of intermediate genes, which in turn control the expression of late genes. During the late phase, after virus assembly, the four distinct viral particles are generated for subsequent infection of new cells [30, 31]. Thus, as it is usually the case with complex pathogens, the immune system activates different mechanisms to combat infection by VACV.

1.2. Role of autophagy in innate and adaptive immunity

1.2.1. Molecular regulation of autophagy

Autophagy was originally characterized by Ashford and Porter in rat hepatocytes and described to be a cellular response to starvation [32]. Autophagy-related genes (Atgs), which were actually identified in yeast, are conserved in eukaryotic cells and participate in autophagosome formation [33-35]. Environmental cues are at the origin of autophagy regulation. In the presence of growth or nutrient factors, mTOR (mammalian target of rapamycin) is stimulated and autophagosome formation is disabled [36]. Energy depletion, starvation or infection, are responsible for activation of autophagy, which involves the induction of a highly sophisticated signalling cascade [37, 38].

mTOR is a 280 kDa large Serine/Threonine rapamycin sensitive protein kinase, implicated into cellular metabolism regulation to monitor protein synthesis, nutrient import and autophagy [39-42]. The mTOR complex constitutes mTOR itself, the beta subunit–like protein (GβL), the regulatory associated protein of mTOR (raptor) and the proline-rich Akt/PKB substrate 40 kDa (PRAS40). mTOR activation is controlled by the class I phosphatidylinositol 3-kinase (PI3K)-AKT pathway through perception of growth factors like insulin [41, 43]. In the case of energy deprivation and ATP decrease, mTOR blockage is mediated via AMP-activated kinase (AMPK) to stimulate autophagy [38, 43].

Autophagy is triggered through activation of the ULK1:Atg13:FIP200 complex by inhibiting mTOR [44-46]. ULK1 (unc51-like kinase 1, Atg1 ortholog) and FIP200 (200 kDa focal adhesion kinase family-interacting protein) interact with Atg13, which in turn is stabilized by the expression of Atg101 [40, 47, 48]. Phagophore nucleation and assembly necessitate the initiation of the PI3K complex, composed of the class III PI3K, the regulatory protein kinase p150, Beclin-1 (Atg6 ortholog) and Atg14L, a Beclin-1-associated key regulator [49, 50]. This results in production of phosphatidylinositol-3-phosphate (PI3P), which enables autophagosome formation (**Figure 1**) [38].

Vesicle elongation is promoted by two ubiquitin-like conjugation systems [36]. For the first system, Atg12 is activated by the E1-like enzyme Atg7 and conjugation to Atg5 is sustained by the E2-like enzyme Atg10. Binding of Atg16L1 to Atg5-Atg12, which exhibits an E3-like enzyme activity, contributes to the generation of a heterotrimeric complex, located at the phagophore membrane. This complex, together with the Atg4B protease, Atg7 and Atg3, encompass the second ubiquitin-like conjugation system, which establishes the interaction between phosphatidylethanolamine (PE) and the microtubule-associated light chain 3 protein (LC3-I, mammalian homolog of Atg8). The conversion of LC3-I to the lipidated and autophagosome-associated form LC3-II (PE conjugated) is a common marker and regulator for autophagy activation. Autophagy is commonly assessed through the determination of the immunoblot signal ratio of LC3-II to LC3-I or LC3-II to β-actin [51, 52]. Thus, an increase in LC3-II molecules is indicative for autophagy induction [36, 38].

After fusion of lysosomes with autophagosomes, specific acidic hydrolases are released inside of the autolysosome, leading to cargo degradation and finally to vesicle breakdown for metabolic recycling. Though, previous investigations demonstrated autophagy to be strongly implicated into the adaptive immune response, especially in regard of MHC class II antigen generation [2, 3, 53], but can also be involved in production of MHC class I peptides and innate immunity [38].

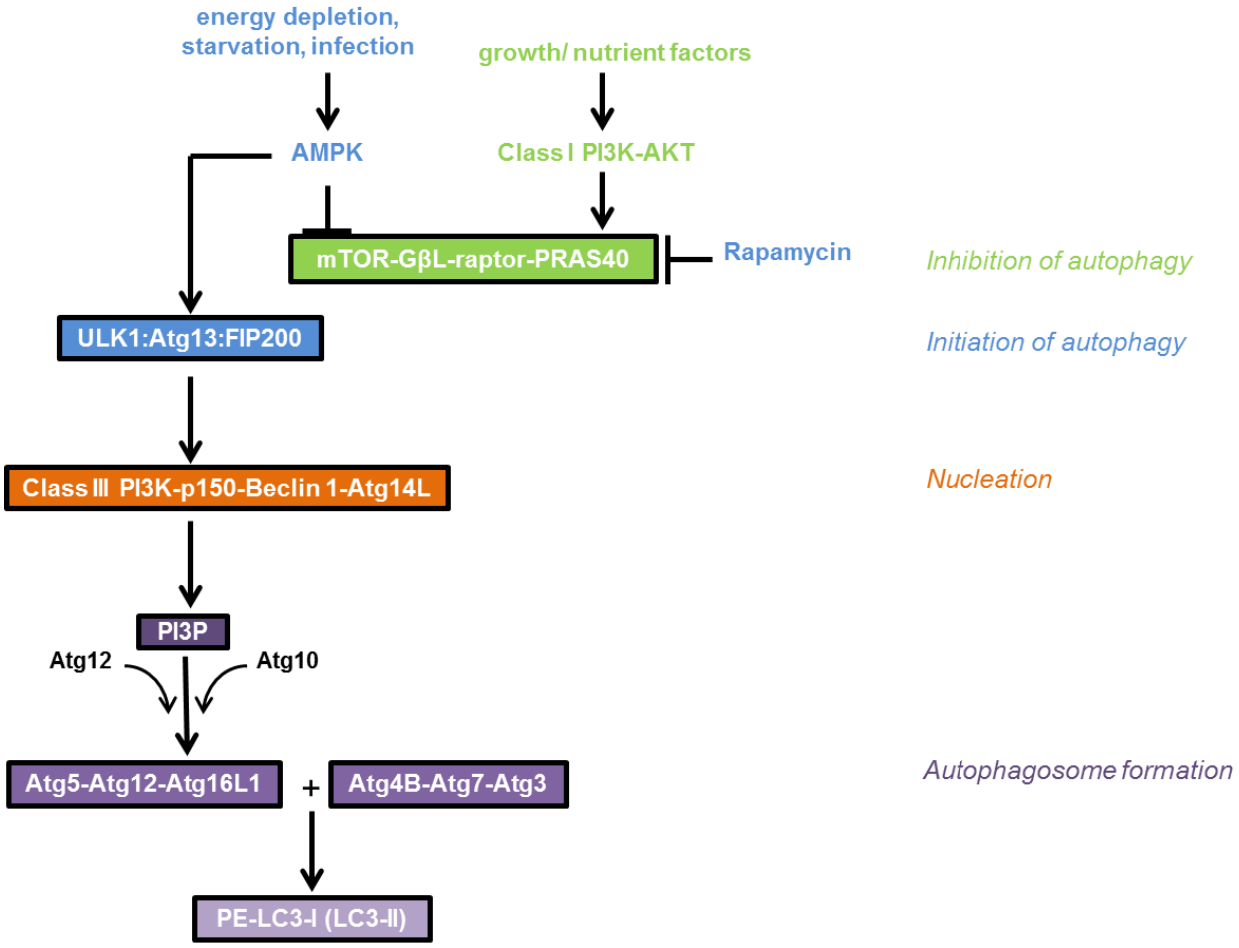

Figure 1: Autophagy signalling cascade. Autophagy can be induced or inhibited by diverse factors. In the case of induction, different complexes are triggered leading to final autophagosome formation. Inhibition of autophagy is mediated by activation of the mTOR complex [38].

1.2.2. Autophagy in adaptive immunity

In the case of an infection, pathogen-derived antigens are presented by major histocompatibility complex (MHC) class I or II molecules to surveilling T-cells. Contrary to MHC class I molecules, which are expressed on all nucleated cells, MHC class II is only found on professional antigen presenting cells (APCs) like dendritic cells (DCs), B-cells, macrophages and certain epithelial cells. Additionally, MHC class I antigens are from cytosolic origin and processed by proteasomes to be translocated into the endoplasmic reticulum (ER) via the transporter associated with antigen processing (TAP) [54]. However, the proteasomal degradation machinery has become a target for numerous viruses in order to avoid antigen presentation and immune recognition. Thus, autophagy has been shown to be also implicated into MHC class I antigen presentation. English *et al.* reported herpes simplex virus 1 (HSV-1) infection of macrophages to implement generation of endogenous MHC class I antigens for $CD8^+$ T-cell stimulation via a vacuolar pathway closely related to autophagy [55]. An autophagy-mediated but TAP-independent endogenous MHC class I peptide loading has also been described for antigens generated from the Human cytomegalovirus

(HCMV)-encoded pUL138 protein, which is either degraded by the conventional route or by lysosomal proteases [38, 56].

MHC class I molecules are also known to present antigens from exogenous origin in APCs to $CD8^+$ T-cells via cross-presentation [57]. The vacuolar cross-presentation implies protein up-take by endocytosis or phagocytosis, degradation by proteases and MHC class I loading within these compartments. Hence, during cytosolic cross-presentation, proteins are translocated trough endosomes and phagosomes to the cytoplasm for proteasomal degradation, and are either transported back into the vesicles they originated from, or into the ER-lumen via TAP for regular MHC class I loading [58-60]. Dysregulation of autophagy by knocking down specific Atgs in tumor cells (e.g. Beclin-1 and Atg12) caused a significant decrease in cross-presentation [38, 61]. Possible explanations could be that autophagosomes themselves serve as compartments for cross-presentation [62] or that peptides traffic via autophagy to these compartments [63].

However, the role of autophagy in MHC class I antigen presentation remains controversial. In absence of Atg5 and Atg7, MHC class I presentation in DCs was significantly increased and upon influenza and lymphocytic choriomeningitis virus (LCMV) infection, $CD8^+$ T-cell responses were upregulated. This could be ascribed to impaired internalization and endocytic degradation of MHC class I molecules [64]. Additionally, autophagy was described to restrict protein ubiquitination and therefore proteasomal degradation for efficient MHC class I peptide generation [65].

Regarding MHC class II antigens, they are mainly generated from exogenous proteins [66, 67] but can also be of nuclear and cytosolic origin if processed through autophagy [66, 68]. In support of this notion, 20-30% of natural MHC class II ligands are derived from endogenous proteins produced through autophagy [2, 69, 70]. To provide efficient antigen presentation, the MHC class II α- and β-chain assemble in the ER and interact with the invariant chain (Ii) to prevent binding of premature epitopes. Thus, this complex is transported to the acidic endosomal MHC class II compartment (MIIC) within APCs, where Ii is digested, leaving a class II associated Ii peptide (CLIP). The binding of MHC class II antigens is mediated by human leukocyte antigen (HLA)-DR, being responsible for the dissociation of CLIP from the peptide binding groove. Antigens generated via autophagy are delivered to MHC class II molecules through direct fusion of autophagosomes with MIIC, or of endosomes which then in turn merge with MIIC [38, 71, 72]. Silencing of Atg12 inhibits biogenesis of autophagosomes and fusion with MIIC [71]. Additionally, Kondylis *et al.* posit the existence of an endosome-mediated autophagy in lipopolysaccharide (LPS)-stimulated DCs, characterized by the formation of MIIC-derived autophagosomes [73]. These outcomes supplementary confirmed the relationship between

autophagy and MHC class II antigen presentation, as well as autophagy to be possibly induced by activation of Toll like receptors (TLRs) signalling. Hence, the MHC class II complex is released from MIIC and peptides are presented to $CD4^+$ T-cells (**Figure 2**) [38, 66].

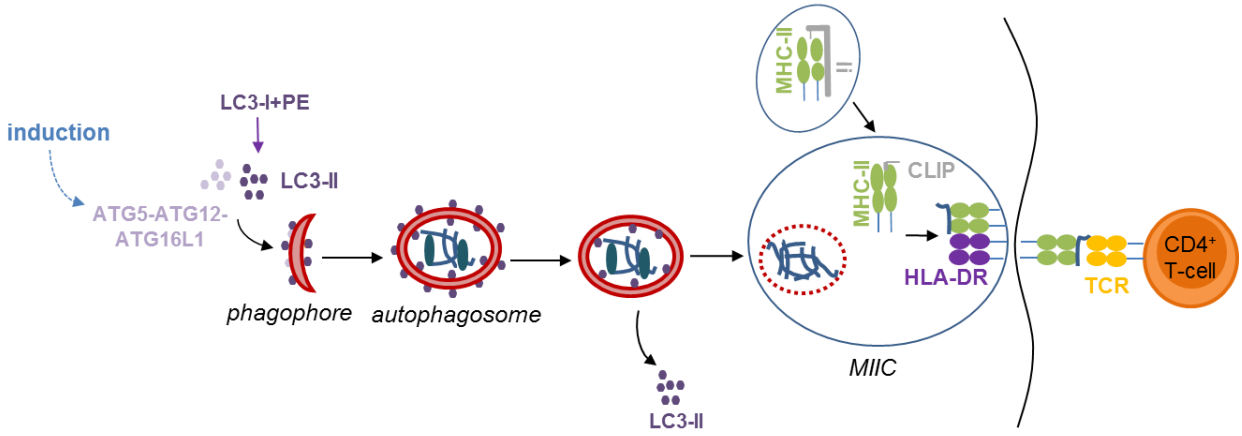

Figure 2: Autophagy-dependent MHC class II antigen presentation. MHC class II molecules and li assemble in the ER. The complex is then conducted from the Golgi to the MIIC through vesicle transport, where li is digested leaving CLIP. Simultaneously, autophagosomes fuse with MIIC for delivery and binding of antigens to MHC class II molecules, after HLA-DR mediated their dissociation from CLIP. Newly peptide-loaded MHC class II complexes are transported to the cell surface and expose their peptides to $CD4^+$ T-cells to be recognized by their specific T-cell receptors (TCR) [38].

The relevance of autophagy for MHC class II antigen presentation, has also been described in terms of viral infections. Reed *et al.* illustrated the constitutive role of Beclin-1 in DCs upon respiratory syncytial virus infection. Mice with severe deficiencies in autophagy emanating from Beclin-1 haplo-insufficiency, exhibited reduced MHC class II expression and down-regulation of innate cytokine synthesis, resulting in serious lung pathology [74]. In another study, DCs, B- and epithelial cells expressing the influenza A matrix protein 1 (M1) in fusion with LC3, demonstrated a 20-fold higher M1-specific MHC class II presentation to $CD4^+$ T-cell clones than cells expressing M1 alone [38, 71]. However, autophagy activation can have a detrimental role too, as it has been shown for mice suffering from herpetic stromal keratitis (HSK). HSK is a blinding ocular disease induced by HSV-1, referable to an inappropriate chronic inflammation by $CD4^+$ T-cells. Autophagy in DCs was responsible for an up-regulation of $CD4^+$ T-cell activation, leading subsequently to corneal inflammation [75].

The role of autophagy was also defined in the context of lymphocyte development and activity. The up-regulation of co-stimulatory signals released by APCs, sustains their migration to lymphoid organs. There, APCs and naive $CD4^+$ T-cells encounter and interact with each other via detection of pathogen-derived peptides presented by MHC class II molecules [76], a process called T-cell priming [77]. Lee and coworkers highlighted the significance of Atg5 for antigen

presentation by DCs, since deletion of Atg5 affected $CD4^+$ T-cell priming upon viral infection [38, 78]. Taken together, these findings support the conclusion of autophagy to be strongly involved in the control of $CD8^+$ and $CD4^+$ T-cell activation, and therefore to be a constitutive part of the adaptive immune system.

1.2.3. Autophagy in innate immunity

As generally known, in the case of an infection, APC activation is conducted through binding of pathogenic motifs to pattern-recognition receptors (PRRs) which are subdivided into different classes, comprising the membrane-bound TLRs. TLRs recognize microbial patterns to induce an innate immune response, which is initially implemented by a downstream signalling cascade, including the adaptor molecules MyD88 (myeloid differentiation primary-response protein 88) and TRIF (TIR domain-containing adaptor protein inducing interferon β), with ensuing release of IFN-I and pro-inflammatory cytokines [79]. MyD88 and TRIF were described to be involved in activation of autophagy by targeting Beclin-1 [80], emphasizing a direct connection between pathogen recognition and autophagy induction [38]. In another study, LPS stimulation of human and mouse macrophages induced autophagy upon TLR4 activation, in a TRIF-dependent but MyD88-independent manner [81]. A screen of multiple PRR ligands revealed the induction of autophagy through RNA stimulation of TLR7, to have the most significant effect [82].

PRR sensing of pathogenic DNA has also been characterized to be closely related to autophagy, especially in regard to the cGAS-STING pathway. DNA is recognized by cGAMP synthase (cGAS) to produce second messenger cyclic GMP-AMP (cGAMP), which in turn activates the heterodimeric stimulator of interferon genes (STING) [83-85]. Thus, STING translocates from the ER to the Golgi where it encounters TBK1, phosphorylates and gets transported together with TBK1to IFN-regulatory factor 3 (IRF3) harboring endosomes [86, 87]. Hence, IRF3 is phosphorylated and translocated to the nucleus to actuate transcription of IFN-I [88]. Saitoh *et al.* delineated a co-localization of STING with Atg9a and LC3 after stimulation with double stranded (ds)DNA. They concluded Atg9a to regulate and inhibit STING trafficking and thereby IFN-production. Loss of Atg9a enhanced STING and TBK1 assembly upon activation via dsDNA [89]. Moreover, identification of interaction between cGAS and Beclin-1 after DNA stimulation or HSV-1 infection, resulted in autophagy-mediated degradation of pathogenic dsDNA and suppression of cGAMP synthesis. Beclin-1 was claimed to have a regulatory function on autophagy but also on cGAS by avoiding excessive cGAMP production and persistent IFN-I synthesis [90]. A further publication exhibits the existence of a connection between STING and ULK1. After being activated and accomplishing its task, STING gets phosphorylated by ULK1,

whose dissociation from AMPK is orchestrated by cGAS-generated cGAMP, in order to initiate a negative feedback-loop control [91]. Thus, autophagy is directly and indirectly, meaning by activation of single Atgs, implicated into the cGAS-STING pathway with a major role in regulating STING activation and uncontrolled stimulation of antimicrobial immune responses.

Since the cGAS-STING pathway constitutes an important part of the immune system, it is evident that viruses have developed immune modulatory or immune evasion factors to protect themselves from being eliminated. This is also the case for VACV. Dai *et al.* [92] could show MVA infection of conventional DCs (cDCs) to cause a cGAS- and STING-dependent IFN-I production. By contrast, VACV infection of cDCs led to a significant down-regulation of IFN-I production. Phosphorylation levels of TBK1 and IRF3 were also reduced. They could ascribe this effect to the expression of VACV N1L protein, which is truncated in MVA [93], and concluded VACV to interfere with the cGAS-STING pathway via N1L [92]. For sure, recognition of viral dsDNA by the cGAS-STING pathway plays a crucial role.

1.2.4. Relevance of autophagy in vaccinia virus infection

The elimination of intracellular pathogens in infected cells occurs via autophagy through lysosomal degradation. This process is commonly referred to as xenophagy [37, 94]. Regarding VACV, there are only a few studies describing its interaction with autophagy.

Moloughney *et al.* [95] noticed a considerable LC3-lipidation after VACV infection, which was probably mediated through direct conjugation of Atg3 to Atg12. However, neither autophagosome formation nor autophagy flux could be detected. Previous investigations reported the capacity of VACV to replicate in autophagy-deficient cells as efficiently as in wild-type cells [96]. Moreover, Whilding *et al.* observed that although LC3 was lipidated upon VACV infection, depending on the cell line and viral strain used, there was no general activation of autophagy in ovarian cancer cells [97]. These outcomes indicate that VACV does not require autophagy for replication and possibly interferes in order to deceive the immune system.

1.3. Aim of PhD thesis

Our latest findings revealed the relevance of the autophagy machinery regarding generation of MHC class II epitopes upon MVA infection. MVA-infected DCs engendered a strong $CD4^+$ T-cell activation through recognition of MHC class II endogenous viral antigens, while uninfected cells were only able to present exogenous peptides and to stimulate $CD4^+$ T-cells to a lower extent. The extensive LC3-lipidation and down-regulation of MHC class II presentation of endogenous

antigens after treatment with an autophagy inhibitor, unraveled the importance of this process for peptide generation [4]. Indeed, supplementary experiments unveiled autophagy induction in MVA-infected APCs, whereas after infection with wild type strain Western Reserve (WR) or co-infection with MVA and WR, autophagy was inhibited. These outcomes raised our interest to analyse this phenomenon in greater detail, to understand how VACV is activating or inhibiting regulatory mechanisms of the immune system, and to identify the inhibitory factors in order to improve design and selection of vectors according to a specific immune response.

2. Materials

2.1. Equipment

Blotting-Equipment	Neolab
Centrifuges	Pico21, Heraeus
	Fresco 21, Heraeus
	5810R, Eppendorf
	Megafuge 16R, Heraeus
Cross-linker	Peqlab
ECL imager	Fusion Fx Vilber Lourmat, Vilber
Electrophoresis chambers	Neolab
Flow cytometry equipment	FACSCanto II™, BD
Freezer (-80°C)	Herafreeze, Thermo Scientific
	Forma 88000 Series, Thermo Scientific
Freezer (-20°C)	GNP 4166 Premium NoFrost, Liebherr
	IG 1166 Premium, Liebherr
Fridge (+ 4°C)	LKUv 1610 MediLine, Liebherr
	FKUv 1610 Premium, Liebherr
	KB 4260 Premium, Liebherr
	KUR18421, AntiBacteria, Bosch
Heating plate	MR Hei-Tec, Neolab
Ice machine	AF124, Scotman
Incubators	Heracell 150i / 240i, Thermo Scientific
Micropipettes	Pipetman P2-1000, Gilson
Microscope	CKX41, Olympus
	LSM 780, Zeiss
Microwave	Gn3431MA
Multi-channel pipette	Pipetman P200N, Gilson
Nitrogen Tank	Biosafe MD, Cryotherm
pH-meter	PB-11, Satorius
Pipetboy	accu-jet pro, Brand
Power-Supplies	MS 3AP, MS Major Science
Sonification machine	Sonopuls HD200/UW200, Bandeline
Spectrophotometer	Nanodrop 1000, Berthold
Thermoblock	Neolab
Thermomixer	Thermomixer Comfort,Eppendorf
Thermocycler	T1 und T3000, Biometra
UV-Transilluminator	UVsolo TS, Biometra
Vortexer	Vortex Genie 2, Scientific Industries

	VV3, VWR
Waterbath	type 1083, GFL
Weighing machine	AEJ 220-4M, KERN & Sohn GmbH
	Ew 4200-2nm, KERN & Sohn GmbH
magnetic shaker	St 5 cat, Neolab
Immunoblot chamber	Neolab
Working sterile bank	Mars Safety class 2, Labogene

2.2. Chemicals

Acetic Acid	Merck
Agarose	Biozym
Ampicillin	Roth
Bacto-Agar	Fluka
β-mercaptoethanol	Roth
Bromophenol blue	Merck
Calcium chloride	Roth
Dimethyl sulfoxide (DMSO)	Roth/ Sigma
DNA-Size Standards Hyperladder I	Bioline
Desoxinucleotides triphosphate (dNTPs)	Qiagen
Dithiothreitol (DTT)	Merck
DNase	Roche
DreamTaq Master Mix (2x)	ThermoFisher
Dulbecco's Modified Eagle's Medium (DMEM)	Gibco
Endonucleases (restriction enzymes)	New England Biolabs
Enzyme buffers (10x)	New England Biolabs
Ethanol absolute	Merck
Ethylenediaminetetraacetic acid (EDTA)	Merck
EZ Vision in gel	Amresco
Fetal bovine serum (FBS)	PAN, Biotech
FS buffer (FSB, 5x)	Invitrogen
Glycerol	Roth
Glycine	Roth
Hydrochloric acid (HCl, 32%)	Roth
Isopropanol	Merck
Kanamycin	Sigma
LB-Broth (Lennox)	Roth
Lumi-light Western Blotting Substrate	Roche
Magnesium chloride	Roth
Methanol	Sigma
Nonfat-dried milk	Sufocin

Paraformaldehyde	Merck
Pharm-Lyse (lysing buffer, BMDC preparation)	BD
Phosphate buffered saline (PBS, 1x)	Gibco
Penicillin/Streptomycin (P/S)	Gibco
Phenol-chlorophorm	Roth
Ponceau S	Roth
Primer p(dT)	Roche
Proteinase K	AGS GmbH
Puromycin dihydrochloride	Sigma
RNasin®	Promega
qPCR Master Mix Precision Plus (2x)	Primerdesign
Roswell Park Memorial Institute medium (RPMI)	Gibco
Rotiphorese Gel 30 (acrylamide)	Roth
Saponin	Sigma
Sodium acetate (NaAc)	Meck
Sodium azide (NaN_3)	Merck
Sodium chloride (NaCl)	Sigma
Sodium dodecyl sulfate (SDS)	Roth
Sodium hydroxide (NaOH)	Merck
Sucrose	VWR
Super script® reverse transcriptase (SuperScript® III)	Invitrogen
T4-DNA-Ligase	New England Biolabs
T4-DNA-Ligase buffer (10x)	New England Biolabs
TEMED	Roth
Tris-Base	Roth
Tris-borate EDTA buffer (TBE, 10x)	Sigma
Triton X-100	Sigma
Trypan blue stain (0.4%)	Gibco
Trypsin-EDTA (0.05%)	Gibco
TurboFect	ThermoFisher
Tween 20	Merck

2.3. Kits

Lenti-X™ Lentiviral Expression Systems	Clontech
MinElute purification Kit	Qiagen
Plasmid Midiprep Kit	Qiagen
QIAquick Gel Extraction Kit	Qiagen
RNA-Isolation Kit	Qiagen

2.4. Solutions and buffers

Growth medium	RPMI/ DMEM 10% FBS 1% P/S
Freezing-medium	90% FCS 10% DMSO
LB-medium	20 g on 1 L H_2O
LB-Agar	1.5% (w/v) Agar in LB-medium
Saponin Solution	0,025% Saponin dd H_2O
6x TBE-Sample buffer	10% (v/v) Glycerol 6x TBE Bromophenol blue
Solutions for Immunoblotting:	
10x Laemmli-running buffer	250 mM Tris-base 2M glycine
Ponceau	0.1% Ponceau S 5% Acetic acid
5x sample loading buffer	250 mM Tris pH 6,8 10% SDS 7.5% Glycine 12.5% β-Mercaptoethanol 0.5% Bromphenol blue
Separating gel (12%), small	7.2 ml Acrylamide 3.75 ml 2 mM Tris/HCl, pH 8.8 90 µl 20% SDS 6.8 ml H_2O 36 µl TEMED 216 µl 10% APS
Stacking gel, small	1.5 ml Acrylamide 1.2 ml 0.5 M Tris/HCl, pH 6.8 45 µl 20% SDS 2.1 ml 60% sucrose 4.2 ml H_2O 12 µl TEMED 120 µl 10% APS
10x TBST	0.1 M Tris/HCl pH 8.0

	1.5 M NaCl 0.5% (v/v) Tween 20
10x Transfer buffer	0.5 M Tris-base 0.4 M Glycine
1x Transfer buffer	100 ml 10x Transfer buffer 200 ml Methanol 700 ml dd H_2O
Tyr-lysis buffer	50 mM Tris-HCl pH 8 150 mM NaCl 0.02% NaN_3 1% Triton X-100

2.5. Plasmids

Table 1: List of used vectors

Name	Provider
ptfLC3	Addgene
pcDNA3.1D-V5-His-Topo	Addgene
pQCXI Puro DsRed-LC3-GFP	Addgene
pLVX-IRES-Puro	Clontech

2.6. Oligonucleotides

Table 2: List of oligonucleotides applied for PCR, Q-PCR and sequencing analysis (from Eurofins)

Sequence 5' → 3'	Application	Name
GGGAATTTCAACGTGGCCCA	Q-PCR	humanSTING_fwd
AGCAGGTTGTTGTAATGCT	Q-PCR	humanSTING_rev
AAGAAGTTAAATGTTGCCCA	Q-PCR	Fwd mouse STING
CCACTGAGCATGTTGTTAT	Q-PCR	Rev mouse STING
ATCCGCATTTCCGAAGAA	Q-PCR	B8_fwd
ACATGTCACCGCGTTTGTAA	Q-PCR	B8_rev
AAACGGCTACCACATCCAAG	Q-PCR	18S rRNA_fwd
CCTCCAATGGATCCTCGTTA	Q-PCR	18S rRNA_rev
CTACGTATGCCGAAGTACTC	PCR/Sequencing	A50R_fwd1
CTGATATCG CATCCGTTTGTAC	PCR/Sequencing	A50R_fwd2
TTCCTAAACTTCCAAACGGGAG	PCR/Sequencing	A50R_rev1
TACCGAGGACCCGCTTTAAT	PCR/Sequencing	A50R_rev2
GTTTCCTATTAGGGTTCCGC	PCR/Sequencing	G5R_fwd1
GTTACCGGATTTATGGAAGAAG	PCR/Sequencing	G5R_fwd2
GTTATAGATGCCCCATAGAGTC	PCR/Sequencing	G5R_rev1
CGTCTCTTG TCTCTAACGTC	PCR/Sequencing	G5R_rev2
GGTTCTTGAGGGTTGTGTTAAA	PCR/Sequencing	H5R_fwd
TTGTCGGTAGCCACCTTTAG	PCR/Sequencing	H5R_rev
TTCAGGAGCAGAGTTTACATCT	PCR/Sequencing	A51R_fwd
CACAGACATCTTTATCCTTTCC	PCR/Sequencing	A51R_rev
GTATGTTGGGGAAATATGAACC	PCR/Sequencing	A52R_fwd
ATAGTACCGAATTGTTCTTCCG	PCR/Sequencing	A52R_rev
ATGGCGGGATATATGGCAAG	PCR/Sequencing	B20R_fwd

GCGGTGTTCCATATTTGCTG	PCR/Sequencing	B20R_rev
GCAATGTAATGGAGAGTTACC	PCR/Sequencing	C19L_fwd
CATAGCAGCGAACAACAACA	PCR/Sequencing	C19L_rev
GGACTCTGGAATCTTAGACG	PCR/Sequencing	C9.5L_fwd
GATCCCGATTGGACACCT	PCR/Sequencing	C9.5L_rev
GTTCCATATTCCACTAGAGGG	PCR/Sequencing	WR015_fwd
GGATACGAGAGCATATGTGC	PCR/Sequencing	WR015_rev
GATGCAATACGGTACCGC	PCR/Sequencing	WR016_fwd
GAGTTCACAGTAGCTCATTC	PCR/Sequencing	WR016_rev
CGTGTCACTGGCTTTGTAGA	PCR/Sequencing	C2L_fwd
TACTTCAAGAATGGAAAGCGTG	PCR/Sequencing	C2L_rev
TTTATCACACGCGTTTGGATCT	PCR/Sequencing	M1L_fwd
CTAAACCAGTGCCTTCTTGACA	PCR/Sequencing	M1L_rev
TACAACATAGGACTAGCCGC	PCR/Sequencing	I3L_fwd
CCGGTGGTTTGTGATTCC	PCR/Sequencing	I3L_rev
CACCACGTGTGTTTCAGGAT	PCR/Sequencing	I6L_fwd
ACCTGCACGATCTATCACTG	PCR/Sequencing	I6L_rev
GAAGGAGACGGCTACTGT	PCR/Sequencing	K7R_fwd
CGTCGGTCATCAGATCTG	PCR/Sequencing	K7R_rev
CTATGCCAAGCGTATGTTGTTC	PCR/Sequencing	L2R_fwd
ATAGGCATATCACTCACCGATG	PCR/Sequencing	L2R_rev
GTCGCGGATATGGAATTCGA	PCR/Sequencing	WR011_fwd
GTACCAATTTACCAACCCTCTT	PCR/Sequencing	WR011_rev
GCATCGACGCTTCCAAAATTG	PCR/Sequencing	F16L_fwd
ACGGAGTATGAGCAGATGCA	PCR/Sequencing	F16L_rev
GGTCCCTATTGTTACAGATGG	PCR/Sequencing	J2R_fwd
CACAGCAGTTAGTTTTACCACC	PCR/Sequencing	J2R_rev
GAGGAGCTGATATAGTCGTAC	PCR/Sequencing	204_fwd
GTAGATGGGTAGTATATTGTACATG	PCR/Sequencing	204_rev
CGT GAT CTA TGA GTT CTT CTT CG	PCR/Sequencing	H4L_fwd
TAT CCA TTC AGA GAT CGG CG	PCR/Sequencing	H4L_rev
GCA ACC AGT GTT TGA TCA TCC	PCR/Sequencing	H4L_fwd_2
CACAACCCTCAAGAACCTTTG	PCR/Sequencing	H4L_rev_2
GGGGGCGGCCGCATGGTGAGCAAGGGCGAGGAG	PCR/cloning	HK_GFP-NotI-fwd
GGGGGCGGCCGCTGATCAGTTATCTAGATCCGGTG	PCR/cloning	HK_GFP-NotI-rev

2.7. Antibodies

Table 3: List of antibodies used for flow cytometry analysis and immunoblot

Antibody	Species	Specificity	Application	Company/ reference
β-actin	mouse	β-/α-actin	WB	Sigma
FVD eFluor®660		Viability dye	FC	eBioscience
Goat anti-rabbit-POD	Goat	Secondary antibody	WB	Jackson ImmunoResearch
LC3B	rabbit	LC3-I and LC3-II	WB	Sigma
TMEM173	rabbit	Human STING	WB	Abcam
Vaccinia virus Serum	rabbit	Vaccinia proteins	WB	

2.8. Cell lines

Table 4: List of used cell lines

Cell line	characteristics	Reference
BHK21	Baby hamster kidney cells	ATCC© CCL-10™
BMDC	Bone marrow dendritic cell	C57/BL6 mice
DC2.4	Immortalized murine dendritic cells	Georg Häcker
HEK293T	Human embryonic kidney cells	Veit Hornung
HeLa	Human cervical carcinoma cells	ATCC© CRM-CCL-2™
J774	Macrophage-like cell line	Georg Häcker
MEF	Murine embryonic fibroblasts	Björn Storck
MJS	Human melanoma cells	Emmanuel Wiertz
Vero76	African-Green-Monkey kidney epithelial cells	ATCC© CRL-1857™

2.9. Viruses

Table 5: List of used vaccinia virus strains and recombinant viruses

Virus	Description
Modified vaccinia virus Ankara (MVA)	Wild type MVA strain
MVA-P7.5-eGFP	Recombinant MVA virus expressing eGFP under early and late promoter P7.5
MVA-P7.5-NP-SIIN-eGFP	Recombinant MVA virus expressing SIINFEKL peptide and eGFP in the nucleus under early and late promoter P7.5
MVA-P11-eGFP	Recombinant MVA virus expressing eGFP under late promoter P11
MVA-P7.5-N1L	Recombinant MVA virus expressing N1L gene from WR strain
Western Reserve (WR)	vaccinia virus strain Western Reserve
WR-P7.5-eGFP	Recombinant WR virus expressing eGFP under early and late promoter P7.5
WR-ΔN1L	Recombinant WR virus having N1L gene deleted
Chorioallantois vaccinia virus Ankara (CVA)	vaccinia virus strain CVA
Copenhagen	vaccinia virus strain Copenhagen
Wyeth	vaccinia virus strain Wyeth
Lister	vaccinia virus strain Lister

2.10. Reagents

Table 6: List of used reagents

Name	Working concentration	Company
AraC	40 µg/ml	Sigma
Bafilomycin A1	100 nM	Santa Cruz
Chloroquine	50 µM	Sigma
3-Methyladenine	5 mM	Sigma
MG132	1 µM	Calbiochem
Psoralen	0.1 mg/ml	Sigma
Rapamycin	50 µg/ml	VWR

3. Methods

3.1. *In vitro* cell culture

3.1.1. Cell culture

Cells were cultivated in RPMI or DMEM supplemented with 10% heat inactivated FBS and 1% penicillin/streptomycin in a 5% CO_2 incubator at 37°C. The cells were split in an interval of three days and were diluted to reach a confluence of 30-50%. The old medium was discarded, the cells were washed once with PBS and detached from surface using 0.05% trypsin-EDTA for 3-5 min in the incubator. The cells were then flushed down, resuspended, split and transferred into a new flask containing fresh medium.

3.1.2. Cell freezing and thawing

To freeze cells, they were harvested as described in 3.1.1 and centrifuged at 160 xg for 5 min at room temperature. The supernatant was discarded, the pellet resuspended in an appropriate volume of freezing medium and aliquoted in 1.5 ml cryotubes. The tubes were placed in a freezing box at -80°C for at least 24 hrs, to be subsequently transferred to the liquid nitrogen tank.

For cell thawing, the frozen cryotube was placed for 2-3 min in a 37°C water bath or incubator. The cells were first collected in 5 ml culture medium and pelleted at 160 xg for 5 min at room temperature. The medium was discarded, the cells were resuspended in 1 ml fresh culture medium and transferred into a cell culture flask. The cells were cultivated in a 5% CO_2 incubator at 37°C.

3.1.3. Preparation of bone marrow dendritic cells (BMDCs)

BMDCs were derived from femurs and tibia of C57/BL6 mice. The bones were set free from fur and muscle tissue, disinfected with 70% EtOH and placed into a dish containing growth medium. Bones were cut at the edges and cells were flushed out with medium twice using a syringe with a 30G needle. The cells were transferred into a 50 ml falcon tube and centrifuged at 420 xg for 5 min at room temperature. The supernatant was discarded and the pellet was resuspended into 5 ml TAC buffer (diluted 1:10 with dd H_2O) for 2 min at 37°C, in order to lyse the erythrocytes. The cells were then centrifuged at 420 xg for 5 min at room temperature and were taken up in 5 ml growth medium. Afterwards, the cells were filtered through a 100 µm filter, counted and seeded into a 10 cm petri dish. Cells were seeded into a 10 cm dish to a density of $5x10^6$ cells per plate in 10 ml growth medium containing 1% GM-CSF. BMDCs were cultivated up to 10 days at 37°C, 5% CO_2. At day 3, 10 ml growth medium supplemented

with 10% GM-CSF were added to the cells. At day 6, 10 ml medium were exchanged with fresh medium containing 10% GM-CSF.

3.1.4. Generation of stably transfected HeLa dsRed-LC3-eGFP cells

HeLa cells stably expressing dsRed-LC3-eGFP were generated by using the Lenti-X™ lentiviral expression system from Clontech, following manufacturer's protocol.

DNA enzyme restriction and ligation

The dsRed-LC3-eGFP fragment was previously cloned from the pQCXI-Puro-dsRed-LC3-GFP plasmid (from Addgene) into the lentiviral pLVX-IRES-puro vector using the NotI and BamHI restriction sites. The digest occurred overnight at 37°C. The DNA fragments were run through an agarose gel, cut out and purified by using the gel extraction kit from Qiagen. pLVX-IRES-puro vector and dsRed-LC3-eGFP insert with compatible overhangs were ligated by using the T4-DNA ligase in a total volume of 15 µl for 1 hr at 25°C and then overnight at 16°C.

Transformation of plasmid DNA into chemical competent E. coli cells

An aliquot of competent *E. coli* bacteria (XL-1-Blue: *recA1 endA1 gyrA96 thi-1 hsdR17 supE44 relA1 lac* [F' *proAB lacI*q*ZΔM15* Tn*10* (Tetr)], Stratagene) was thawed on ice for 15 min. A volume of 7.5 µl of the ligation mix was added to the bacteria, mixed by pipetting up and down and incubated for 30 min on ice. The bacterial cells were heat-shocked for 1 min at 42°C and immediately cooled down on ice for 2 min. Through this procedure, the cellular membrane gets permeabilized to take up the DNA. One ml LB-medium was added to the sample, which was then shaken at 37°C for 1 hr. Afterwards, the bacteria were centrifuged at 3200 xg for 3 min at room temperature and the LB-medium was discarded leaving around 100 µl in the tube, in which the pellet was resuspended. The bacteria were plated on an agar-plate with the respective antibiotic for selective growth overnight at 37°C.

Lentiviral transduction of HeLa cells

HeLa cells were transduced with dsRed-LC3-eGFP-pLVX-IRES-puro using the Lenti-X™ lentiviral expression system kit from Clontech according to manufacturer's protocol. For this purpose, HEK293T cells were seeded in 10 ml in a 10 cm dish 24 hrs prior to transfection for a confluency of 80-90% the next day. The transfection reaction consisted of two mixtures, which were prepared individually as described below:

Tube 1:	**Tube 2:**
557 µl Xfect reaction buffer	592.5 µl Xfect reaction buffer
36 µl Lenti-X HTX packaging mix	7.5 µl Xfect polymer
7 µl vector DNA (1 µg/µl)	600 µl total volume
600 µl total volume	

Each tube was vortexed well before and after mixing tube 2 with tube 1. The mixture was incubated for 10 min at room temperature and was then added dropwise to the HEK293T cells, which were incubated at 37°C, 5% CO_2. Transfection medium was exchanged with 10 ml fresh growth medium at the next day and cells were incubated for further 48 hrs at 37°C, 5% CO_2.

The lentiviral supernatants were harvested and filtered through a 0.45 µm filter to get rid of cellular debris. The lentiviruses were then either aliquoted and stored at -80°C or directly used to infect target cells. For this purpose, HeLa cells were plated in a 10 cm dish in 10 ml growth medium 12-18 hrs prior to infection. Polybrene (10 µg/ml) was added to the cells to increase transduction efficiency, by reducing charge repulsion between virus and cell. The virus supernatant was added to the cells and the plates were centrifuged at 1200 xg for 90 min at 32°C to improve infection efficiency. At 24 hrs p.i. the virus containing medium was replaced by 10 ml fresh growth medium and cells were incubated for further 2 to 3 days. Selection occurred by using 2-4 µg/ml puromycin for 3 days.

3.1.5. Cell transfection

Cells were seeded in a 6 well-plate at a density of $2.5x10^5$ cells per well 24 hrs prior to transfection. The cells were transfected using TurboFect reagent following manufacturer's protocol. Transfection efficiency was determined after 24-48 hrs by fluorescence microscopy.

3.1.6. Cell infection

HeLa cells were seeded in a 6 well-plate at a density of $5x10^5$ cells per well in 1.5 ml medium. The cells were infected the next day with MVA or WR in 300 µl under regular shaking for 1 hr. The wells were filled up with medium to 1 ml and the plate was placed back at 37°C, 5% CO_2 for the remaining infection time.

DC2.4 cells and BMDCs were harvested, counted an infected on the same day. Two million cells were infected in approximately 200 µl medium in a 15 ml falcon tube for 1 hr at 37°C, 5% CO_2 under regular shaking. The cells were then transferred to a 6 well-plate and medium was adjusted to 1 ml.

For the AraC treatment, HeLa or DC2.4 cells were first incubated for 30 min with AraC (40 µg/ml) at 37°C, 5% CO_2 and then infected as described previously.

In the case of PUVA-treatment, 0.1 mg/ml psoralen were added to 500µl virus containing medium in a well of a 6-well plate and was pre-incubated for 15 min at 37°C, 5% CO_2. UV-inactivation of virus occurred in the cross-linker for 15-30 min at 0.1 Joules and was then added to the cells.

3.1.7. Virus titration ($TCID_{50}$)

To determine the titer of WR and WR-derived mutants, $2x10^4$ Vero76 cells were seeded in 100 µl/well RPMI supplemented with 5% FBS of a flat bottom 96-well plate. Virus suspension was serially diluted starting from 10^{-1} to 10^{-9} using RPMI supplemented with 2% FBS. A volume of 100 µl of diluted virus suspension was added to the respective well of Vero76 cells. In total 16 wells per dilution were infected. The plates were analysed for plaque formation at 4-6 days p.i. and virus titers were calculated according to the number of infected wells using the following formula:

$$\text{vp/ml} = 10^{\,a + 0.5 + \sum \left(\frac{b}{n}\right)} \times 10$$

vp: virus particles

a: last dilution with 100% CPE

b: number of wells with CPE in further dilutions

n: number of wells per dilution

3.2. DNA protocols

3.2.1. Extraction of viral DNA

BHK cells were seeded in a 6-well plate to a density of 4.10^5 cells per well for infection with MOI 10 the next day. The infected cells were harvested 24 hrs p.i. in 400 µl dd H_2O and transferred into a 1.5 ml tube. A volume of 50 µl 10x TEN pH 7.4 buffer was added to the cells. After freezing and thawing them three times at -80°C, the samples were mixed by vortexing and centrifuged at 450 xg for 5 min at room temperature to remove cellular debris. The supernatant was then transferred into a new 1.5 ml tube and subjected to 50 µl proteinase K as well as 23 µl 20% SDS. The samples were incubated for 3 hrs at 56°C. DNA extraction occurred through phenol-chloroform precipitation. Therefore, equal volume of phenol-chloroform (around 523 µl) was added to the samples, which were mixed by vortexing for 10-15 sec and centrifuged at top speed for 5 min at room temperature. The upper suspension was transferred into a clean 1.5 ml tube and extracted again with phenol-chloroform. After the second

extraction, 1/10 volume of 3 M sodium acetate and 2 volumes of absolute ethanol were added. The samples were placed for 30 min at -80°C and centrifuged at top speed for 10 min at 4°C. The supernatant was discarded, the DNA pellet was washed twice with 1 ml 70% ethanol and centrifuged for 5 min at 4°C. The pellet was air dried for 10-20 min until all drops of ethanol were completely evaporated. The DNA was finally resuspended in 30 µl dd H_2O and stored at 4°C until further usage.

3.2.2. Polymerase chain reaction (PCR)

To ensure that enough material was submitted for successful sequencing, we amplified the isolated viral DNA by using specific primers (**Table 2**), binding upstream and downstream of the region of interest. Every sample was pipetted on ice, placed in the thermocycler afterwards and processed as described below:

PCR-mix:

DreamTaq Master Mix (2x)	25 µl
Forward primer (10 µM)	2.5 µl
Reverse primer (10 µM)	2.5 µl
Template DNA	100 ng
dd H_2O	X µl
	∑50 µl

PCR-program:

95°C	2 min	
95°C	30 sec	30x
Tm=57°C	30 sec	
72°C	5 min	
72°C	15 min	
4°C	∞	

3.2.3. Agarose gel electrophoresis

PCR products were loaded on a 1% agarose gel parallel to a DNA ladder and run in 1x TBE buffer through electrophoresis at 100 V for 60 min. The DNA was visualized using an UV-transilluminator.

3.2.4. Quantitative reverse transcriptase polymerase chain reaction (qRT-PCR)

RNA isolation occurred by using the Qiagen RNA Extraction Kit according to manufacturer's protocol. For cDNA synthesis, 3 µg RNA were mixed with 1 µl DNAse (10U/µl) to a total volume of 10 µl. The mix was incubated for 20 min at 37°C for DNA digest and cooled down for 10 min at room temperature. The DNAse was heat inactivated for 5 min at 70°C. The samples were briefly spun down and promptly placed on ice. The RNA-mix for cDNA synthesis was pipetted as follows:

RNA (after DNAse digest)	4.5 µl
dd H_2O	6.5 µl
dNTPs (10 mM)	1 µl
Primer p(dT)	1 µl
	∑13 µl

The samples were incubated for 5 min at 65°C for RNA denaturation and then placed on ice. The cDNA reaction was pipetted as described below:

RNA-mix	13 µl
FSB (5x)	4 µl
DTT (100 mM)	1 µl
RNAsin (40U/µl)	1 µl
SuperScript® III (200U/µl)	1 µl
	∑20 µl

The cDNA reaction mix was incubated for 1 hr at 50°C and 15 min at 72°C. The samples were either stored at -20°C or directly used for Q-PCR. In this case, Q-PCR products were synthesized from cDNA samples using SYBR®Green according to the following reaction:

qPCR Master Mix Precision Plus (2x)	10 µl
Forward primer (10 µM)	1 µl
Reverse primer (10 µM)	1 µl
cDNA	2 µl
dd H_2O	6 µl
	∑20 µl

Every sample was run in two replicates according to the following program:

95°C	10 min	
95°C	15 sec	⎫
55°C	15 sec	⎬ 42x
72°C	30 sec	⎭
40°C	30 sec	

3.2.5. DNA sequencing

The samples were sent to Eurofins for sequencing. Sequencing of DNA was performed according to the cycle sequencing technology (dideoxy chain termination /cycle sequencing), which is based on Sanger sequencing method (Sanger *et al*., 1977). The cycle sequencing technology utilizes a thermo stable DNA polymerase, which allows the repetition of sequencing reactions, and tagged ddNTP terminators that are fluorescently labeled with different dyes. A laser beam within an automated DNA sequencing machine excites these fluorescent molecules for analysis of the DNA fragments produced. Every reaction contained 15 µl of 5-10 ng/µl template DNA and 2 µl of 10 µM primer.

3.3. Immunological methods

3.3.1. Immunoblot

Cell lysis and protein extraction

Cells were seeded and infected as described in 3.1.6. After infection time, the cells were scraped from the plate, harvested into a 1.5 ml tube and centrifuged at 900 xg for 3 min at 4°C. The supernatant was discarded and the cellular pellet was washed one time with cold PBS. Afterwards, the cells were resuspended in 60-80 µl TYR-lysis buffer and placed for 20 min at

-20°C. After thawing the lysates, they were sonified two times for one minute to break up the membranes, and centrifuged at 20.000 xg for 15 min at 4°C to get rid of cellular debris. The supernatants were then transferred into fresh tubes and stored at -20°C for short term or -80°C for long term.

Sodium dodecyl sulfate (SDS)- polyacrylamide gel electrophoresis (PAGE)

Electrophoretic separation of proteins was performed on the basis of their apparent molecular weight using SDS-PAGE (Laemmli, 1970). Discontinuous gels consisted of a stacking and a 12% separating gel. The separating gel was first poured in the gel apparatus. A layer of isopropanol was given to the unpolymerized gel to keep the surface flat. Afterwards, the isopropanol layer was poured off, the stacking gel was added and the comb was inserted. After polymerization, the gels were inserted into the electrophoresis chamber. The comb was removed and the wells were rinsed with Laemmli running buffer. Meanwhile proteins were denatured by adding 5x sample loading buffer and boiling them for 5 min at 95°C. The samples as well as a protein size marker were loaded on the gel. Small gels were run at 30 mA and 300 V for 1 hr and large gels were run at 60 mA and 300V for 2.5-3 hrs.

Protein transfer to membrane

After electrophoresis, the gel was removed carefully from the glass plates and cropped to the separating gel. The gel was placed in the blotter on a stack of three Whatman filter papers and a nitrocellulose membrane which were previously soaked in transfer buffer solution. The gel was then covered by three supplementary Whatman filter papers at the top. The proteins were pulled from the gel into the membrane by an electric current of 300 mA, 17 V for 1 hr. Then, the membrane was stained for 2-3 min in Ponceau-red solution to verify protein transfer. The staining was removed by washing the membrane three times with 1x TBST buffer. In order to avoid unspecific binding of the antibody, the membrane was saturated in a 5-10% nonfat milk or 3% BSA blocking solution for 1 hr at room temperature or overnight at 4°C under shaking.

Protein detection

For protein detection the required primary antibody was diluted in blocking solution. Thus, the membrane was incubated with the antibody for 1 hr at room temperature or overnight at 4°C under shaking. The blot was then washed one time with 1x TBST buffer for 5-10 min, and incubated with a horseradish peroxidase (HRP)-conjugated secondary antibody for 1 hr at room temperature. The membrane was extensively washed three times for 10 min with 1x TBST buffer and shortly dried using whatman paper, before being coated with enhanced

chemiluminescent (ECL) substrate for 5 min. Proteins were detected through chemiluminescence and captured by using a photographic film or a CCD camera.

Membrane stripping

In order to be able to detect other specific proteins on the same blot by using a primary antibody with a different specificity, it is necessary to strip the membrane and eliminate the bound antibodies by using a so-called reblot solution. To this end, the membrane was washed two times with 1x TBST buffer and two times with deionized water for 5 min, before being subjected to re-blot solution and incubated for 30 min at room temperature under shaking. The membrane was then rinsed again two times with 1x TBST buffer and blocked for 1 hr at room temperature before incubating with new antibodies as described previously.

3.3.2. Flow cytometry

Cells were seeded and infected as described in 3.1.6. After infection, the cells were trypsinized, transferred into a 1.5 ml tube and centrifuged for 3 min at 600 xg and 4°C. The supernatant was discarded and the cells were washed once with 1x PBS. The live/dead staining occurred by resuspending the cells in 500 µl viability dye (1:2000 dilution), which were then seeded in a 12 well-plate and incubated for 20 min on ice in the dark. The samples were transferred back into a new 1.5 ml tube, centrifuged for 3 min at 600 xg and 4°C and washed once with 1x PBS. In case a saponin wash was carried out, the cells were rinsed with 200 µl 0.05% saponin solution and incubated for 2 min on ice. The volume was filled up to 1 ml with PBS and the pellet was resuspended gently. The samples were then centrifuged again for 3 min at 600 xg and 4°C. The cells were taken up into 150 µl PBS and transferred to a FACS tube containing 150 µl 2% PFA. Flow cytometry measurement occurred by using FACS Diva from BD and results were analysed through FlowJo.

3.4. Statistics

Immunoblots were analysed by comparing the protein band intensities and calculating their densitometry through ImageJ software. Statistics were calculated with Graphpad Prism and using the student t-test with $p \leq 0.05$ considered as significant: one star * indicates $p \leq 0.05$, two stars ** indicate $p \leq 0.01$, three stars *** indicate $p \leq 0.001$.

4. Results

4.1. Deciphering the impact of VACV infection on autophagy

We first investigated the overall impact of VACV on autophagy, considering that the effect might alter depending on the viral strain (**Figure 3**). As expected, MVA infection of HeLa cells resulted in a strong up-regulation of autophagy. We wondered if the MVA parental strain CVA was behaving the same way. Although LC3-II band intensity and LC3-II/LC3-I ratio were slightly stronger than for the other VACV strains, they were not as significant as for MVA. The other VACV strains, including Copenhagen (Cop.), WR, Wyeth and Lister demonstrated considerably lower lipidation, which was comparable to the basal level of autophagy (mock). We then studied whether these outcomes, with a special focus on MVA and WR strains, were cell type-specific (**Figure 4**). We observed MVA-mediated induction of autophagy also in several other cell lines like dendritic cell-like DC2.4 or the macrophage-like cell line J774 (**Supplementary figure 1**), as well as in primary BMDCs (as shown in later experiments). Interestingly, co-infection with MVA and WR activated autophagy to a lower extend than MVA alone, which strongly supports the inhibitory property of WR. In regard of cellular infection, distinct infectious forms of VACV virions are available (EEV, CEV, IMV), infecting target cells via different routes and depending on diverse cellular factors, which are produced at different amounts among the various VACV strains [7, 98]. Thus, the virulence and infection efficacy might strongly differ between these two strains. We analysed the infection rates in HeLa and DC2.4 cells by using eGFP expressing recombinant viruses by flow cytometry and adjusted the infection rates, respectively (**Figure 5**). Multiplicity of infection (MOI) 10 for WR equalled to an infectivity of MOI 20 for MVA, although infecting cells with MOI 10 for MVA already revealed and infection efficiency of around 70% in HeLa and 60% in DC2.4 cells.

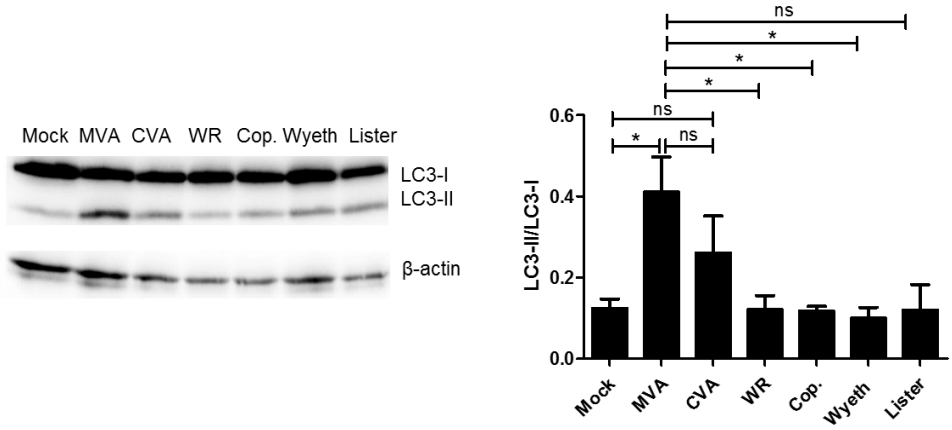

Figure 3: Impact of different VACV strains on autophagy. HeLa cells were infected with VACV for 4 hrs at MOI 10. The cells were then harvested and protein synthesis was analysed through immunoblotting (n=3).

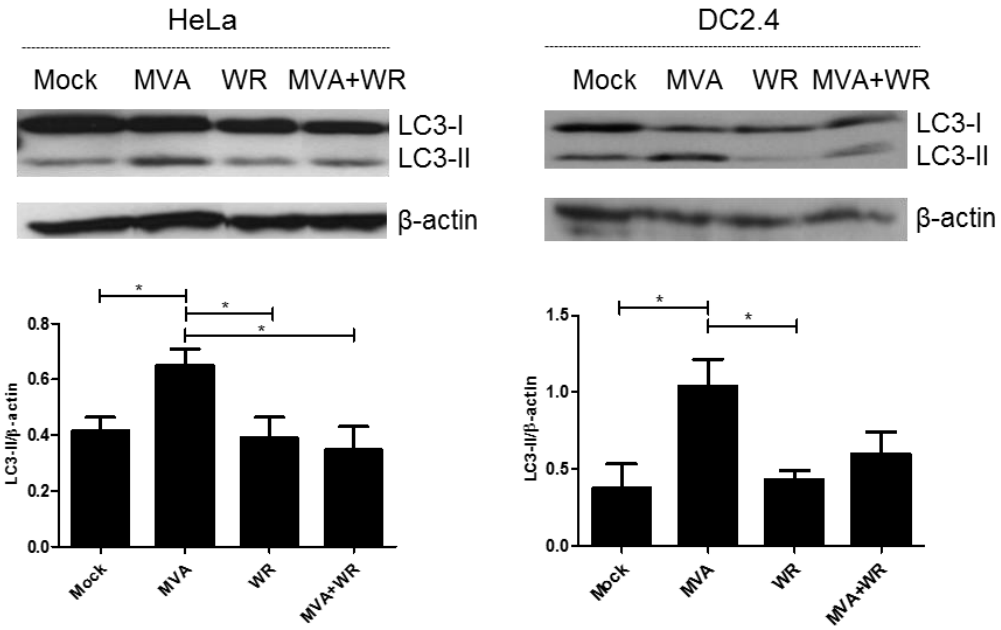

Figure 4: LC3-lipidation in MVA- and WR-infected cells. HeLa and DC2.4 cells were infected with MVA or WR using MOI 10. At 4 hrs p.i. the cells were harvested for lysate preparation and immunoblot analysis (n=3).

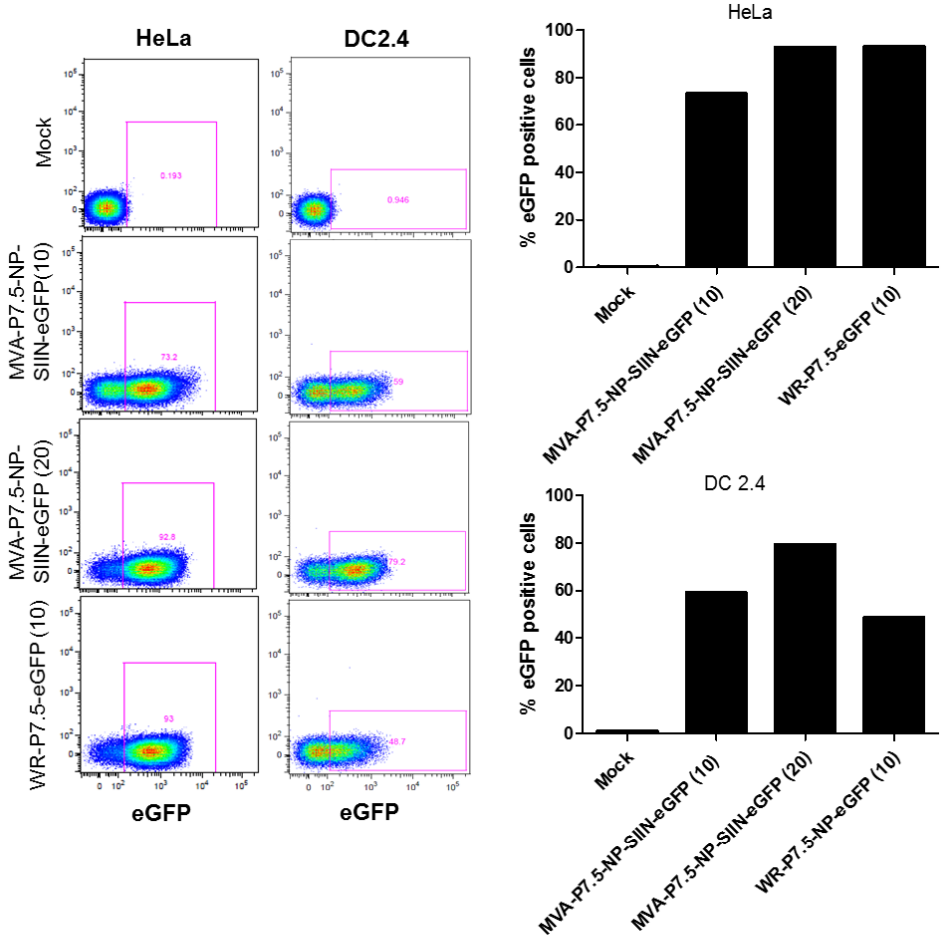

Figure 5: Infection efficiency of MVA and WR. HeLa and DC2.4 cells were infected with MVA or WR expressing eGFP under the P7.5 promoter with MOI 10 or 20 as indicated in brackets. At 8 hrs p.i. the cells were harvested and prepared for flow cytometry analysis. MVA-P7.5-NP-SIIN-eGFP virus expressed eGFP in the nucleus, whereas WR-P7.5-eGFP encoded for cytoplasmic eGFP (n=1).

Analysis of LC3-lipidation through immunoblotting has very often been described to be inadequate and time consuming [99]. In order to exclude that our observations were due to inappropriate quantification, we aimed to establish a system to measure autophagy by using a reliable, easy and rapid quantification method like flow cytometry (**Figure 6**). To this end, we generated HeLa cells stably expressing LC3 fused with two fluorophores, dsRed at the N-terminus and eGFP at the C-terminus (**Figure 6A**) [100]. When autophagy is induced, LC3 gets naturally cleaved at the C-terminus to enable PE conjugation and generate LC3-II. Thus, after autophagy activation, eGFP would be degraded and only dsRed would be present. We were able to monitor autophagy simply by analysing the amount of dsRed-only positive cells through flow cytometry, or the number of exclusively dsRed-LC3-II dots by confocal microscopy (data not shown). Transduction of HeLa cells resulted in 76% of cells stably expressing the fusion gene dsRed-LC3-eGFP (**Figure 6B**). To increase the specificity of dsRed signals and to get rid of soluble cytoplasmic proteins, for example not fully degraded eGFP, that might falsify the results, we introduced a washing step by using a 0.05% saponin solution (**Figure 6C**). Saponin permeabilizes the cellular membrane, and through extensive washing, only insoluble and membrane attached proteins, like the autophagosome-bound dsRed-LC3-II, would remain within the cell [101]. As expected, under conditions where autophagy was not induced, we got an almost complete loss of eGFP and dsRed signals. However, as demonstrated in **Figure 7**, when autophagy was stimulated, e.g. after MVA infection or rapamycin treatment, we detected a three times increase (percentage) of dsRed positive cells if compared to mock cells. Infection with WR did not result in any up-regulation of autophagy. Although treatment with 3-MA delivered minimal higher values than for mock or WR, which could be related to toxicity and cellular stress, the mean percentage of dsRed positive cells was still below the positive control. These outcomes were confirmed by analysis of the mean fluorescence intensity (MFI) (**Figure 7**). Taken together, MVA induces autophagy, while WR infection causes inhibition of autophagy. According to the fact that MVA and WR strongly differ in genome size and gene content, we were particularly interested to characterize and identify the WR encoded inhibitory factor(s) that prevent autophagy from being activated.

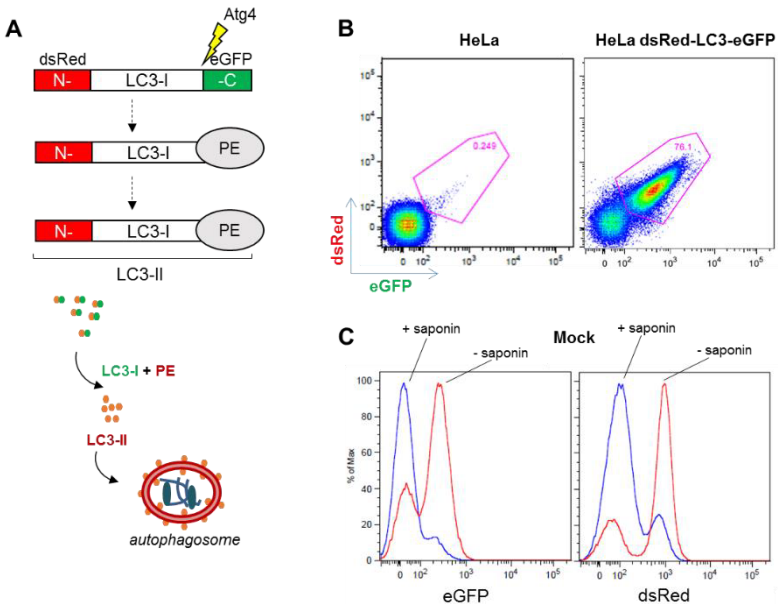

Figure 6: Establishment of a system to track autophagosome induction via flow cytometry analysis. A. Schematic representation of autophagosome induction in HeLa dsRed-LC3-eGFP cells. **B**. Transduction efficiency of HeLa cells stably expressing dsRed-LC3-eGFP was analysed by flow cytometry. **C.** HeLa dsRed-LC3-eGFP cells were either left untreated or washed for 2 min with 0.05% saponin solution on ice, and were subsequently fixed before being analysed through flow cytometry (n=1).

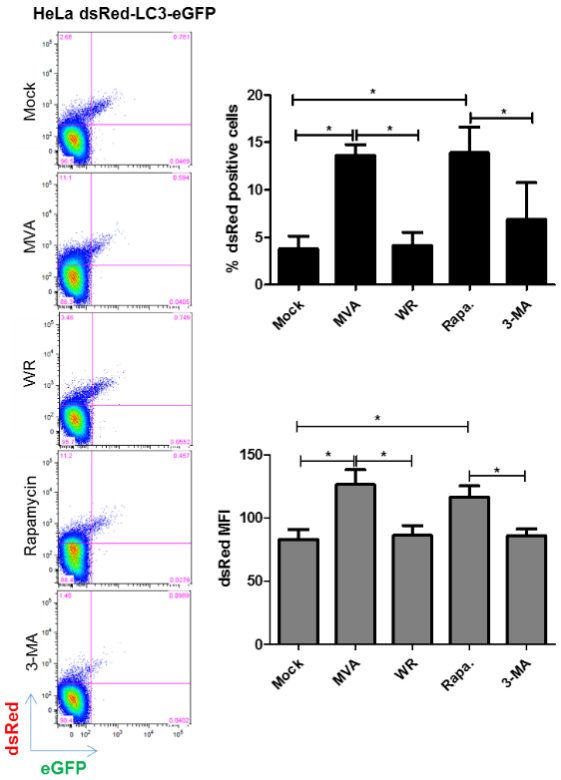

Figure 7: MVA infection induces autophagy as determined by increase in the number of dsRed positive cells and intensity of the dsRed signal per cell (MFI). HeLa dsRed-LC3-eGFP cells were infected with MVA at MOI 20 or WR at MOI 10 for 4 hrs. Rapamycin (Rapa., 50 µg/ml) was used as a positive and 3-MA (5 mM) as a negative control for autophagy induction. The cells were washed with 0.05% saponin before being fixed and analysed through flow cytometry (n=4).

4.2. MVA-mediated induction and WR-mediated inhibition of autophagy occurs at the early time phase of infection

VACV gene expression is transcriptionally regulated into an early, intermediate and late phase. To explore whether the effects can be attributed to any specific class of genes, we performed a kinetic analysis in which HeLa cells were infected and harvested at different time intervals for LC3 immunoblot analysis (**Figure 8**). Interestingly, autophagy was already slightly induced by MVA at 1 hr p.i. From 4 hrs on, the differences between uninfected and MVA- or WR- infected cells became more significant. These outcomes prompt us to test, whether autophagy inhibition was dependent on early genes (**Figure 9**). The reagent cytosine arabinoside (AraC) intercalates into viral DNA to prevent its replication [102], so that only early genes may be expressed. AraC treatment of DC2.4 cells did not show any differences regarding LC3-lipdation, if compared to untreated cells (**Figure 9A**). As a control, DC2.4 cells were infected with MVA expressing eGFP under regulation of late promoter P11 (**Figure 9B and C**). In presence of AraC, eGFP expression was completely disabled, indicating that the treatment was successful. These results were also confirmed for HeLa cells through flow cytometry (**Figure 10**). As depicted in **Figure 10B**, AraC treatment of HeLa dsRed-LC3-eGFP cells did not show any relevant changes regarding the percentage of dsRed positive cells in comparison to the untreated cells, meaning autophagy was still activated or blocked, although intermediate and late genes were efficiently repressed. These observations strongly indicate that inhibition of autophagy by WR and activation of autophagy by MVA was mediated in the early phase of infection.

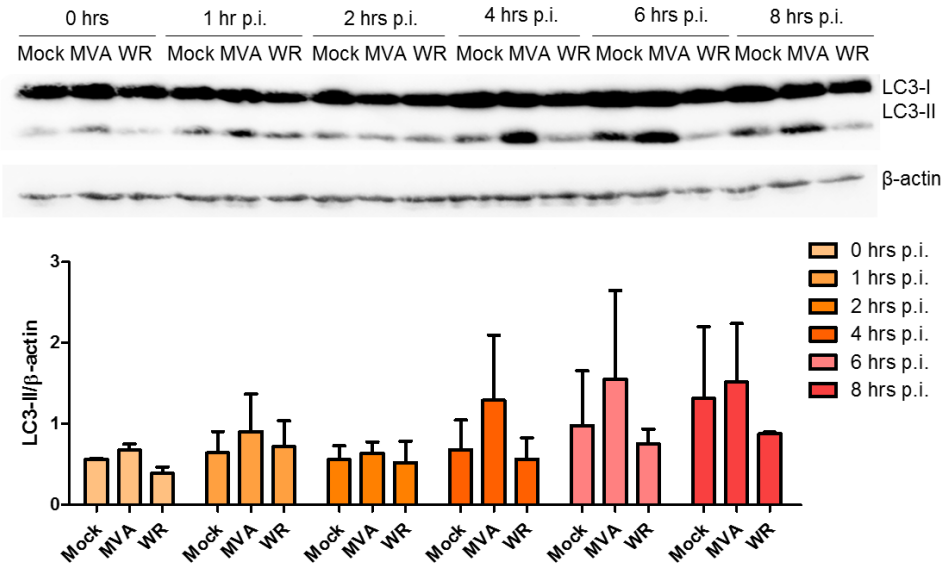

Figure 8: VACV-mediated regulation of autophagy occurs early after infection. HeLa cells were infected with MVA at MOI 20 or WR at MOI 10 and harvested at the indicated time point for immunoblot analysis. For time point 0, the cells were infected with virus and incubated for 30 min at room temperature before being lysed (n=2).

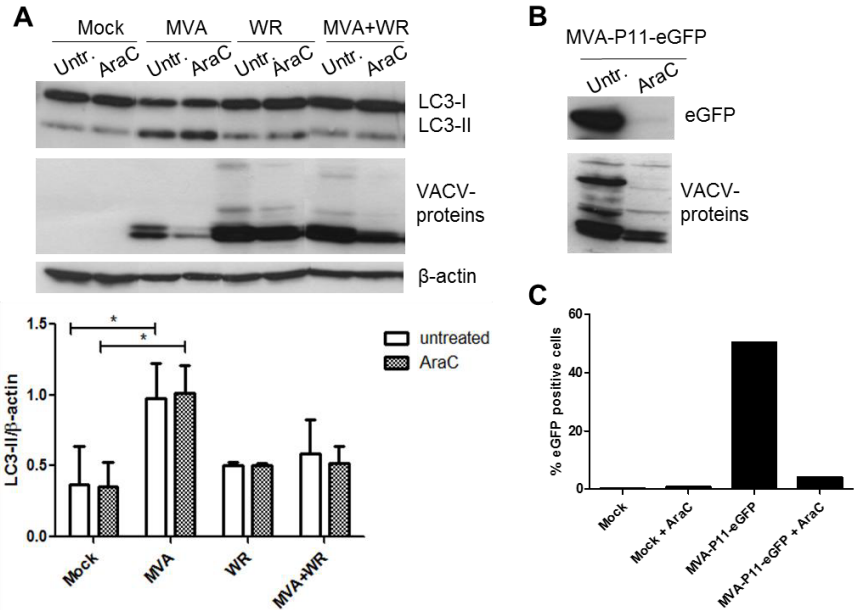

Figure 9: AraC treatment has no impact on MVA-dependent induction or WR-mediated inhibition of autophagy. DC2.4 cells were either treated with AraC (40 µg/ml) and infected or just infected (untr.) with **A.** MVA at MOI 20 or WR at MOI 10. At 4 hrs p.i. the cells were harvested for immunoblot analysis (n=3). **B.** and **C.** DC2.4 cells were infected with MVA-P11-eGFP for 8 hrs and harvested for immunoblot or flow cytometry analysis (n=1). VACV-specific serum (VACV proteins) served as an infection control.

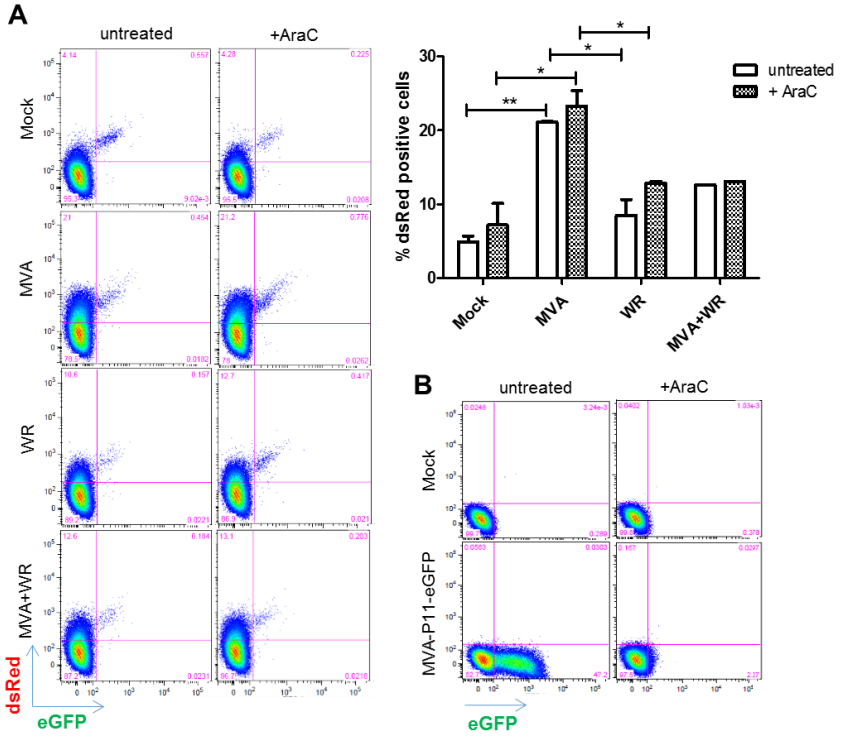

Figure 10: AraC treatment does not influence autophagosome formation (percentage of dsRed positive cells). A. HeLa dsRed-LC3-eGFP cells were incubated for 30 min with AraC (40 µg/ml) before being infected with MVA MOI 20, WR MOI 10 or co-infected with MVA and WR using MOI 10 and 5 respectively. At 4 hrs p.i. the cells were washed with 0.05% saponin and fixed for flow cytometry analysis. **B.** Normal HeLa cells were either left untreated or treated with AraC (40 µg/ml). Infection with MVA-P11-eGFP occurred at MOI 20 for 8 hrs. The cells were analysed through flow cytometry (n=2).

4.3. MVA-mediated induction of autophagy does not necessitate viral DNA replication but efficient virus entry, while WR-mediated inhibition additionally relies on early gene expression

To investigate if initiation of viral replication is necessary for autophagy activation or inhibition, VACV particles were subjected to UV-inactivation. UV-light provokes nucleic acid dimerization leading to the inability of the virus to replicate its DNA and also impairs early gene expression to a certain extend [103, 104]. We did not see any significant changes regarding autophagy induction after MVA infection (**Figure 11**). Though, we noticed a significant upregulation of LC3-lipidation in WR-infected cells, although the values remained below those of MVA-infected cells. Since AraC which also inhibits DNA replication, but allows for efficient early gene expression, had no effect on the inhibitory potential of WR, one may anticipate that early gene expression is required to interfere with autophagy. To explore whether virus entry is necessary for autophagy induction by MVA, or if virus attachment to cells is enough, we incubated HeLa cells with bafilomycin A1 1 hr prior to infection (**Figure 12**). Bafilomycin A1 is an inhibitor of vesicle acidification and autolysosme formation [105]. We observed that after MVA infection, autophagy was not induced anymore. We deduced from these experiments that DNA replication is not a prerequisite for autophagy induction, however efficient VACV cellular entry and not only cellular adsorption is compulsory.

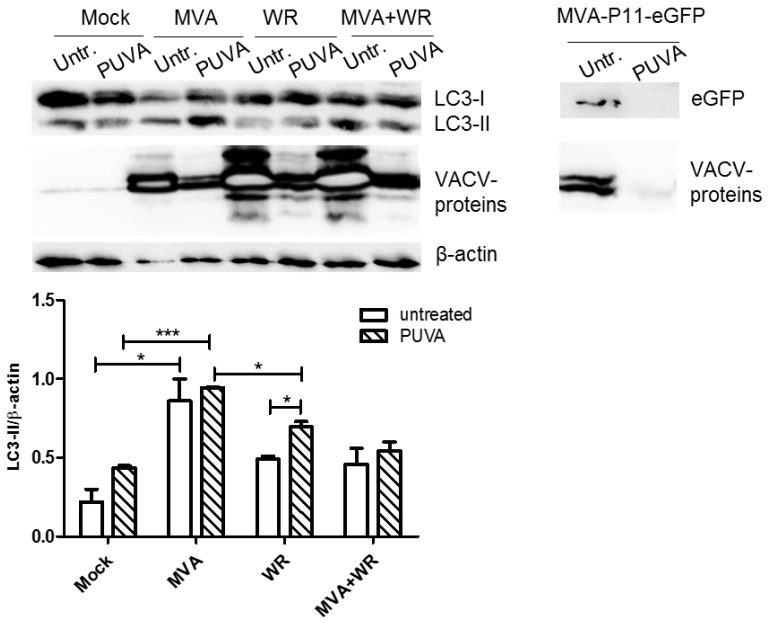

Figure 11: UV-inactivation has no impact on MVA-induced autophagy. DC2.4 cells were infected with MVA MOI 20, WR MOI 10 or co-infected with MVA and WR using MOI 10 and 5 respectively. Viruses were subjected to 0.1 mg/ml psoralen, UV-inactivated for 15 min and then added to the cells. MVA and WR infected cells were harvested at 4 hrs p.i., and MVA-P11-eGFP infected cells at 8 hrs p.i. for immunoblot analysis (n=2).

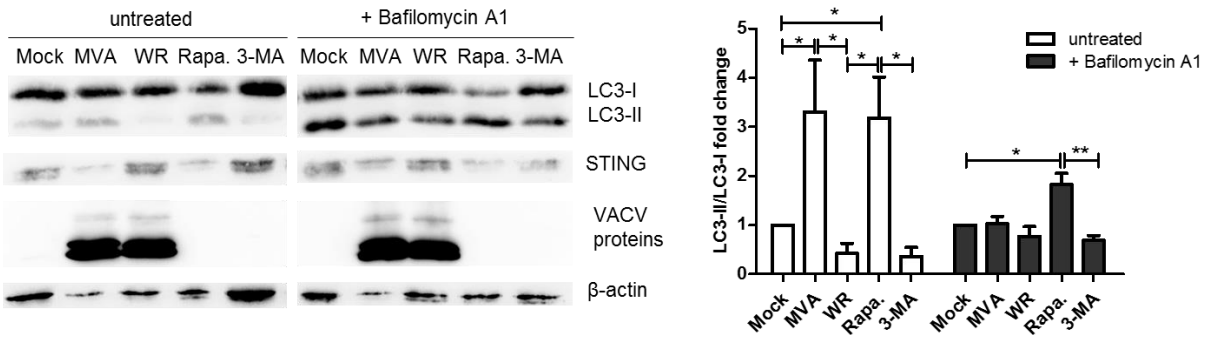

Figure 12: MVA-mediated autophagy activation requires efficient virus entry. HeLa cells were incubated for 1 hr with bafilomycin A1 (100 nM), before being infected with MVA at MOI 20 or WR at MOI 10. Treatment with rapamycin (Rapa.) occurred at a concentration of 5 mM or 50 µg/ml for 3-MA. At 4 hrs p.i. cells were harvested and analysed through immunoblotting (n=3).

4.4. Screen of potential viral candidates for autophagy interference

The previous outcomes pushed us to investigate the relevance of specific viral genes for autophagy interference. Twenty potential candidates, encoded by WR but not MVA, were selected according to their function and expression profile (early gene) (**Supplementary figure 2**). We generated viral deletion mutants using the CRISPR (Clustered Regularly Interspaced Short Palindromic Repeats)-Cas9 (CRISPR-associated protein 9) system, which is a method for directed gene editing. By designing specific guide RNAs (gRNAs) complementary to a defined target sequence, the endonuclease Cas9 is guided to that site and leads to a double strand break and deletion. Through non-homologous end-joining, the DNA strands are re-joined together. In case the deletion succeeds in a truncation or frameshift of the genetic open-reading frame (ORF), the genetic information is disrupted and the gene will not be correctly expressed anymore [106]. However, if mutations take place, which would not result in a frameshift or truncation e.g. an amino acid exchange or deletion, the gene function would most likely not be affected. The efficiency of this system strongly depends on the gene of interest and binding site of the gRNA. Therefore, for every potential candidate three different gRNAs were designed. The viral mutants were generated through primary infection of MJS cells, a human melanoma cell line stably transduced with the respective gRNA and Cas9, with WR-P7.5-eGFP virus. We started using a very low MOI of 0.01 or 0.001, to ensure that every viral particle is sucessfully targeted by the gRNA and cleaved. We tracked the overall infection efficiency by observing the number of green fluorescent plaques through microscopy. At 6 days p.i. the infected cells were harvested and lysed to release progeny of virus, which was used for a second infection round using MOI 0.01. In the last step, freshly seeded MJS cells were infected with MOI 1 for virus amplification. It took around 4 weeks for complete generation and evaluation of one

deletion mutant. Before screening them, we first determined the viral titer, sent the isolated viral DNA for sequencing, and analysed the infection efficiency of the mutants as depicted in **Figure 13**. All candidates showed an infection rate of at least more than 50% in HeLa cells. The viral mutants were then tested through flow cytometry for their capacity to induce autophagy (**Figure 14**). In case the deleted gene would have encoded for an inhibitory factor, its deletion would have allowed for induction of autophagy. Although some mutants indicated a higher percentage of dsRed-positive cells than the control WR-infected cells (WR-ctrl_58) (**Figure 14A**), none of them showed a significant up-regulation as compared to MVA (**Figure 14B**).

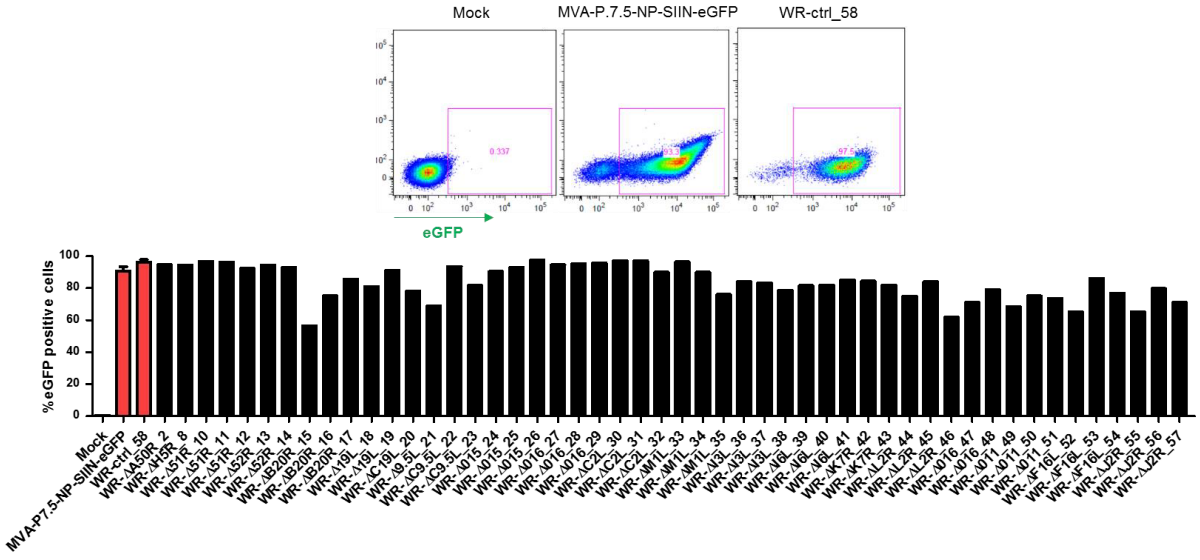

Figure 13: Infection rate of viral deletion mutants. HeLa cells were infected with MVA-P7.5-NP-SIIN-eGFP at MOI 20 or with control virus WR-ctrl_58 expressing eGFP under P7.5 promoter or with the indicated viral mutants WR-ΔA50R_2 to WR-ΔJ2R_57 at MOI 10. At 8 hrs p.i. the cells were harvested and processed for flow cytometry analysis (n=1).

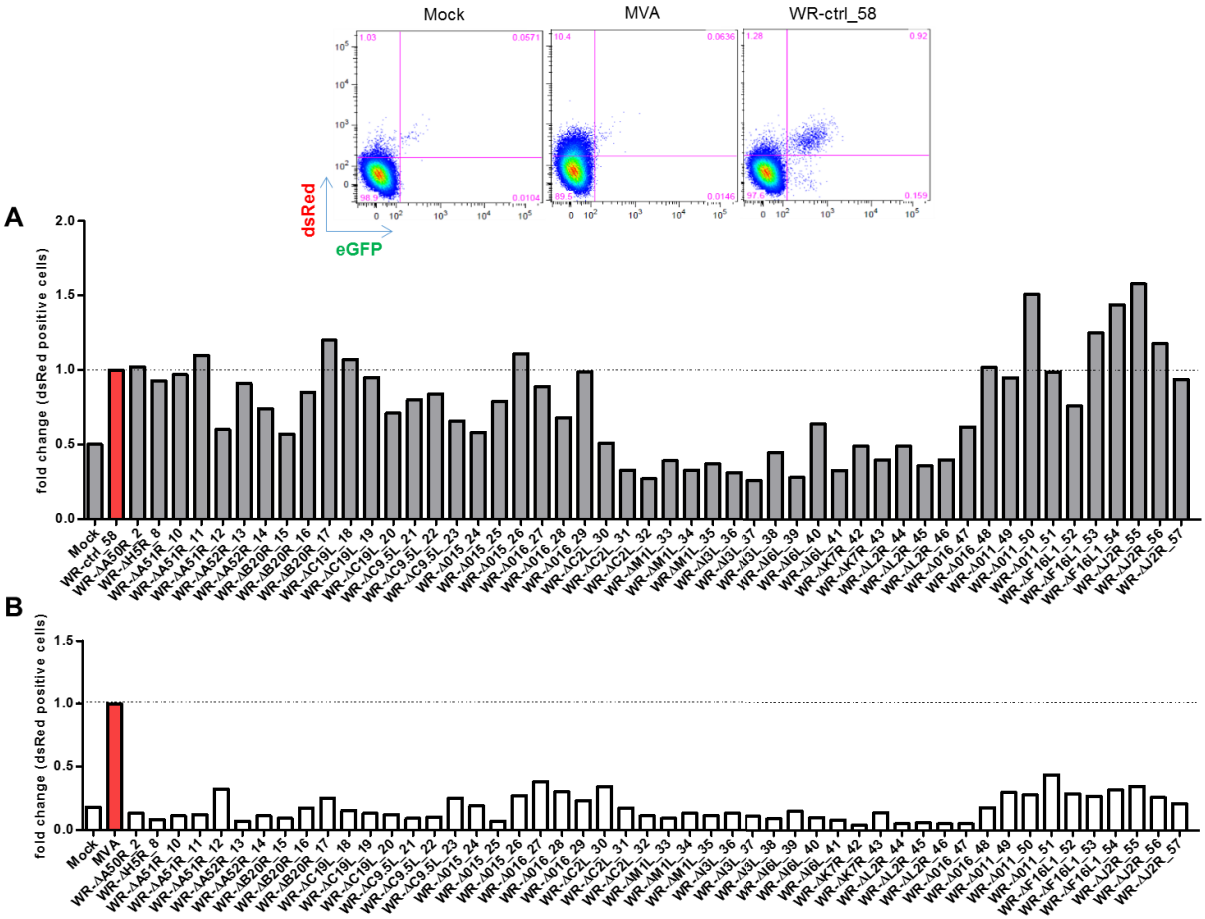

Figure 14: Screen of viral deletion mutants for autophagy induction. HeLa dsRed-LC3-EGFP cells were infected with MVA at MOI 20, with control virus WR-ctrl_58 at MOI 10, or with the viral mutants WR-ΔA50R_2 to WR-ΔJ2R_57 at MOI 10. At 4 hrs p.i. the cells were harvested, washed with 0.05% saponin solution and analysed through flow cytometry (n=1). **A.** number of dsRed positive cells was normalized to WR-infected cells, **B.** number of dsRed positive cells was normalized to MVA-infected cells.

Like previously mentioned, gene editing by using the CRISPR-Cas9 method either resulted in a silent-, missense- or non-sense mutation, as exhibited by the sequencing results (**Supplementary figure 3 and 5**). Moreover in some samples, the sequences were very ambiguous, meaning that nucleotides from either forward or reverse strand were not conform to the corresponding reference sequence, which suggests that we were dealing with a mixed virus population (**Supplementary figure 4**). Some viral particles did probably not efficienctly go through the deletion procedure and remained wild type, developed a revertant phenotype or resistance against restriction by Cas9. To circumvent this problem, we reanalysed the nucleotide sequences, selected the genes for which we had clear deletions, but with a mixed or wt contaminated phenotype. We perfomed a limiting dilution assay from previously generated viral stocks, through which we were able to select and amplify single mutant clones. For every gene one to three clonal mutants were tested by flow cytometry (**Figure 15**). Although the DNA

sequences demonstrated clear results in regard of nucleotide deletion, none of the investigated genes had a phenotype that seemed to be functionally associated with autophagy.

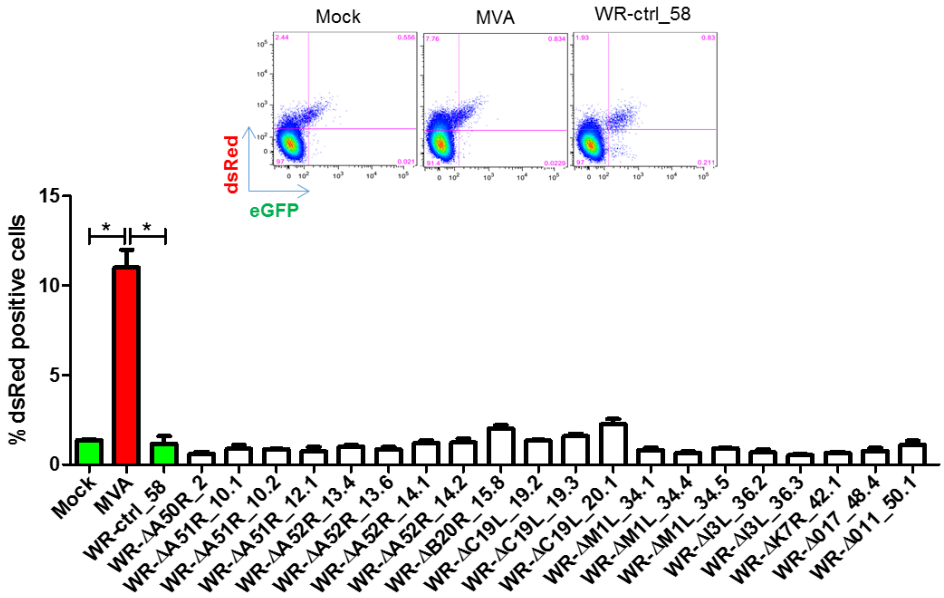

Figure 15: screen of clonal viral mutants with deletions resulting in a gene frameshift (performed by Bastian Gorn)**.** HeLa dsRed-LC3-eGFP cells were infected with MVA at MOI 20, with control virus WR-ctrl_58 at MOI 10, or with the viral mutants WR-ΔA50R_2 to WR-Δ11_50.1 at MOI 10. At 4 hrs p.i. the cells were harvested, washed with 0.05% saponin and analysed through flow cytometry for autophagy induction (n=2).

4.5. cGAS-STING-dependent activation of autophagy upon MVA infection

In order to identify the inhibitory gene candidate, we were looking for alternative methods. We aimed to perform a screen of a commercially available ORF library, constituted of 257 plasmid-encoded VACV genes. We intended to investigate the function of these genes in regard to autophagy, by transfecting HeLa cells with the respective vector-encoded gene and subsequently testing its ability to repress autophagy. However, transfection with a control plasmid itself already engendered strong up-regulation of LC3-lipidation, to a level that we were not able to differentiate between induction and inhibition anymore (**Figure 16**). We considered the possibility of autophagy to get activated by dsDNA and addressed the question, whether there is a connection between autophagy and recognition of dsDNA, by taking into account that VACV is a dsDNA virus.

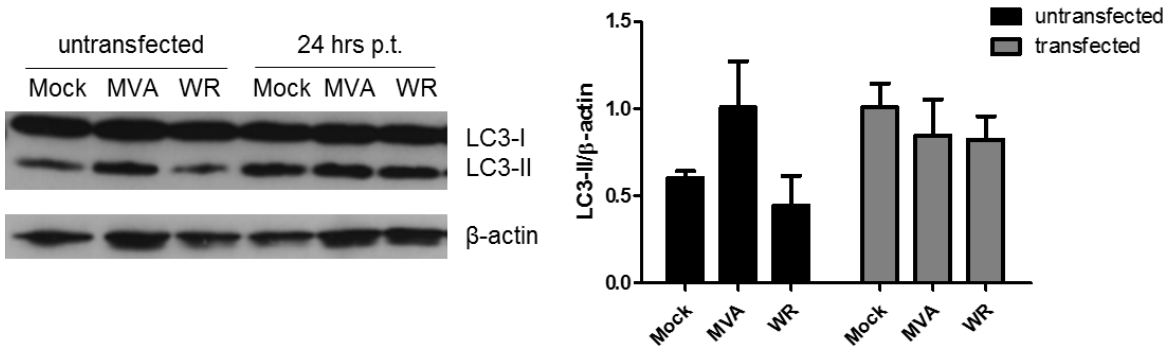

Figure 16: Plasmid-DNA transfection induces LC3-lipidation. HeLa cells were either left untransfected or were transfect with the plasmid pcDNA-3.1D-eGFP using the transfection reagent Turbofect. At 24 hrs p.t. the cells were infected with MVA or WR at MOI 10 for 4 hrs. The cells were then harvested and analysed through immunoblotting.

At that time, a quite recently described mechanism for recognition of dsDNA was the cGAS-STING pathway. Previous findings revealed VACV to interfere with STING, via the viral protein N1L [92]. We wondered, if this pathway played any relevant role regarding MVA-induced autophagy. Therefore, we used wild type (wt) or BMDCs STING-/- and tested first of all their capacity to be infected (**Figure 17**). We obtained comparable infection rates for the two cell types. Next, we analysed the LC3-lipidation upon infection (**Figure 18**). In BMDCs wt, autophagy was efficiently activated by MVA and inhibited by WR as expected. However, in BMDCs STING-/- the up-regulating effect transmitted by MVA was abolished, although rapamycin treatment led to a four- to five-fold increase. We came to the conclusion that MVA-mediated induction of autophagy likely requires STING expression.

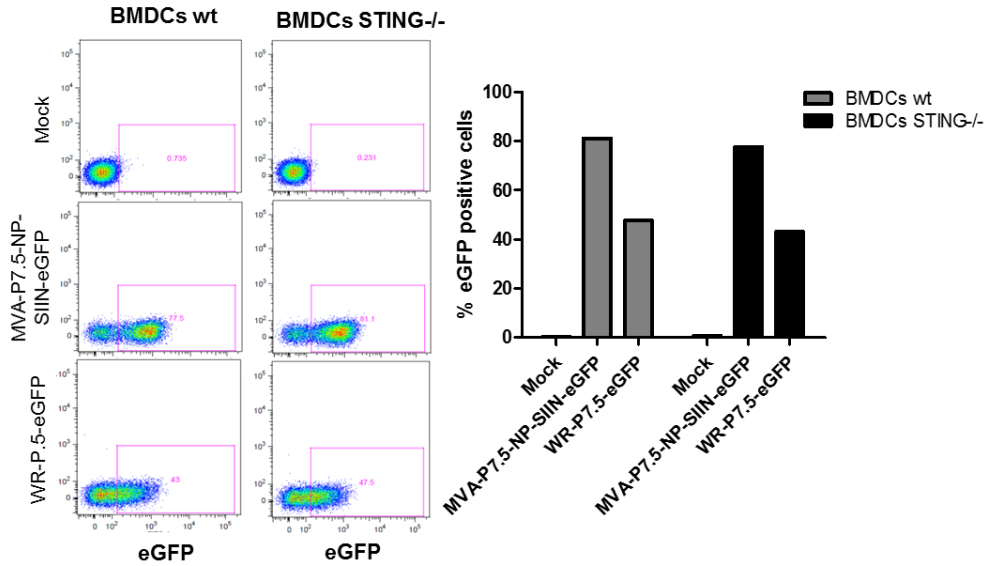

Figure 17: Infection efficiency of MVA and WR in BMDCs. BMDCs wt or BMDCs STING-/- cells were infected with MVA or WR expressing eGFP under control of the P7.5 promoter with MOI 20 or 10, respectively. At 8 hrs p.i. the cells were harvested and processed for flow cytometry analysis (n=1).

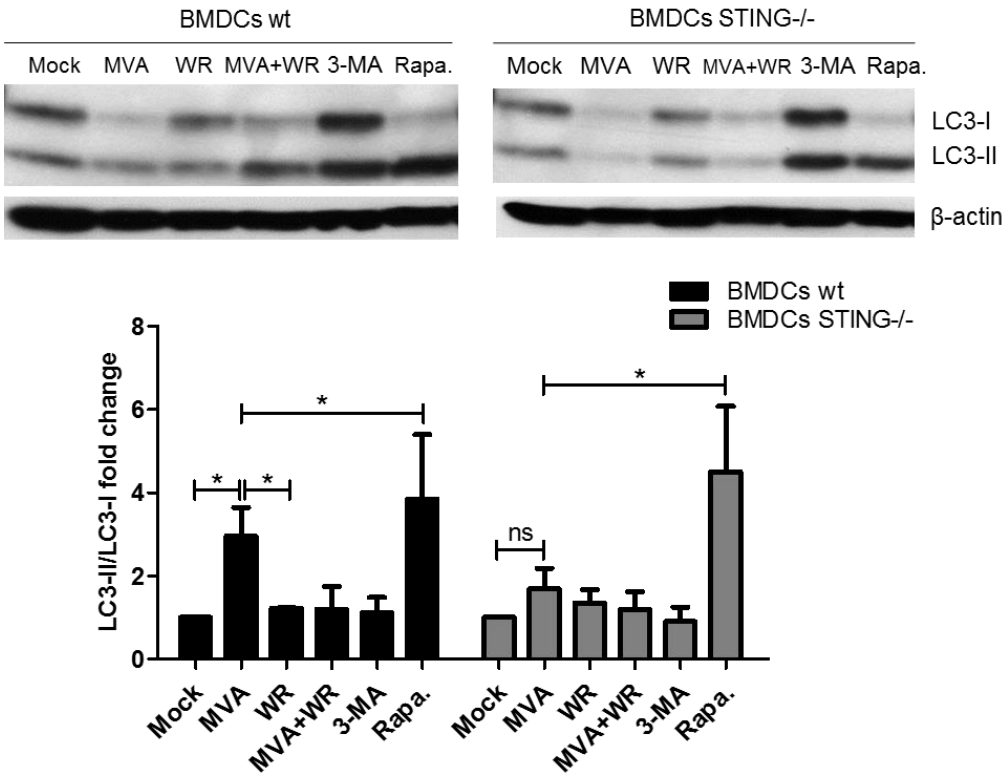

Figure 18: STING-dependent MVA-mediated induction of autophagy. Eight days old BMDCs were infected with MVA-P7.5-NP-SIIN-eGFP at MOI 20, WR at MOI 10 or co-infected with MVA and WR at MOI 10 and 5, respectively, for 5 hrs. The autophagy inhibitor 3-MA was added at a concentration of 5 mM and rapamycin (Rapa.), which induces autophagy, at a concentration of 50 µg/ml (n=4).

Afterwards, we attested the relevance of STING for MVA-mediated autophagy by using STING-deficient HEK293T cells. MVA infection of these cells did not induce, but rather led to a slight decrease of LC3-lipidation if compared to uninfected cells (**Figure 19**). These findings are consistent with the previous results and emphasize autophagy activation to depend on STING.

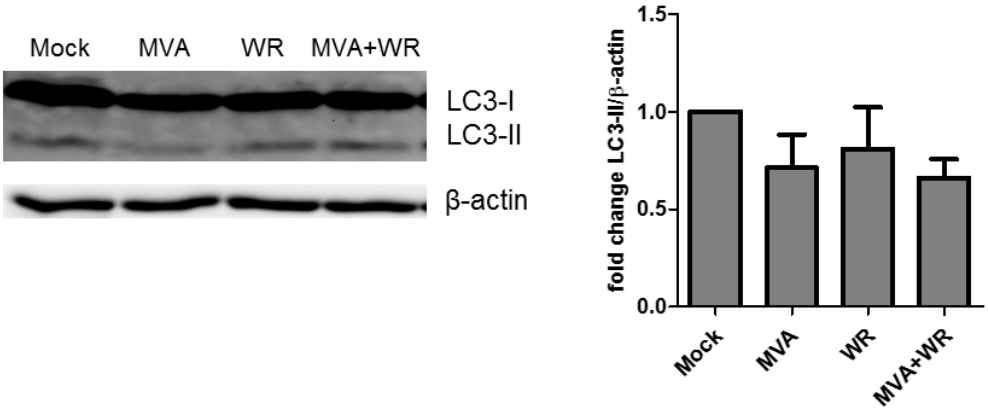

Figure 19: MVA does not induce autophagy in the absence of functional STING (HEK293T cells). HEK293T cells (provided by V. Hornung, LMU München) were infected with MVA or WR using MOI 10 or were co-infected with MVA and WR at MOI 5 each. At 4 hrs p.i. cells were lysed and proteins were analysed through immunoblotting (n=3).

4.6. VACV interferes with a non-canonical autophagy pathway

Numerous studies report the implication and regulatory function of Atgs in regard of the cGAS-STING pathway [90, 91]. The maintained rapamycin-dependent autophagy induction in BMDCs STING-/- (**Figure 18**), suggests autophagy to be controlled differently in VACV-infected cells. These findings motivated us to explore how autophagy proceeds upon VACV infection.

Rapamycin triggers autophagy via inhibition of mTOR. The downstream signalling cascade implies activation of the ULK1:ATG13:FIP200 complex [44-46]. In a first step, we investigated whether this complex is also required for MVA-mediated activation of autophagy. We infected wild type MEFs (wt) and MEFs lacking either ATG13 or ULK1/2 and analysed the LC3-lipidation (**Figure 20**). Although MVA-mediated induction of autophagy in the ATG13 control cells MEF wt was not significant, which is due to strong deviations between the values for the individual experiments, we saw a clear activation beyond the level of basal autophagy in mock cells. However, we could observe a down-regulation of rapamycin induced autophagy in the knock-out cells, which was more significant in MEF ATG13-/- than for MEF ULK1/2-/-, while the LC3-lipidation in MVA-infected cells was kept at comparable levels. These data indicate that ATG13 and ULK1/2 are not required for stimulation of MVA-mediated autophagy, which points to a non-canonical pathway.

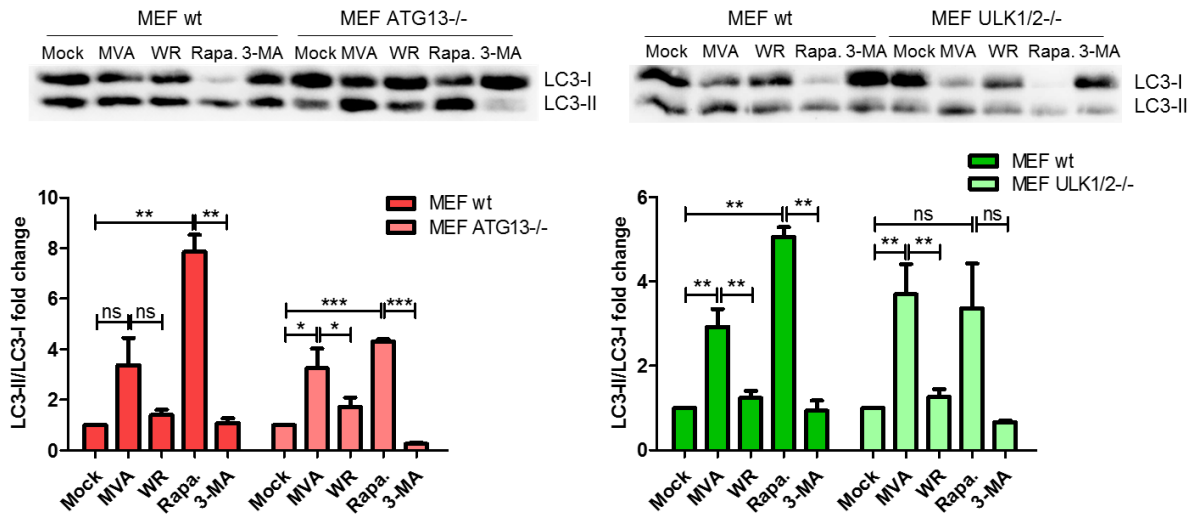

Figure 20: MVA-mediated induction of autophagy is independent from ATG13 and ULK1/2. MEF cells (gift from Björn Storck, HHU Düsseldorf) were infected with MVA at MOI 20 or WR at MOI 10 and additionally treated with 5 mM rapamycin or 50 µg/ml 3-MA. At 4 hrs p.i. the cells were harvested, lysed and analysed through immunoblotting (n=4).

In the following experiment, we confirmed the previously described results (**Figure 21**). HeLa cells were infected and additionally subjected to rapamycin or 3-MA. After rapamycin

treatment, autophagy was strongly activated, which was preserved even after WR infection. However, in case of 3-MA treatment and MVA infection, autophagy was not blocked as we would have expected, but was rather induced by MVA. These results indicate that MVA and WR act on an alternative autophagy pathway, distinct from the one which is regulated by rapamycin and 3-MA. Besides these outcomes, we perceived another interesting phenotype regarding STING stability (**Figure 21**). After treating the cells with rapamycin, the STING protein was not detectable, contrary to the untreated cells or those which were subjected to 3-MA only. In the latter case, the STING band intensity was even stronger, which indicates autophagy to play a role in STING regulation. Interestingly, also upon MVA infection and rapamycin treatment, STING protein was not detectable, while in WR- or 3-MA-treated cells it was present. Intriguingly, STING was absent in MVA-infected and 3-MA-treated cells, which implies canonical autophagy not to be responsible for the loss of STING in regard of MVA infection. Hence, we had a closer look on how STING is regulated upon VACV infection.

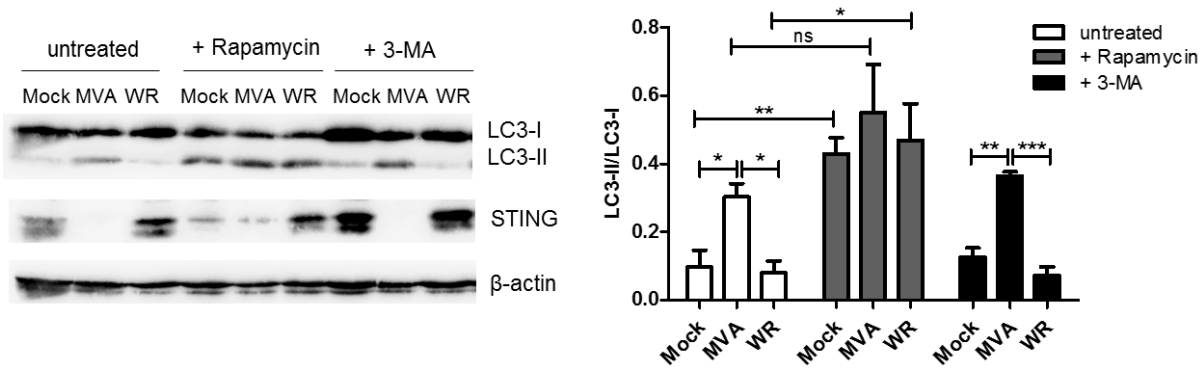

Figure 21: MVA induces LC3-lipidation via an alternative autophagy signalling pathway. HeLa cells were infected with MVA at MOI 20 or WR at MOI 10 and additionally treated with 5 mM rapamycin or 50 µg/ml 3-MA. At 4 hrs p.i. the cells were harvested, lysed and analysed through immunoblotting (n=3).

4.7. MVA infection causes degradation of STING

To find out if the missing STING protein band corresponded to a delayed or abrogated expression, we infected HeLa cells for 4 and 8 hrs and analysed the samples through immunoblotting (**Figure 22**). Even at 8 hrs p.i. we were not able to detect any STING protein. Nevertheless, qRT-PCR analysis showed normal STING mRNA levels, which were comparable between MVA- and WR-infected cells. These results would rather argue for MVA-mediated STING degradation than for down-regulation or retarded expression.

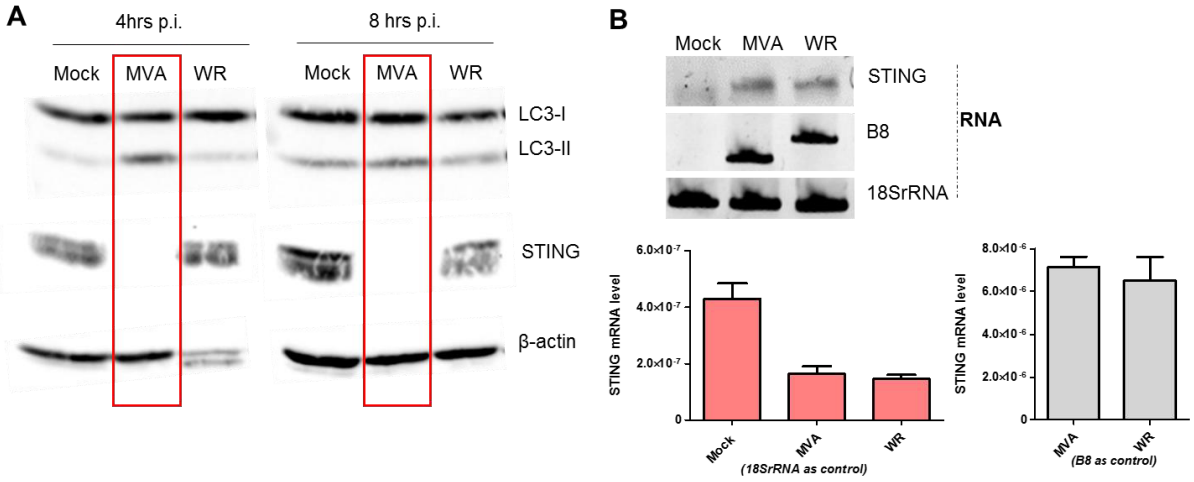

Figure 22: STING is degraded upon MVA infection in HeLa cells. HeLa cells were infected with MVA at MOI 20 or WR at MOI 10 and harvested for **A.** immunoblot analysis at 4 or 8 hrs p.i. (n>3) **B.** RNA was isolated from MVA- and WR-infected cells and subjected to qRT-PCR analysis using STING-specific primers. 18SrRNA was used as cellular housekeeping control and B8 as viral infection control (n=3).

Hence, we wanted to explore the mechanism behind STING degradation and whether there is a direct link to autophagy. We analysed STING expression upon addition of AraC or PUVA (**Figure 23**). STING was still degraded in MVA-infected cells, independently from the treatment with either of the two chemical compounds. These results are indicative for STING degradation to occur early and to be independent from viral DNA replication, as previously shown for autophagy induction by MVA.

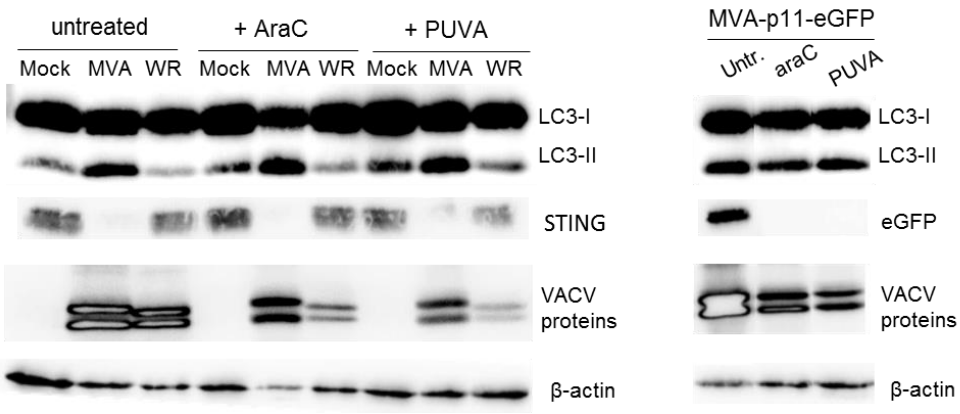

Figure 23: STING is degraded at the early time phase of infection and is independent from viral DNA replication. HeLa cells were infected with MVA at MOI 20 or WR at MOI 10 for 4 hrs. HeLa cells were incubated with AraC (40 µg/ml) for 30 min prior to infection. For PUVA treatment, the virus was incubated with psoralen (0.1 mg/ml), inactivated for 30 min in the UV-cross-linker and subsequently added to the cells. Infection with MVA-P11-eGFP expressing GFP under control of the P11 late promoter occurred using MOI 10 for 8 hrs. After lysis, the samples were analysed through immunoblotting (n=2).

Next, we tested if proteasomes could be responsible for STING degradation (**Figure 24**), since ubiquitin-ligase RNF5 has been described to be implicated in the cGAS-STING pathway [107]. HeLa cells were subjected to MG132, a proteasome inhibitor, before being infected. However, STING protein stability was not restored and LC3-lipidation after MVA infection or rapamycin treatment was increased. VACV protein synthesis was decreased due to inhibition of intermediate and late gene expression, indicating more or less that the treatment was successful.

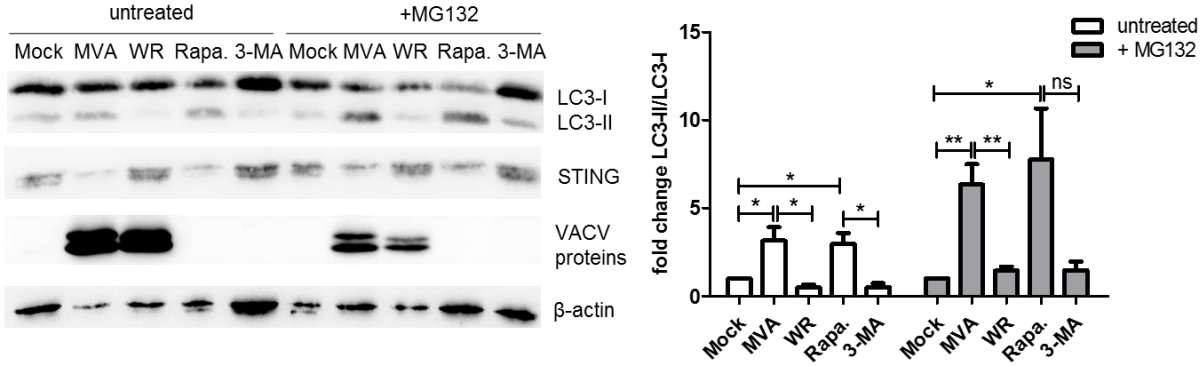

Figure 24: STING degradation is proteasome-independent. HeLa cells were incubated for 30 min with MG132 (1 µM) before being infected with MVA at MOI 20 or WR at MOI 10. Treatment with rapamycin (Rapa.) occurred at a concentration of 5 mM or 50 µg/ml for 3-MA. At 4 hrs p.i. the cells were harvested and analysed through immunoblotting (n=4).

In another approach, we tried to rescue STING from degradation via expression of the N1L gene, which is trunctated in MVA but contained full-length in WR (**Figure 25**) [11]. N1L was described to interfere with the cGAS-STING-type I interferon pathway [92]. To this end, we infected cells with recombinant MVA expressing N1L or WR having N1L deleted. None of the two viruses showed a variant phenotype in regard of STING degradation or autophagy, when compared to the corresponding wild type viruses. The results assume neither autophagy inhibition by WR nor STING degradation by MVA to rely on N1L.

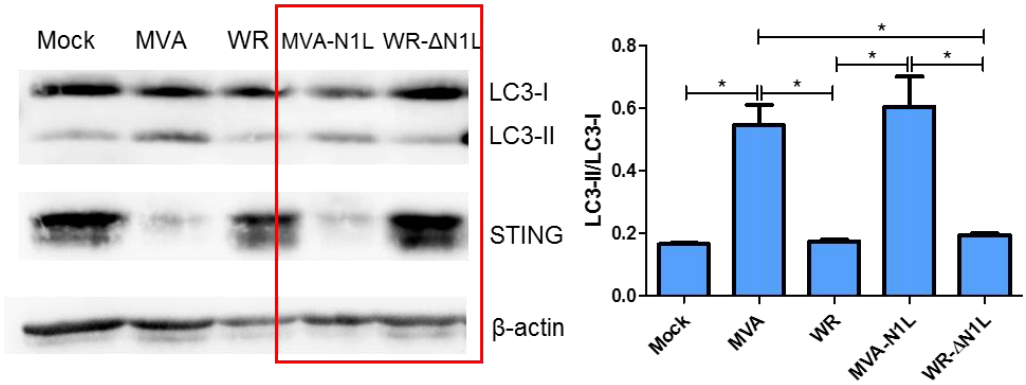

Figure 25: STING is degraded and LC3 is lipidated in presence of N1L. HeLa cells were either infected with MVA or MVA-N1L at MOI 20 or WR or WR-ΔN1L at MOI 10 for 4 hrs, before being harvested for immunoblot analysis (n=2).

DNA viruses, as vaccinia virus, produced out of cGAS expressing cells are able to activate the cGAS-STING pathway, since the viral progeny will encapsulate the produced cGAMP and will transmit it to newly infected cells resulting in an antiviral state [108, 109]. In this regard, we were interested to see whether exogenous cGAMP could induce LC3-lipidation, which would allow to draw a direct connection between autophagy and cGAS-STING pathway. In the last experiment, we investigated the requirement of cGAMP for autophagy activation and STING degradation (**Figure 26**). As a control, we transfected cells with plasmid DNA, that caused a prominent up-regulation of autophagy and degradation of STING. Transfection with synthetic cGAMP or cGAMP agonist (Agn) led to autophagy induction, however we did not observe STING degradation. By contrast, incubation with cGAMP engendered definite STING degradation, which was not the case for Agn incubated cells, although autophagy was induced in both cases. We inferred from these results, that autophagy induction does not specifically depend on cGAMP, while STING degradation is mediated i.a. by cGAMP.

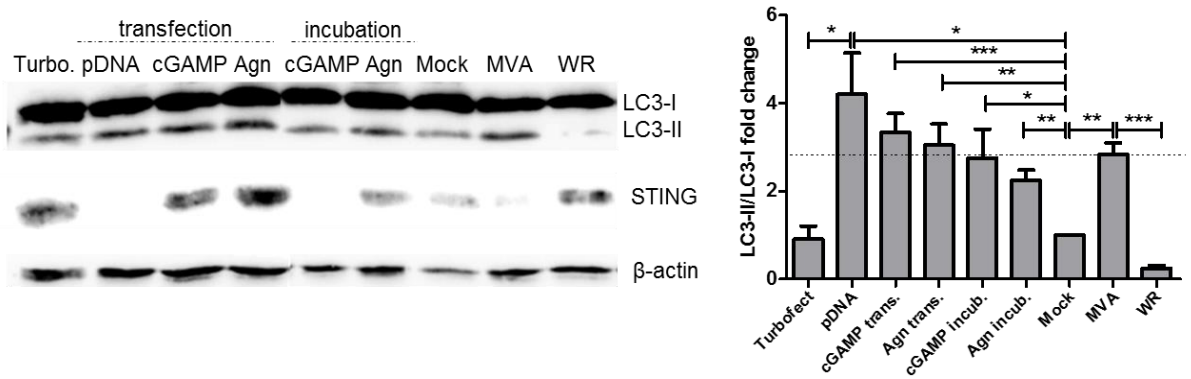

Figure 26: cGAMP induces autophagy, but inconsistently conveys STING degradation. HeLa cells were transfected (trans.) using Turbofect reagent with 4 µg plasmid DNA (pDNA), synthetic cGAMP or cGAMP agonist (Agn) for 24 hrs. Meanwhile, HeLa cells were incubated with 20 µg/ml cGAMP or Agn for 24 hrs. On the next day, HeLa cells were infected with MVA at MOI 20 or WR at MOI 10 for 4 hrs. The cells were harvested and processed together for immunoblot analysis (n=3).

5. Discussion

After repeated epidemics of variola disease and its successful eradication through vaccination, VACV has raised the overall interest and is commonly employed as a viral vector vaccine against other diseases [8-10]. Due to its safety profile, MVA has become one of the preferential strains for recombinant vaccine generation. Therefore, it is of huge importance to investigate and understand the immune responses against VACV infection and recombinant VACV vaccination, in order to increase the quality of these vaccines and to avoid possible side effects during treatment. Since VACV antigens for MHC class II presentation have been shown to be also generated through autophagy [4], the aim of this PhD project was to analyse the relation of autophagy to VACV infection and how it is orchestrated.

5.1. Differences between VACV strains are not limited to their genome size, but influence diverse cellular mechanisms that contribute to immune defence

To study the overall impact of VACV on autophagy, we infected HeLa cells with different vaccinia viral strains. LC3-lipidation was significantly up-regulated upon MVA infection, while the other strains did not show any induction of autophagy. CVA infection demonstrated an intermediate phenotype, however LC3-lipidation was still below the level in MVA infected cells. CVA has a genome size of around 192 kbp and belongs to the ancestral strain of MVA. As compared to the other strains, CVA possesses 51 fragmented genes that are full-length in other orthopoxviruses, but presumably do not encode for functional proteins [110]. Still, we have to consider, that the potential inhibitory candidate we are seeking might not be expressed, fragmented or dysfunctional in CVA.

We focused on MVA, being preferentially used for vaccine development, and WR, known to be the most virulent vaccinia strain in animal models [111, 112]. In human as well as in murine cells, MVA had an up-regulating effect on autophagy contrary to WR. A co-infection of MVA and WR resulted in a dominant negative effect mediated by WR, and emphasized its inhibitory impact on autophagy, which was also attributable to the other VACV strains. MVA is characterized by six major deletions, that affect genes encoding for host range and immune evasion factors. Due to replication deficiency of MVA in mammalian cells, it is self-evident that the virus is less virulent than WR. These may be the major reasons for the incapacity of MVA to overcome or manipulate the autophagy process for its own advantage. On the other side, WR has a completely autophagy-independent replication and survival capacity [96].

Therefore, it is intriguing to uncover the benefit WR has by inhibition of autophagy and also to elucidate the mechanism behind it.

5.2. Autophagy inhibition by WR is a process mediated early after infection

We further characterized the impact of VACV infection on autophagy. According to our findings, VACV interference with autophagy occurs at the early time phase of infection. The kinetic experiment revealed an up-regulation of LC3-lipidation within the first hours. The strongest inhibitory effect was observed at 4 hrs post WR infection. Beyond this time point, after the late phase has started [7, 113], the discrepancy between autophagy induction and repression was getting smaller, and LC3-lipidation upon WR infection was enhanced nearly as strong as in MVA-infected cells (**Supplementary figure 6**). Our presumptions were confirmed, when we observed that AraC treatment did not alter autophagy induction or inhibition in MVA- or WR-infected cells, respectively. AraC blocks DNA replication and disables the intermediate and late gene expression, while the early transcription machinery is actuated [114, 115]. Thus, the results implied the inhibition of autophagy to be mediated by early genes. Interestingly, it was also reported that within the first 2 hrs p.i., around half of VACV ORFs are expressed, including host immune modulatory factors [7, 113] and probably the inhibitory gene candidate we were looking for. Next, we analysed whether virus replication was required to efficiently stimulate autophagy. Surprisingly, there were no significant differences between cells infected with UV-inactivated or untreated MVA. However, UV-inactivated WR led to a significant up-regulation of autophagy, which remained below the induction observed in MVA-infected cells. UV-inactivated viral particles are still infectious, however they are not able to replicate and late, intermediate, as well as to some extend early genes (particularly large ones) are no longer expressed [103, 104]. Partial block of viral early genes justified the induction of autophagy upon infection with UV-inactivated WR and emphasize the role of an early gene for inhibition. To follow up on this, one could try to repress early gene expression and *de novo* protein synthesis by pre-incubating infected cells with cycloheximide and monitor whether autophagy is still induced [116]. In another assay, HeLa cells were subjected to the proteasome inhibitor MG132, which supplementary promoted LC3-lipidation after MVA infection or addition of rapamycin, two times higher than for cells without MG132. In line with these outcomes, MG132 was also reported to inhibit VACV intermediate and late gene expression [117]. Furthermore, proteasomal degradation and autophagy where described to have complementary functions. Hence, when proteasomes are blocked, their degradative function is taken over by autophagy and vice versa [118, 119]. We concluded the WR-mediated inhibition of autophagy

to be independent from intermediate and late gene expression, from viral replication, and to be mediated by early expressed gene products.

In a further approach, we addressed whether viral entry is required for autophagy induction, or if viral cell attachment is sufficient to induce autophagy. VACV internalization occurs via endocytosis that requires vacuolar and vesicular acidification or through fusion with the cellular plasma membrane [20, 120, 121]. By pre-treating cells with Bafilomycin A1, an endosomal acidification inhibitor, we were able to prevent VACV from entering host cells. Interestingly, VACV protein synthesis, which was used as an infection control, was not reduced in the presence of bafilomycin A1 neither for MVA nor for WR. A plausible explanation would be that the detected proteins were derived from viruses that were attached to the cells, but not necessarily internalized, and were lysed together with the cellular proteins. Bafilomycin A1 is also able to impede autolysosome formation and to block the autophagy flux [105]. In regard of MVA-infected cells, we would have expected an accumulation of LC3-II molecules superior to uninfected cells. However, the reduced up-regulation of autophagy in presence of MVA to the level of uninfected cells, claimed that the treatment was successful and was an additional proof for inefficient virus entry. Via confocal microscopy, one could test whether bafilomycin A1 treatment is really able to obstruct VACV entry, by infecting cells with an eGFP expressing virus, and tracking if it has successfully penetrated the cellular plasma membrane or not. Another possibility would be generation of fusion-deficient viruses, by mutating or deleting A27, D8 or H3 genes [122-125], which are involved in cellular attachment and full-length in MVA and WR [11], by using the CRISPR-Cas9 method for example. Collectively, these data show that influence of VACV on autophagy is an early phenomenon, which necessitates efficient virus entry.

5.3. Screening of CRISPR-Cas9 generated viral mutants did not deliver any potential candidate for autophagy interference

We selected twenty VACV encoded genes that might interfere with autophagy according to specific criteria: the gene had to be an early expressed one, which is encoded exclusively by WR and not by MVA. We screened the complete genome and picked those early genes, with known or unknown functions (**Supplementary figure 2**) [11, 126]. We engineered WR viral mutants using the CRISPR-Cas9 method. Among the 54 mutants that have been sequenced, 20% were resistant to mutagenesis (no changes in gene sequences), 6% displayed a single nucleotide exchange, 7% showed a 1-3 nucleotide insertion and 66% deletion of one nucleotide

up to a whole gene fragment. Additionally, five of the 20 selected and tested genes were reported to be essential and to be expressed in MVA as well as in WR [11, 127]. Nevertheless, we tried, but failed to generate mutants for these genes. Either the viruses were not replicating, or the resulting progeny did not exhibit mutations. These outcomes strongly emphasized the capacity of the virus to overcome the CRISPR-Cas9 machinery, if the respective gene is essentially required for its own survival and replication. Genome editing using the CRISPR-Cas9 method has been described to be very successful in organisms naturally expressing the system like bacteria (up to 100% efficacy) [128], however to vary between 2% and 38% efficiency in human cell lines [129, 130]. Recognition and cleavage of the target site via Cas9, introduces double strand break and repair through non-homologous end-joining. This process is error prone, and can lead to unspecific insertions, deletions or mutations [131, 132] as observed for our viral mutants. Though, we were struggling with another major issue throughout the assay. The sequencing results demonstrated that in nearly every case, we were dealing with a mixed virus population probably consisting of deletion mutants and wild type virus (**Supplementary figure 4**). This could be due to the fact that not all viral particles were adequately subjected to the CRISPR-Cas9 deletion procedure, if for example derived from cells, which have lost the expression plasmid. Regular selection procedures of the CRISPR-Cas9 transduced cells are therefore compulsory. Another plausible reason might be that the viruses have developed a resistance beyond the gene editing system with the passage of time and over the infection cycles, or have acquired a revertant phenotype as demonstrated for HIV-1 [133, 134] or HCMV [135]. Additionally, the forward and reverse sequences of the viral DNA showed nucleotide changes or deletions at distinct sites that did not coincide with each other (**Supplementary figure 4**). If taking into account that the non-homologous end-joining repair mechanism of the double strand break results in unpredictable insertions and deletions for every individual targeted gene [131, 132], it is understandable that the mutated genes would display heterogeneous nucleic acid sequences if compared to the reference. To overcome this problem, we started a clonal infection with one viral particle of the previously generated mutants based on a limiting dilution assay, and amplified the clones for final infection and screening. Although sequencing confirmed frameshift mutations, truncations or deletions in these mutant clones, we did not observe significant changes in the capacity of these mutants to stimulate autophagy. Altogether, the study did not deliver any inhibitory candidate for autophagy induction. Either the gene of interest has not been among the selected ones for mutagenesis, or the inhibition could be mediated by co-interaction of two or more genes. It is also probable that the inhibitory

function is redundant among the viral proteins, meaning that the function is taken over by another protein, when the gene of interest is deleted.

Disregarding the rapidity and simplicity of the CRISPR-Cas9 technique compared to e.g. homologous recombination, a strict quality control of mutants needs to be assured. Some genes might require more than one deletion to get fully functional knocked-down. This could be achieved by transfecting cells with two or more instead of one gRNA expressing plasmid, or by submitting the mutants having been generated using gRNA-1 to a second infection round in cells expressing gRNA-2 distinct from the originally used one. Through the CRISPR-Cas9 method it is also possible to generate deletions of two different genes simultaneously by following the same procedure as described [136]. Another idea would be to excise large fragments of the WR genome, relative to the six major deletions in MVA, or to consecutively reintroduce genome fragments into MVA and to look for autophagy interference. For future perspectives, we are planning to take the advantage of an automated, high-throughput siRNA screen, targeting early VACV mRNA, and to trace autophagy induction [137]. The cellular interaction partner can equally be identified by using a RNAi silencing screen for host cell factors [138].

5.4. VACV interferes with a non-canonical autophagy pathway, which is different from rapamycin-activated autophagy

While we were looking for an alternative method to identify the inhibitory gene candidate, we intended to perform a screen of a VACV ORF library by transfecting cells with plasmids expressing the respective gene candidates. Although we tried different cell lines and transfection reagents, we constantly observed a strong autophagy induction upon transfection with plasmid DNA, to a level that did not allow to differentiate between induction and inhibition anymore, which was a prerequisite for our assay. Thus, we sought for cellular receptors that recognize dsDNA and are related to autophagy. At that time, J. Chen lab discovered the cGAS-STING pathway for activation of IFN-I transcription [84]. This was followed by a number of publications, describing the implication of Atgs in regulation of cGAS-STING signalling cascade [89-91]. With the intention to use STING-deficient cells, in order to compass recognition of plasmid DNA and thus unspecific autophagy activation, we ascertained the MVA-mediated autophagy to be STING-dependent, but also to be different from the canonical and rapamycin-induced autophagy. Thus, in order to identify Atgs that could play a role in the VACV-dependent alternative autophagy pathway, we examined the requirement of ATG13 and

ULK1 molecules, which belong to the initiator complex of the rapamycin-induced autophagy machinery [44-46]. Interestingly, neither ATG13 nor ULK1, nor its homolog ULK2 [139] seemed to be essential for the MVA-mediated autophagy. However, LC3-lipidation in rapamycin-treated MEF ULK1/2-/- cells was slightly but not significantly reduced. Interestingly, two further variants ULK3 and ULK4 have been described to exist in mammalian cells, with a sequence similarity of 52% and 41% respectively to the ULK1 kinase region [140]. Since ULK3 is able to activate autophagy upon amino acid and serum depletion [141] it is possible that rapamycin induces autophagy via ULK3 in MEFs ULK1/2-/-, however the actual mechanism has to be investigated in greater detail. To rule out the requirement of ULK1 for activation of alternative autophagy, one should analyse the autophagy flux by inhibiting autolysosme formation via bafilomycin A1 [105] and assess if MVA and rapamycin still induce autophagy. One could also test whether the analysed expression of LC3 is related to normal or aberrant formation of autophagosomes, and track other autophagy markers like p62 [142] or WIPI2 (WD repeat domain phosphoinositide-interacting protein 2) [143]. These results might also give more certainty regarding role of ULK1 in the cGAS-STING pathway upon VACV infection [91].

Our hypothesis of VACV to interfere with an alternative autophagy pathway was strengthened, when we observed that in rapamycin-treated and WR-infected HeLa cells autophagy was not blocked anymore, although in previous experiments we clearly demonstrate the dominant negative effect of WR over MVA. In contrast, for cells which were treated with 3-MA and additionally infected with MVA, we would have expected the 3-MA inhibitory effect to prevail, especially because the chemical operates relatively at the beginning of the autophagy cascade [144], which however was not the case. These results clearly emphasize VACV and the tested reagents to act on distinct autophagy pathways.

So far, two alternative autophagy pathways have been described: the Beclin-1-independent [145-147] and the Atg5/Atg7-independent autophagy [148]. Latter is reported to require ULK1, but to be LC3-independent and therefore can be excluded from being the pathway we are interested in [149]. Though, the Beclin-1-independent autophagy was declared to be 3-MA insensitive [148], which would correlate with our findings, since 3-MA and MVA infection together did not down-regulate LC3-lipidation. Moreover, proteasome inhibitors like MG132 were demonstrated to further activate the Beclin-1-independent autophagy in ovarian cancer cells [150], which again would be conform to our results, in which MVA-mediated autophagy was fostered after MG132 treatment. Both alternative pathways can be inhibited via brefeldin A, without impacting canonical autophagy [151], which might deliver further proofs. Thus, one

should be careful when using this reagent, since it was notified to block production of VACV EVs, but to have no influence on intracellular MVs [152].

We also thought about the ability of VACV to enhance LC3-associated phagocytosis (LAP), a process which is triggered following phagocytosis, wherein LC3 is conjugated to phagosomes through autophagy proteins [153-156]. LAP is activated by TLR recognition of pathogens [153, 157]. Contrary to the conventional autophagy pathway, LAP does not require the pre-initiation complex composed of ULK1, ATG13 and FIP200 [157-159], but necessitates expression of Beclin-1, Atg7 and Atg5 [153, 160], which would coincide with our results. Additionally, Martinez *et al*. [161] observed that silencing of Rubicon promoted autophagy-related LC3-lipidation, while recruitment of LC3 molecules to LAP-phagosomes was abolished. These findings exhibited Rubicon to negatively regulate autophagy, but to be essential for LAP [161]. One more feature of LAP is the formation of single membrane phagosomes, different from the double-membraned autophagosomes [153, 160], that could be investigated via correlative light and electron microscopy, a method which unifies light and electron microscopy together and facilitates study of membranous structures [156, 162].

Last, Moloughney *et al*. emphasized the VACV-induced LC3-lipidation to be Atg5/Atg7-independent [95], but similarly to Zhang *et al*., autophagy not to be required for VACV replication [95, 96]. However, these results would rather argue for the use of an alternative autophagy pathway, or VACV to encode for Atg homologs.

5.5. Is MVA-mediated autophagy responsible for STING degradation?

While we were exploring the role of STING in relation to autophagy, we observed a complete degradation of STING upon MVA infection. This process turned out to occur early, because addition of AraC or infection with PUVA-virus did not prevent STING from being degraded. However, it was unclear how and why the degradation is taking place, since in WR-infected cells STING protein was intact. We very quickly could deny canonical autophagy to be responsible for STING degradation, as in 3-MA-treated and MVA-infected cells STING protein stability was not restored. Next, we inspected the possibility of STING to be targeted by proteasomes, since the ubiquitin-ligase RNF5 was described to cause STING degradation (**Figure 27**) [107]. In this regard, RNF5 was also shown to regulate autophagy by controlling stability of ATG4B ligase, and thus to limit LC3-II formation [163]. Treatment of HeLa cells with the proteasome inhibitor MG132 did not spare STING from being degraded, which likely refutes RNF5 to be at the origin of STING degradation.

Furthermore, we studied the role of the VACV protein N1L, which is truncated in MVA but full-length in WR [11]. Expression of that gene was previously reported to inhibit NF-κB and IRF3 activation by binding to TBK1 [93], and thus to interfere with the cGAS-STING pathway, having a down-regulatory effect on IFN-I production [92]. Due to its Bcl-2-like structure, N1L could also have been a potential candidate for autophagy interference. Members of the Bcl-2 family have been shown to indirectly affect autophagy activation. However, with did not see any differences concerning LC3-lipidation or STING degradation in presence or absence of N1L (**Figure 27**).

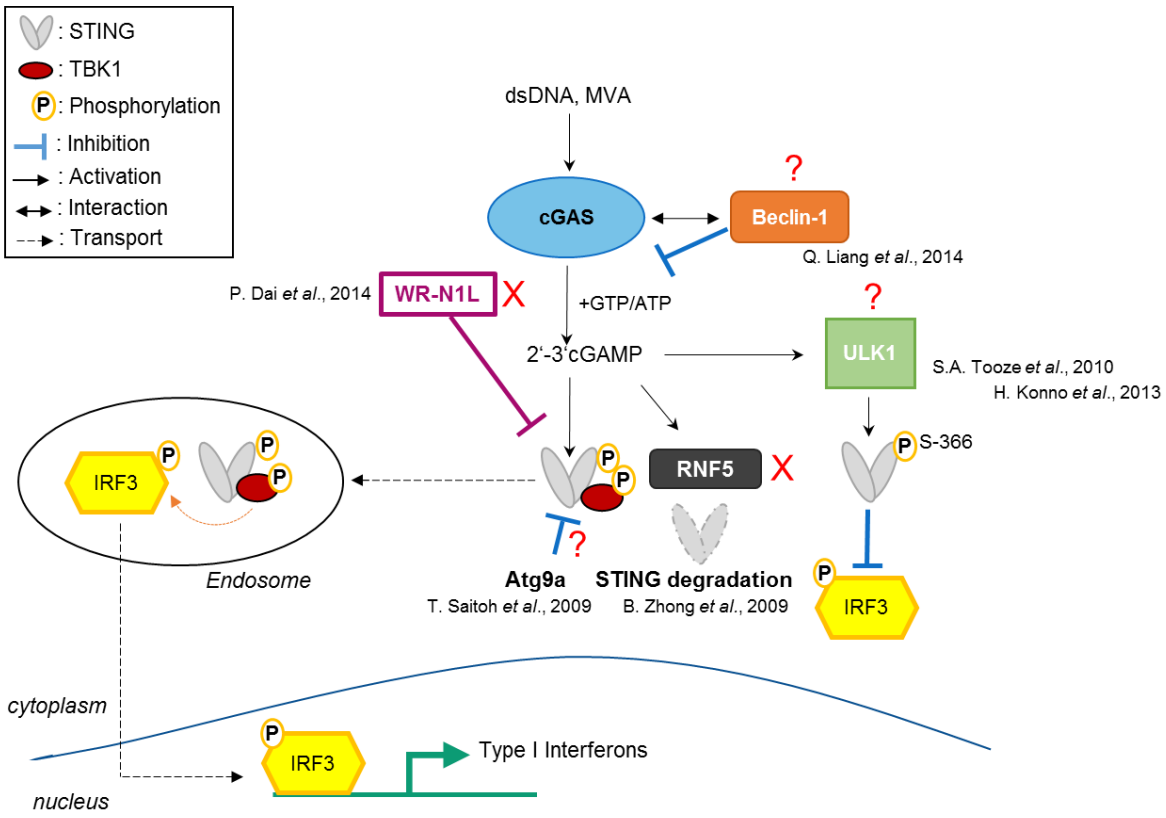

Figure 27: Autophagy related trafficking and degradation of STING. STING is activated via cGAMP produced by cGAS after recognition of dsDNA. TBK1 is recruited to STING and traffics to IRF3 harbouring endosomes. Thus, the phosphorylated IRF3 is translocated into the nucleus to initiate IFN-I transcription and translation. Autophagy related genes like Atg9a, ULK1 or Beclin-1, as well as the ubiquitin ligase RNF5 are implicated into regulation of IFN-I synthesis via a negative feedback-loop. VACV is able to inhibit STING activation through N1L protein, which abolishes IFN-I production. "X" indicates the pathways that have already been investigated, while "?" stands for those that still have to be more intensely examined.

Still, we did not elucidate whether and how non-canonical VACV-dependent autophagy could be related to STING degradation. One could test this by treating infected cells with chloroquine, which prevents endosomal acidification and autolysosme formation [164], without affecting VACV infection [165]. Thus, in a first experiment STING was still degraded in the presence of

chloroquine in MVA-infected cells, which however has to be confirmed and repeated with increasing dosage (**Supplementary figure 7**). Nevertheless, there are numerous other degradative mechanisms that need to be considered.

Neddylation is a post-translational protein modification, which is closely related to ubiquitination with a sequence similarity of 76% [166]. This mechanism occurs through conjugation of NEDD8 to its substrate e.g. cullins, which in turn are molecular scaffold proteins for E3-ubiquitin ligases [167] and implicated in many regulatory processes, including VACV infection [138]. Neddylation of cullins in the cullin-RING-E3 ligase mediates proteolysis of the target protein [168]. Interestingly, NEDD8 inhibitor MLN4924 was characterized to stimulate autophagy to rescue cell from MLN4924 induced apoptosis [169, 170]. One could use this inhibitor, to analyse the relevance of neddylation for STING degradation.

Another possibility could be STING degradation via calpains, which are calcium-dependent, non-lysosomal cysteine proteases [171-173]. Calpains mainly recognize the overall tertiary structure of their substrate instead of direct amino acid sequences [174, 175]. Calpain activity can be easily tracked by using commercially available kits, constituted of a substrate bound to a fluorogenic molecule that upon calpain cleavage gets released and activated. Additionally, different computational softwares for calpain cleavage prediction sites are available. Analysis of the STING amino acid sequence resulted in 11 potential cleavage sites for the human protein (**Figure 28A**), and 8 sites for murine STING (**Figure 28B**), if using a high threshold with a high substrate specificity fixed to 95% [176]. Thus, it is worth to test whether calpains play a role in STING degradation.

A

Predicted Sites

Position	Peptide
5	*****MPHSS|LHPS
269	EYATPLQTLF|AMSQ
274	LQTLFAMSQY|SQAG
344	QEEKEEVTVG|SLKT
347	KEEVTVGSLK|TSAV
349	EVTVGSLKTS|AVPS
352	VGSLKTSAVP|STST
354	SLKTSAVPST|STMS
355	LKTSAVPSTS|TMSQ
357	TSAVPSTSTM|SQEP
358	SAVPSTSTMS|QEPE

B

Predicted Sites

Position	Peptide
268	EYATPLQTLF|AMSQ
341	IRQEEKEEVT|MNAP
343	QEEKEEVTMN|APMT
347	EEVTMNAPMT|SVAP
348	EVTMNAPMTS|VAPP
349	VTMNAPMTSV|APPP
350	TMNAPMTSVA|PPPS
357	SVAPPPSVLS|QEPR

Figure 28: Prediction of calpain restriction sites for targeting STING molecules. A. Prediction of calpain restriction sites for A. human STING sequence and B. for murine STING sequence, using a high threshold for increased calpain specificity. Software was downloaded from following website: http://ccd.biocuckoo.org/.

Although we were not able to identify the source of STING degradation, there are different opportunities that still have to be explored. Even if the original degradation machinery would be successfully inhibited and identified, it could be possible that another proteolytic pathway gets activated, which would make it difficult to understand how and why STING is degraded.

5.6. cGAMP is required for STING degradation, but not specifically for autophagy induction

Upon recognition of dsDNA via cGAS, 2'3'-cGAMP binds and activates STING, which escorts TBK1 to IRF3 to trigger IFN-I transcription [83-88] (**Figure 27**). It is reported, that viruses are able to encapsulate cGAMP from the originally infected cell, and to transmit it to the next target cell to activate STING independently from recogniton of viral DNA [108, 109]. We queried whether this is also true for MVA and enough to promote STING degradation. Therefore, we transfected HeLa cells with plasmid DNA, synthetic 2'3'-cGAMP or with a cGAMP agonist. LC3-lipidation was significantly induced, with no differences between plasmid DNA, cGAMP or cGAMP agonist transfected or incubated cells, showing that autophagy is not specifically activated by cGAMP but stimulated as soon as foreign substrates enter the cell. Hence, we were quite surprised to see that transfection with cGAMP did not cause STING degradation. A plausible explanation could be that cGAMP concentration of 1 µg/ml was way too low, as it was seven times below the required cGAMP concentration of 10 nM, which was reported to deliver robust IFN-β mRNA levels [83]. Incubation with 20 µg/ml cGAMP, which corresponds to 28.5 nM, provoked clear STING degradation, which was not the case when incubating with cGAMP agonist. These results assume two options: STING degradation occurs either directly after cGAS recognition of dsDNA from MVA, or via cGAMP delivered by MVA. It is also obvious, that STING degradation proceeds after the molecule has been activated. Although cGAMP is important for STING degradation, it is not a prerequisite for autophagy stimulation.

Still, the inhibitory factor which prevents STING from being degraded in WR-infected cells, needs to be identified. DNA-tumor oncogenes were described to encode for proteins that are able to block the cGAS-STING pathway. Proteins with the consensus motif LXCXE, where X stands for any other amino acid, are implied in antagonizing STING [177]. We identified two VACV proteins with that consensus motif, namely WR204 and H4L. WR204 is an early expressed gene and a member of the serine protease inhibitor (SPI)-1 family [178], while essential H4L is late expressed and presumably incorporated in the virion, since it belongs to

the early transcription machinery [179]. However both genes are expressed in MVA and WR [11], and can therefore be excluded from being responsible for STING degradation.

5.7. Concluding remarks

Without doubt, VACV infection impacts autophagy as well as the cGAS-STING pathway. While autophagy is induced and STING is degraded after MVA infection, we observed a total inhibition of autophagy and stabilization of STING upon WR infection. MVA-mediated stimulation of autophagy is independent from viral DNA replication, but requires efficient virus entry. Still, the inhibitory mechanism is not fully scrutinized. We unveiled a temporal overlap between STING degradation and onset of autophagy, but up to now were not able to find a direct link between these two processes. Autophagy related genes like Beclin-1 or ULK1, remain to be investigated in regard of the cGAS-STING pathway, although ULK1 has already been shown not to be required for VACV-dependent alternative autophagy.

A similar phenomenon was observed in α-herpesviruses, for which autophagy activation was transmitted through recognition of dsDNA via the cGAS-STING pathway [180]. Likewise, detection of mycobacterium tuberculosis by cGAS was accompanied by enhanced autophagy [181]. Hence, it seems to be a commonly active process related to DNA pathogens.

Due to its antiviral activity, autophagy can easily negatively impact the efficacy of vaccines. By gaining deeper knowledge on how VACV interferes with autophagy, we would be able to characterize how and to which level antigen presentation is affected. Accordingly, one could inhibit the non-canonical autophagy pathway without affecting the host's cellular homeostasis that might be required for other crucial regualtory functions.

6. Appendix

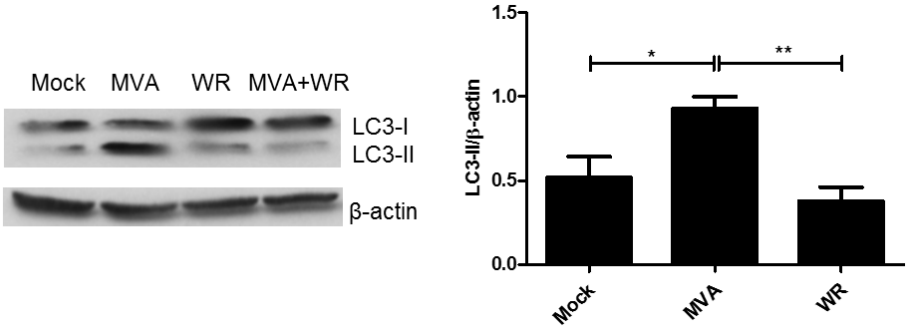

Supplementary figure 1: Impact of VACV infection on autophagy induction in J774 cells. J774 cells were infected with MVA or WR at MOI 10. The cells were harvested at 8 hrs p.i. for immunoblot analysis (n=4).

Name	Gene expression	VV-mutant	function
A50R	early	1, 2, 3	DNA ligase gene [182]
G5R	early	4, 5, 6	hypothetical protein
H5R	early, intermediate, late	7, 8, 9	late transcription factor [183]
A51R	early	10, 11, 12	hypothetical protein
A52R	early	13, 14	MyD88 homolog [184, 185]
B20R	unknown	15, 16, 17	ankyrin-like protein
C19L	unknown	18, 19 20	ankyrin-like protein
C9.5L	unknown	21, 22, 23	ankyrin repeat protein
VV_WR_015	unknown	24, 25, 26	ankyrin repeat protein
VV_WR_016	unknown	27, 28, 29	ankyrin repeat protein
C2L	unknown	30, 31, 32	intracellular kelch protein homolog [186]
M1L	early	33, 34, 35	ankyrin-like protein
I3L	early, intermediate	36, 37, 38	DNA-binding phosphoprotein
I6L	unknown	39, 40, 41	hypothetical protein
K7R	unknown	42, 43	Suppressor of DDX3-mediated IRF activation and INFβ promoter induction [187]
L2R	early	44, 45, 46	hypothetical protein
VV_WR_017	unknown	47, 48	ankyrin repeat protein
VV_WR_011	early	49, 50, 51	zinc finger-like protein
F16L	early	52, 53, 54	hypothetical protein
J2R	early	55, 56, 27	thymidine-kinase

Supplementary figure 2: Selection of 20 potential viral gene candidates for autophagy interference. VACV genes were selected according to their expression profile (early), function and to their exclusive expression in WR strain (not MVA). The red highlighted genes turned out to be essential and to be expressed in MVA and WR [11]. For every gene 2-3 mutants were generated.

Supplementary figure 3: Sequencing results for WR-ΔA50R_2 deletion mutant. The results are representative for sequences from other deletion mutants. **A.** Viral DNA was sent after PCR for sequencing using forward and reverse primers binding close to CRISPR region, which is indicated in the red frame. ^{X} shows nucleotides, which were simultaneously deleted in the forward and reverse DNA strand. **B.** Amino acid sequence after deletion of ^{XX} nucleotides (A50R deletion), resulted in an early stop codon (*) and therefore encoded for a truncated and non-functional protein.

Supplementary figure 4: Sequencing results for WR-ΔC19L_20 deletion mutant. These results are representative for sequences from DNA isolated from a sample with mixed virus populations. Viral DNA was sent after PCR for sequencing using forward and reverse primers binding close to CRISPR region, which is indicated in the red frame. Nucleotide deletions occurred at different sites, which did not coincide with each other in the forward and reverse strand.

Supplementary figure 5: Sequencing results for WR-ΔC2L_31 deletion mutant. These results are representative for sequences from mutants with a clear deletion. **A.** Viral DNA was sent after PCR for sequencing using forward and reverse primers binding close to the CRISPR region, which is indicated in the red frame. [X] shows nucleotides, which were simultaneously deleted in the forward and reverse DNA strand. B. Amino acid sequence after deletion of the single nucleotide (C2L deletion), resulted in a frameshift and early stop codon (*) and therefore encoded for a truncated and most likely non-functional protein.

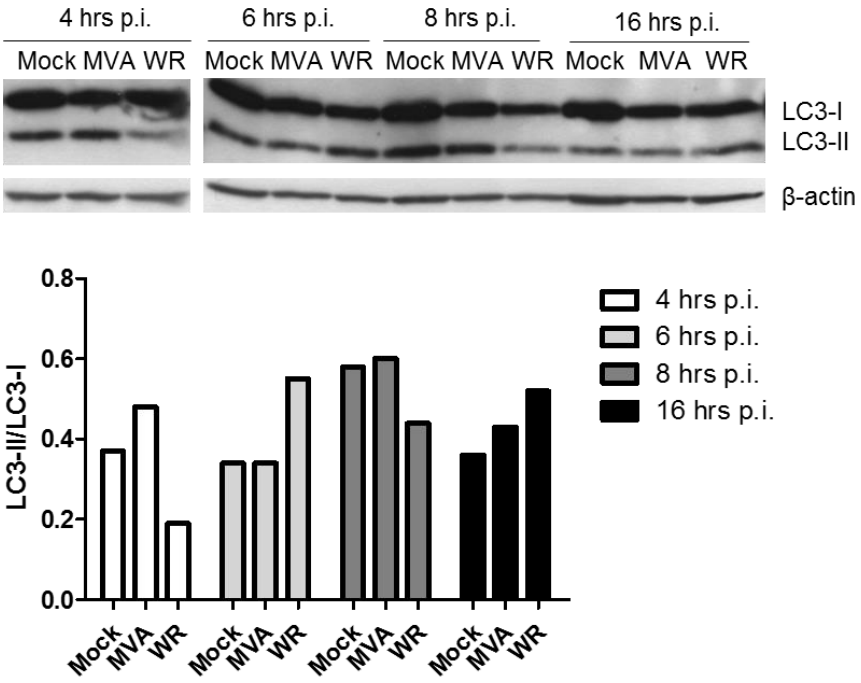

Supplementary figure 6: Increase of LC3-lipidation as WR infection proceeds. HeLa cells were infected with MVA or WR at MOI 10 and were harvested at the indicated time points for immunoblot analysis. (n=1).

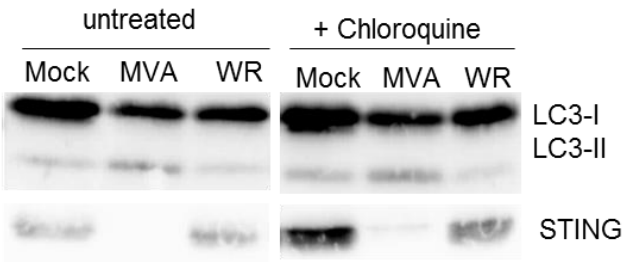

Supplementary figure 7: STING is probably not degraded by lysosomal activity. HeLa cells were infected with MVA at MOI 20 or WR at MOI 10 and were either left untreated or were additionally treated with 50 µM chloroquine. The cells were harvested at 4 hrs p.i. for immunoblot analysis.

7. References

1. Meyer, H., G. Sutter, and A. Mayr, *Mapping of deletions in the genome of the highly attenuated vaccinia virus MVA and their influence on virulence.* J Gen Virol, 1991. **72 (Pt 5)**: p. 1031-8.

2. Dengjel, J., et al., *Autophagy promotes MHC class II presentation of peptides from intracellular source proteins.* Proc Natl Acad Sci U S A, 2005. **102**(22): p. 7922-7.

3. Nimmerjahn, F., et al., *Major histocompatibility complex class II-restricted presentation of a cytosolic antigen by autophagy.* Eur J Immunol, 2003. **33**(5): p. 1250-9.

4. Thiele, F., et al., *Modified vaccinia virus Ankara-infected dendritic cells present CD4+ T-cell epitopes by endogenous major histocompatibility complex class II presentation pathways.* J Virol, 2015. **89**(5): p. 2698-709.

5. Lefkowitz, E.J., C. Wang, and C. Upton, *Poxviruses: past, present and future.* Virus Res, 2006. **117**(1): p. 105-18.

6. Moutaftsi, M., et al., *Uncovering the interplay between CD8, CD4 and antibody responses to complex pathogens.* Future Microbiol, 2010. **5**(2): p. 221-39.

7. Moss, B., *Poxviridae: The Viruses and Their Replication*. Fields' Virology, ed. L.W.a. Wilkins. 2007, USA.

8. Henderson DA, M.B., *Smallpox and Vaccinia* Vaccines, ed. O. Plotkin. Vol. 3rd edition. 1999, Philadelphia.

9. Bazin, H., *The Eradication of Smallpox*, ed. A. Press. Vol. 1st Edition. 1999, London.

10. Moss, B., *Vaccinia virus: a tool for research and vaccine development.* Science, 1991. **252**(5013): p. 1662-7.

11. Antoine, G., et al., *The complete genomic sequence of the modified vaccinia Ankara strain: comparison with other orthopoxviruses.* Virology, 1998. **244**(2): p. 365-96.

12. Drexler, I., C. Staib, and G. Sutter, *Modified vaccinia virus Ankara as antigen delivery system: how can we best use its potential?* Curr Opin Biotechnol, 2004. **15**(6): p. 506-12.

13. Drexler, I., et al., *Highly attenuated modified vaccinia virus Ankara replicates in baby hamster kidney cells, a potential host for virus propagation, but not in various human transformed and primary cells.* J Gen Virol, 1998. **79 (Pt 2)**: p. 347-52.

14. Bengali, Z., P.S. Satheshkumar, and B. Moss, *Orthopoxvirus species and strain differences in cell entry.* Virology, 2012. **433**(2): p. 506-12.

15. Bengali, Z., et al., *Drosophila S2 cells are non-permissive for vaccinia virus DNA replication following entry via low pH-dependent endocytosis and early transcription.* PLoS One, 2011. **6**(2): p. e17248.

16. Smith, G.L., A. Vanderplasschen, and M. Law, *The formation and function of extracellular enveloped vaccinia virus.* J Gen Virol, 2002. **83**(Pt 12): p. 2915-31.

17. Gallego-Gomez, J.C., et al., *Differences in virus-induced cell morphology and in virus maturation between MVA and other strains (WR, Ankara, and NYCBH) of vaccinia virus in infected human cells.* J Virol, 2003. **77**(19): p. 10606-22.

18. Sutter, G. and B. Moss, *Nonreplicating vaccinia vector efficiently expresses recombinant genes.* Proc Natl Acad Sci U S A, 1992. **89**(22): p. 10847-51.

19. Bengali, Z., A.C. Townsley, and B. Moss, *Vaccinia virus strain differences in cell attachment and entry.* Virology, 2009. **389**(1-2): p. 132-40.

20. Carter, G.C., et al., *Entry of the vaccinia virus intracellular mature virion and its interactions with glycosaminoglycans.* J Gen Virol, 2005. **86**(Pt 5): p. 1279-90.

21. Whitbeck, J.C., et al., *Vaccinia virus exhibits cell-type-dependent entry characteristics.* Virology, 2009. **385**(2): p. 383-91.

22. Payne, L.G., *Significance of extracellular enveloped virus in the in vitro and in vivo dissemination of vaccinia.* J Gen Virol, 1980. **50**(1): p. 89-100.

23. Smith, G.L., B.J. Murphy, and M. Law, *Vaccinia virus motility.* Annu Rev Microbiol, 2003. **57**: p. 323-42.

24. Schmidt, F.I., C.K. Bleck, and J. Mercer, *Poxvirus host cell entry.* Curr Opin Virol, 2012. **2**(1): p. 20-7.

25. Mercer, J. and A. Helenius, *Vaccinia virus uses macropinocytosis and apoptotic mimicry to enter host cells.* Science, 2008. **320**(5875): p. 531-5.

26. Schmidt, F.I., et al., *Vaccinia extracellular virions enter cells by macropinocytosis and acid-activated membrane rupture.* Embo j, 2011. **30**(17): p. 3647-61.

27. Moss, B., *Poxvirus cell entry: how many proteins does it take?* Viruses, 2012. **4**(5): p. 688-707.

28. Cairns, J., *The initiation of vaccinia infection.* Virology, 1960. **11**: p. 603-23.

29. Dahl, R. and J.R. Kates, *Intracellular structures containing vaccinia DNA: isolation and characterization.* Virology, 1970. **42**(2): p. 453-62.

30. Broyles, S.S., *Vaccinia virus transcription.* J Gen Virol, 2003. **84**(Pt 9): p. 2293-303.

31. Roberts, K.L. and G.L. Smith, *Vaccinia virus morphogenesis and dissemination.* Trends Microbiol, 2008. **16**(10): p. 472-9.

32. Ashford, T.P. and K.R. Porter, *Cytoplasmic components in hepatic cell lysosomes.* J Cell Biol, 1962. **12**: p. 198-202.

33. Klionsky, D.J., et al., *A unified nomenclature for yeast autophagy-related genes.* Dev Cell, 2003. **5**(4): p. 539-45.

34. Thumm, M., et al., *Isolation of autophagocytosis mutants of Saccharomyces cerevisiae.* FEBS Lett, 1994. **349**(2): p. 275-80.

35. Tsukada, M. and Y. Ohsumi, *Isolation and characterization of autophagy-defective mutants of Saccharomyces cerevisiae.* FEBS Lett, 1993. **333**(1-2): p. 169-74.

36. Ravikumar, B., et al., *Regulation of mammalian autophagy in physiology and pathophysiology.* Physiol Rev, 2010. **90**(4): p. 1383-435.

37. Choi, A.M., S.W. Ryter, and B. Levine, *Autophagy in human health and disease.* N Engl J Med, 2013. **368**(7): p. 651-62.

38. Khatif, H.D., I *Autophagy and Its Implication in Antiviral Immunity.* SOJ Immunol, 2014. **2(2): 1-8**: p. Page 2 of 8.

39. Arsham, A.M. and T.P. Neufeld, *Thinking globally and acting locally with TOR.* Curr Opin Cell Biol, 2006. **18**(6): p. 589-97.

40. Bhaskar, P.T. and N. Hay, *The two TORCs and Akt.* Dev Cell, 2007. **12**(4): p. 487-502.

41. Lee, C.H., K. Inoki, and K.L. Guan, *mTOR pathway as a target in tissue hypertrophy.* Annu Rev Pharmacol Toxicol, 2007. **47**: p. 443-67.

42. Sarbassov, D.D., S.M. Ali, and D.M. Sabatini, *Growing roles for the mTOR pathway.* Curr Opin Cell Biol, 2005. **17**(6): p. 596-603.

43. Pattingre, S., et al., *Regulation of macroautophagy by mTOR and Beclin 1 complexes.* Biochimie, 2008. **90**(2): p. 313-23.

44. Ganley, I.G., et al., *ULK1.ATG13.FIP200 complex mediates mTOR signaling and is essential for autophagy.* J Biol Chem, 2009. **284**(18): p. 12297-305.

45. Hosokawa, N., et al., *Nutrient-dependent mTORC1 association with the ULK1-Atg13-FIP200 complex required for autophagy.* Mol Biol Cell, 2009. **20**(7): p. 1981-91.

46. Jung, C.H., et al., *ULK-Atg13-FIP200 complexes mediate mTOR signaling to the autophagy machinery.* Mol Biol Cell, 2009. **20**(7): p. 1992-2003.

47. Mercer, C.A., A. Kaliappan, and P.B. Dennis, *A novel, human Atg13 binding protein, Atg101, interacts with ULK1 and is essential for macroautophagy.* Autophagy, 2009. **5**(5): p. 649-62.

48. Hosokawa, N., et al., *Atg101, a novel mammalian autophagy protein interacting with Atg13.* Autophagy, 2009. **5**(7): p. 973-9.

49. Itakura, E., et al., *Beclin 1 forms two distinct phosphatidylinositol 3-kinase complexes with mammalian Atg14 and UVRAG.* Mol Biol Cell, 2008. **19**(12): p. 5360-72.

50. Sun, Q., et al., *Identification of Barkor as a mammalian autophagy-specific factor for Beclin 1 and class III phosphatidylinositol 3-kinase.* Proc Natl Acad Sci U S A, 2008. **105**(49): p. 19211-6.

51. Kadowaki, M. and M.R. Karim, *Cytosolic LC3 ratio as a quantitative index of macroautophagy.* Methods Enzymol, 2009. **452**: p. 199-213.

52. Barth, S., D. Glick, and K.F. Macleod, *Autophagy: assays and artifacts.* The Journal of pathology, 2010. **221**(2): p. 117-124.

53. Paludan, C., et al., *Endogenous MHC class II processing of a viral nuclear antigen after autophagy.* Science, 2005. **307**(5709): p. 593-6.

54. Donaldson, J.G. and D.B. Williams, *Intracellular assembly and trafficking of MHC class I molecules.* Traffic, 2009. **10**(12): p. 1745-52.

55. English, L., et al., *Autophagy enhances the presentation of endogenous viral antigens on MHC class I molecules during HSV-1 infection.* Nat Immunol, 2009. **10**(5): p. 480-7.

56. Tey, S.K. and R. Khanna, *Autophagy mediates transporter associated with antigen processing-independent presentation of viral epitopes through MHC class I pathway.* Blood, 2012. **120**(5): p. 994-1004.

57. Bevan, M.J., *Cross-priming.* Nat Immunol, 2006. **7**(4): p. 363-5.

58. Joffre, O.P., et al., *Cross-presentation by dendritic cells.* Nat Rev Immunol, 2012. **12**(8): p. 557-69.

59. Rock, K.L. and L. Shen, *Cross-presentation: underlying mechanisms and role in immune surveillance.* Immunol Rev, 2005. **207**: p. 166-83.

60. Blander, J.M., *The comings and goings of MHC class I molecules herald a new dawn in cross-presentation.* Immunol Rev, 2016. **272**(1): p. 65-79.

61. Li, Y., et al., *Efficient cross-presentation depends on autophagy in tumor cells.* Cancer Res, 2008. **68**(17): p. 6889-95.

62. Li, H., et al., *Alpha-alumina nanoparticles induce efficient autophagy-dependent cross-presentation and potent antitumour response.* Nat Nanotechnol, 2011. **6**(10): p. 645-50.

63. De Luca, A., et al., *CD4(+) T cell vaccination overcomes defective cross-presentation of fungal antigens in a mouse model of chronic granulomatous disease.* J Clin Invest, 2012. **122**(5): p. 1816-31.

64. Loi, M., et al., *Macroautophagy Proteins Control MHC Class I Levels on Dendritic Cells and Shape Anti-viral CD8(+) T Cell Responses.* Cell Rep, 2016. **15**(5): p. 1076-87.

65. Loi, M., M. Gannage, and C. Munz, *ATGs help MHC class II, but inhibit MHC class I antigen presentation.* Autophagy, 2016: p. 0.

66. Neefjes, J., et al., *Towards a systems understanding of MHC class I and MHC class II antigen presentation.* Nat Rev Immunol, 2011. **11**(12): p. 823-36.

67. Vyas, J.M., A.G. Van der Veen, and H.L. Ploegh, *The known unknowns of antigen processing and presentation.* Nat Rev Immunol, 2008. **8**(8): p. 607-18.

68. Crotzer, V.L. and J.S. Blum, *Autophagy and adaptive immunity.* Immunology, 2010. **131**(1): p. 9-17.

69. Kim, H.J., S. Lee, and J.U. Jung, *When autophagy meets viruses: a double-edged sword with functions in defense and offense.* Semin Immunopathol, 2010. **32**(4): p. 323-41.

70. Dongre, A.R., et al., *In vivo MHC class II presentation of cytosolic proteins revealed by rapid automated tandem mass spectrometry and functional analyses.* Eur J Immunol, 2001. **31**(5): p. 1485-94.

71. Schmid, D., M. Pypaert, and C. Munz, *Antigen-loading compartments for major histocompatibility complex class II molecules continuously receive input from autophagosomes.* Immunity, 2007. **26**(1): p. 79-92.

72. Berg, T.O., et al., *Isolation and characterization of rat liver amphisomes. Evidence for fusion of autophagosomes with both early and late endosomes.* J Biol Chem, 1998. **273**(34): p. 21883-92.

73. Kondylis, V., et al., *Endosome-mediated autophagy: an unconventional MIIC-driven autophagic pathway operational in dendritic cells.* Autophagy, 2013. **9**(6): p. 861-80.

74. Reed, M., et al., *Autophagy-Inducing Protein Beclin-1 in Dendritic Cells Regulates CD4 T Cell Responses and Disease Severity during Respiratory Syncytial Virus Infection.* J Immunol, 2013.

75. Jiang, Y., et al., *Dendritic Cell Autophagy Contributes to Herpes Simplex Virus-Driven Stromal Keratitis and Immunopathology.* MBio, 2015. **6**(6): p. e01426-15.

76. Swain, S.L., K.K. McKinstry, and T.M. Strutt, *Expanding roles for CD4(+) T cells in immunity to viruses.* Nat Rev Immunol, 2012. **12**(2): p. 136-48.

77. Janeway, C.A., Jr., *The priming of helper T cells.* Semin Immunol, 1989. **1**(1): p. 13-20.

78. Lee, H.K., et al., *In vivo requirement for Atg5 in antigen presentation by dendritic cells.* Immunity, 2010. **32**(2): p. 227-39.

79. Akira, S. and K. Takeda, *Toll-like receptor signalling.* Nat Rev Immunol, 2004. **4**(7): p. 499-511.

80. Shi, C.S. and J.H. Kehrl, *MyD88 and Trif target Beclin 1 to trigger autophagy in macrophages.* J Biol Chem, 2008. **283**(48): p. 33175-82.

81. Xu, Y., et al., *Toll-like receptor 4 is a sensor for autophagy associated with innate immunity.* Immunity, 2007. **27**(1): p. 135-44.

82. Delgado, M.A., et al., *Toll-like receptors control autophagy.* Embo j, 2008. **27**(7): p. 1110-21.

83. Wu, J., et al., *Cyclic-GMP-AMP Is An Endogenous Second Messenger in Innate Immune Signaling by Cytosolic DNA.* Science (New York, N.Y.), 2013. **339**(6121): p. 10.1126/science.1229963.

84. Sun, L., et al., *Cyclic GMP-AMP Synthase is a Cytosolic DNA Sensor that Activates the Type-I Interferon Pathway.* Science (New York, N.Y.), 2013. **339**(6121): p. 10.1126/science.1232458.

85. Burdette, D.L., et al., *STING is a direct innate immune sensor of cyclic-di-GMP.* Nature, 2011. **478**(7370): p. 515-518.

86. Ishikawa, H. and G.N. Barber, *STING is an endoplasmic reticulum adaptor that facilitates innate immune signalling.* Nature, 2008. **455**(7213): p. 674-8.

87. Ishikawa, H., Z. Ma, and G.N. Barber, *STING regulates intracellular DNA-mediated, type I interferon-dependent innate immunity.* Nature, 2009. **461**(7265): p. 788-92.

88. Abe, T., et al., *STING recognition of cytoplasmic DNA instigates cellular defense.* Mol Cell, 2013. **50**(1): p. 5-15.

89. Saitoh, T., et al., *Atg9a controls dsDNA-driven dynamic translocation of STING and the innate immune response.* Proceedings of the National Academy of Sciences of the United States of America, 2009. **106**(49): p. 20842-20846.

90. Liang, Q., et al., *Crosstalk between the cGAS DNA sensor and Beclin-1 autophagy protein shapes innate antimicrobial immune responses.* Cell Host Microbe, 2014. **15**(2): p. 228-38.

91. Konno, H., K. Konno, and G.N. Barber, *Cyclic dinucleotides trigger ULK1 (ATG1) phosphorylation of STING to prevent sustained innate immune signaling.* Cell, 2013. **155**(3): p. 688-98.

92. Dai, P., et al., *Modified vaccinia virus Ankara triggers type I IFN production in murine conventional dendritic cells via a cGAS/STING-mediated cytosolic DNA-sensing pathway.* PLoS Pathog, 2014. **10**(4): p. e1003989.

93. DiPerna, G., et al., *Poxvirus protein N1L targets the I-kappaB kinase complex, inhibits signaling to NF-kappaB by the tumor necrosis factor superfamily of receptors, and inhibits NF-kappaB and IRF3 signaling by toll-like receptors.* J Biol Chem, 2004. **279**(35): p. 36570-8.

94. Levine, B., N. Mizushima, and H.W. Virgin, *Autophagy in immunity and inflammation.* Nature, 2011. **469**(7330): p. 323-35.

95. Moloughney, J.G., et al., *Vaccinia virus leads to ATG12-ATG3 conjugation and deficiency in autophagosome formation.* Autophagy, 2011. **7**(12): p. 1434-47.

96. Zhang, H., et al., *Cellular autophagy machinery is not required for vaccinia virus replication and maturation.* Autophagy, 2006. **2**(2): p. 91-5.

97. Whilding, L.M., et al., *Vaccinia virus induces programmed necrosis in ovarian cancer cells.* Mol Ther, 2013. **21**(11): p. 2074-86.

98. Spehner, D., et al., *Enveloped virus is the major virus form produced during productive infection with the modified vaccinia virus Ankara strain.* Virology, 2000. **273**(1): p. 9-15.

99. Mizushima, N. and T. Yoshimori, *How to interpret LC3 immunoblotting.* Autophagy, 2007. **3**(6): p. 542-5.

100. Sheen, J.H., et al., *Defective regulation of autophagy upon leucine deprivation reveals a targetable liability of human melanoma cells in vitro and in vivo.* Cancer Cell, 2011. **19**(5): p. 613-28.

101. Eng, K.E., et al., *A novel quantitative flow cytometry-based assay for autophagy.* Autophagy, 2010. **6**(5): p. 634-41.

102. Taddie, J.A. and P. Traktman, *Genetic characterization of the vaccinia virus DNA polymerase: cytosine arabinoside resistance requires a variable lesion conferring phosphonoacetate resistance in conjunction with an invariant mutation localized to the 3'-5' exonuclease domain.* J Virol, 1993. **67**(7): p. 4323-36.

103. Hanson, C.V., *Photochemical inactivation of viruses with psoralens: an overview.* Blood Cells, 1992. **18**(1): p. 7-25.

104. Tsung, K., et al., *Gene expression and cytopathic effect of vaccinia virus inactivated by psoralen and long-wave UV light.* J Virol, 1996. **70**(1): p. 165-71.

105. Mauvezin, C. and T.P. Neufeld, *Bafilomycin A1 disrupts autophagic flux by inhibiting both V-ATPase-dependent acidification and Ca-P60A/SERCA-dependent autophagosome-lysosome fusion.* Autophagy, 2015. **11**(8): p. 1437-8.

106. Swiech, L., et al., *In vivo interrogation of gene function in the mammalian brain using CRISPR-Cas9.* Nat Biotechnol, 2015. **33**(1): p. 102-6.

107. Zhong, B., et al., *The ubiquitin ligase RNF5 regulates antiviral responses by mediating degradation of the adaptor protein MITA.* Immunity, 2009. **30**(3): p. 397-407.

108. Bridgeman, A., et al., *Viruses transfer the antiviral second messenger cGAMP between cells.* Science, 2015. **349**(6253): p. 1228-32.

109. Gentili, M., et al., *Transmission of innate immune signaling by packaging of cGAMP in viral particles.* Science, 2015. **349**(6253): p. 1232-6.

110. Meisinger-Henschel, C., et al., *Genomic sequence of chorioallantois vaccinia virus Ankara, the ancestor of modified vaccinia virus Ankara.* J Gen Virol, 2007. **88**(Pt 12): p. 3249-59.

111. Thorne, S.H., et al., *Rational strain selection and engineering creates a broad-spectrum, systemically effective oncolytic poxvirus, JX-963.* J Clin Invest, 2007. **117**(11): p. 3350-8.

112. Naik, A.M., et al., *Intravenous and isolated limb perfusion delivery of wild type and a tumor-selective replicating mutant vaccinia virus in nonhuman primates.* Hum Gene Ther, 2006. **17**(1): p. 31-45.

113. Rubins, K.H., et al., *Comparative Analysis of Viral Gene Expression Programs during Poxvirus Infection: A Transcriptional Map of the Vaccinia and Monkeypox Genomes.* PLoS ONE, 2008. **3**(7): p. e2628.

114. Kates, J.R. and B.R. McAuslan, *Messenger RNA synthesis by a "coated" viral genome.* Proc Natl Acad Sci U S A, 1967. **57**(2): p. 314-20.

115. Schramm, B. and J.K. Locker, *Cytoplasmic organization of POXvirus DNA replication.* Traffic, 2005. **6**(10): p. 839-46.

116. Mss, B. and R. Filler, *Irreversible effects of cycloheximide during the early period of vaccinia virus replicaon.* J Virol, 1970. **5**(2): p. 99-108.

117. Satheshkumar, P.S., et al., *Inhibition of the ubiquitin-proteasome system prevents vaccinia virus DNA replication and expression of intermediate and late genes.* J Virol, 2009. **83**(6): p. 2469-79.

118. Wang, X.J., et al., *A novel crosstalk between two major protein degradation systems: regulation of proteasomal activity by autophagy.* Autophagy, 2013. **9**(10): p. 1500-8.

119. Lilienbaum, A., *Relationship between the proteasomal system and autophagy.* Int J Biochem Mol Biol, 2013. **4**(1): p. 1-26.

120. Townsley, A.C., et al., *Vaccinia virus entry into cells via a low-pH-dependent endosomal pathway.* J Virol, 2006. **80**(18): p. 8899-908.

121. Armstrong, J.A., D.H. Metz, and M.R. Young, *The mode of entry of vaccinia virus into L cells.* J Gen Virol, 1973. **21**(3): p. 533-7.

122. Chung, C.S., et al., *A27L protein mediates vaccinia virus interaction with cell surface heparan sulfate.* J Virol, 1998. **72**(2): p. 1577-85.

123. Hsiao, J.C., C.S. Chung, and W. Chang, *Cell surface proteoglycans are necessary for A27L protein-mediated cell fusion: identification of the N-terminal region of A27L protein as the glycosaminoglycan-binding domain.* J Virol, 1998. **72**(10): p. 8374-9.

124. Niles, E.G. and J. Seto, *Vaccinia virus gene D8 encodes a virion transmembrane protein.* J Virol, 1988. **62**(10): p. 3772-8.

125. Lin, C.L., et al., *Vaccinia virus envelope H3L protein binds to cell surface heparan sulfate and is important for intracellular mature virion morphogenesis and virus infection in vitro and in vivo.* J Virol, 2000. **74**(7): p. 3353-65.

126. Meisinger-Henschel, C., et al., *Introduction of the six major genomic deletions of modified vaccinia virus Ankara (MVA) into the parental vaccinia virus is not sufficient to reproduce an MVA-like phenotype in cell culture and in mice.* J Virol, 2010. **84**(19): p. 9907-19.

127. Dobson, B.M. and D.C. Tscharke, *Redundancy complicates the definition of essential genes for vaccinia virus.* J Gen Virol, 2015. **96**(11): p. 3326-37.

128. Jiang, W., et al., *RNA-guided editing of bacterial genomes using CRISPR-Cas systems.* Nat Biotechnol, 2013. **31**(3): p. 233-9.

129. Mali, P., et al., *RNA-guided human genome engineering via Cas9.* Science, 2013. **339**(6121): p. 823-6.

130. Peng, R., G. Lin, and J. Li, *Potential pitfalls of CRISPR/Cas9-mediated genome editing.* Febs j, 2016. **283**(7): p. 1218-31.

131. Paquet, D., et al., *Efficient introduction of specific homozygous and heterozygous mutations using CRISPR/Cas9.* Nature, 2016. **533**(7601): p. 125-9.

132. Hsu, P.D., E.S. Lander, and F. Zhang, *Development and applications of CRISPR-Cas9 for genome engineering.* Cell, 2014. **157**(6): p. 1262-78.

133. Wang, Z., et al., *CRISPR/Cas9-Derived Mutations Both Inhibit HIV-1 Replication and Accelerate Viral Escape.* Cell Rep, 2016. **15**(3): p. 481-9.

134. Wang, G., et al., *CRISPR-Cas9 Can Inhibit HIV-1 Replication but NHEJ Repair Facilitates Virus Escape.* Mol Ther, 2016. **24**(3): p. 522-6.

135. van Diemen, F.R., et al., *CRISPR/Cas9-Mediated Genome Editing of Herpesviruses Limits Productive and Latent Infections.* PLoS Pathogens, 2016. **12**(6): p. e1005701.

136. Yuan, M., et al., *Efficiently editing the vaccinia virus genome by using the CRISPR-Cas9 system.* J Virol, 2015. **89**(9): p. 5176-9.

137. Kilcher, S., et al., *siRNA screen of early poxvirus genes identifies the AAA+ ATPase D5 as the virus genome-uncoating factor.* Cell Host Microbe, 2014. **15**(1): p. 103-12.

138. Mercer, J., et al., *RNAi screening reveals proteasome- and Cullin3-dependent stages in vaccinia virus infection.* Cell Rep, 2012. **2**(4): p. 1036-47.

139. McAlpine, F., et al., *Regulation of nutrient-sensitive autophagy by uncoordinated 51-like kinases 1 and 2.* Autophagy, 2013. **9**(3): p. 361-73.

140. Jung, C.H., et al., *mTOR regulation of autophagy.* FEBS letters, 2010. **584**(7): p. 1287-1295.

141. Young, A.R.J., et al., *Autophagy mediates the mitotic senescence transition.* Genes & Development, 2009. **23**(7): p. 798-803.

142. Bjorkoy, G., et al., *Monitoring autophagic degradation of p62/SQSTM1.* Methods Enzymol, 2009. **452**: p. 181-97.

143. Dooley, H.C., et al., *WIPI2 links LC3 conjugation with PI3P, autophagosome formation, and pathogen clearance by recruiting Atg12-5-16L1.* Mol Cell, 2014. **55**(2): p. 238-52.

144. Blommaart, E.F., et al., *The phosphatidylinositol 3-kinase inhibitors wortmannin and LY294002 inhibit autophagy in isolated rat hepatocytes.* Eur J Biochem, 1997. **243**(1-2): p. 240-6.

145. Scarlatti, F., et al., *Role of non-canonical Beclin 1-independent autophagy in cell death induced by resveratrol in human breast cancer cells.* Cell Death Differ, 2008. **15**(8): p. 1318-29.

146. Grishchuk, Y., et al., *Beclin 1-independent autophagy contributes to apoptosis in cortical neurons.* Autophagy, 2011. **7**(10): p. 1115-31.

147. Seo, G., et al., *Hydrogen peroxide induces Beclin 1-independent autophagic cell death by suppressing the mTOR pathway via promoting the ubiquitination and degradation of Rheb in GSH-depleted RAW 264.7 cells.* Free Radic Res, 2011. **45**(4): p. 389-99.

148. Juenemann, K. and E.A. Reits, *Alternative macroautophagic pathways.* Int J Cell Biol, 2012. **2012**: p. 189794.

149. Nishida, Y., et al., *Discovery of Atg5/Atg7-independent alternative macroautophagy.* Nature, 2009. **461**(7264): p. 654-8.

150. Liu, C., et al., *Autophagy-independent enhancing effects of Beclin 1 on cytotoxicity of ovarian cancer cells mediated by proteasome inhibitors.* BMC Cancer, 2012. **12**: p. 622.

151. Grose, C. and D.J. Klionsky, *Alternative autophagy, brefeldin A and viral trafficking pathways.* Autophagy, 2016. **12**(9): p. 1429-30.

152. Ulaeto, D., D. Grosenbach, and D.E. Hruby, *Brefeldin A inhibits vaccinia virus envelopment but does not prevent normal processing and localization of the putative envelopment receptor P37.* J Gen Virol, 1995. **76 (Pt 1)**: p. 103-11.

153. Sanjuan, M.A., et al., *Toll-like receptor signalling in macrophages links the autophagy pathway to phagocytosis.* Nature, 2007. **450**(7173): p. 1253-7.

154. Sanjuan, M.A. and D.R. Green, *Eating for good health: linking autophagy and phagocytosis in host defense.* Autophagy, 2008. **4**(5): p. 607-11.

155. Shui, W., et al., *Membrane proteomics of phagosomes suggests a connection to autophagy.* Proc Natl Acad Sci U S A, 2008. **105**(44): p. 16952-7.

156. Lai, S.-c. and R.J. Devenish, *LC3-Associated Phagocytosis (LAP): Connections with Host Autophagy.* Cells, 2012. **1**(3): p. 396-408.

157. Henault, J., et al., *Noncanonical autophagy is required for type I interferon secretion in response to DNA-immune complexes.* Immunity, 2012. **37**(6): p. 986-97.

158. Florey, O. and M. Overholtzer, *Autophagy proteins in macroendocytic engulfment.* Trends Cell Biol, 2012. **22**(7): p. 374-80.

159. Florey, O., et al., *Autophagy machinery mediates macroendocytic processing and entotic cell death by targeting single membranes.* Nat Cell Biol, 2011. **13**(11): p. 1335-43.

160. Martinez, J., et al., *Microtubule-associated protein 1 light chain 3 alpha (LC3)-associated phagocytosis is required for the efficient clearance of dead cells.* Proc Natl Acad Sci U S A, 2011. **108**(42): p. 17396-401.

161. Martinez, J., et al., *Molecular characterization of LC3-associated phagocytosis reveals distinct roles for Rubicon, NOX2 and autophagy proteins.* Nat Cell Biol, 2015. **17**(7): p. 893-906.

162. Razi, M. and S.A. Tooze, *Correlative light and electron microscopy.* Methods Enzymol, 2009. **452**: p. 261-75.

163. Kuang, E., et al., *Regulation of ATG4B stability by RNF5 limits basal levels of autophagy and influences susceptibility to bacterial infection.* PLoS Genet, 2012. **8**(10): p. e1003007.

164. Pasquier, B., *Autophagy inhibitors.* Cell Mol Life Sci, 2016. **73**(5): p. 985-1001.

165. Chillakuru, R.A., D.D. Ryu, and T. Yilma, *Propagation of recombinant vaccinia virus in HeLa cells: adsorption kinetics and replication in batch cultures.* Biotechnol Prog, 1991. **7**(2): p. 85-92.

166. Whitby, F.G., et al., *Crystal structure of the human ubiquitin-like protein NEDD8 and interactions with ubiquitin pathway enzymes.* J Biol Chem, 1998. **273**(52): p. 34983-91.

167. Pan, Z.Q., et al., *Nedd8 on cullin: building an expressway to protein destruction.* Oncogene, 2004. **23**(11): p. 1985-97.

168. Petroski, M.D. and R.J. Deshaies, *Function and regulation of cullin-RING ubiquitin ligases.* Nat Rev Mol Cell Biol, 2005. **6**(1): p. 9-20.

169. Luo, Z., et al., *The Nedd8-activating enzyme inhibitor MLN4924 induces autophagy and apoptosis to suppress liver cancer cell growth.* Cancer Res, 2012. **72**(13): p. 3360-71.

170. Luo, Z., et al., *Inactivation of the Cullin (CUL)-RING E3 ligase by the NEDD8-activating enzyme inhibitor MLN4924 triggers protective autophagy in cancer cells.* Autophagy, 2012. **8**(11): p. 1677-9.

171. Goll, D.E., et al., *The calpain system.* Physiol Rev, 2003. **83**(3): p. 731-801.

172. Liu, J., M.C. Liu, and K.K. Wang, *Calpain in the CNS: from synaptic function to neurotoxicity.* Sci Signal, 2008. **1**(14): p. re1.

173. Sorimachi, H., S. Hata, and Y. Ono, *Calpain chronicle—an enzyme family under multidisciplinary characterization.* Proceedings of the Japan Academy. Series B, Physical and Biological Sciences, 2011. **87**(6): p. 287-327.

174. Hosfield, C.M., et al., *Crystal structure of calpain reveals the structural basis for Ca(2+)-dependent protease activity and a novel mode of enzyme activation.* Embo j, 1999. **18**(24): p. 6880-9.

175. Strobl, S., et al., *The crystal structure of calcium-free human m-calpain suggests an electrostatic switch mechanism for activation by calcium.* Proc Natl Acad Sci U S A, 2000. **97**(2): p. 588-92.

176. Liu, Z., et al., *GPS-CCD: a novel computational program for the prediction of calpain cleavage sites.* PLoS One, 2011. **6**(4): p. e19001.

177. Lau, L., et al., *DNA tumor virus oncogenes antagonize the cGAS-STING DNA-sensing pathway.* Science, 2015. **350**(6260): p. 568-71.

178. Kotwal, G.J. and B. Moss, *Vaccinia virus encodes two proteins that are structurally related to members of the plasma serine protease inhibitor superfamily.* J Virol, 1989. **63**(2): p. 600-6.

179. Yang, Z. and B. Moss, *Interaction of the vaccinia virus RNA polymerase-associated 94-kilodalton protein with the early transcription factor.* J Virol, 2009. **83**(23): p. 12018-26.

180. Rasmussen, S.B., et al., *Activation of autophagy by alpha-herpesviruses in myeloid cells is mediated by cytoplasmic viral DNA through a mechanism dependent on stimulator of IFN genes.* J Immunol, 2011. **187**(10): p. 5268-76.

181. Watson, R.O., et al., *The Cytosolic Sensor cGAS Detects Mycobacterium tuberculosis DNA to Induce Type I Interferons and Activate Autophagy.* Cell Host Microbe, 2015. **17**(6): p. 811-9.

182. Colinas, R.J., et al., *A DNA ligase gene in the Copenhagen strain of vaccinia virus is nonessential for viral replication and recombination.* Virology, 1990. **179**(1): p. 267-75.

183. D'Costa, S.M., et al., *Vaccinia H5 is a multifunctional protein involved in viral DNA replication, postreplicative gene transcription, and virion morphogenesis.* Virology, 2010. **401**(1): p. 49-60.

184. Harte, M.T., et al., *The poxvirus protein A52R targets Toll-like receptor signaling complexes to suppress host defense.* J Exp Med, 2003. **197**(3): p. 343-51.

185. Bowie, A., et al., *A46R and A52R from vaccinia virus are antagonists of host IL-1 and toll-like receptor signaling.* Proc Natl Acad Sci U S A, 2000. **97**(18): p. 10162-7.

186. Pires de Miranda, M., et al., *The vaccinia virus kelch-like protein C2L affects calcium-independent adhesion to the extracellular matrix and inflammation in a murine intradermal model.* J Gen Virol, 2003. **84**(Pt 9): p. 2459-71.

187. Benfield, C.T., et al., *Vaccinia virus protein K7 is a virulence factor that alters the acute immune response to infection.* J Gen Virol, 2013. **94**(Pt 7): p. 1647-57.

Acknowledgments

This work has been performed at the Institute of Virology in the group of Prof. Dr. Ingo Drexler and was supported by the Jürgen Manchot foundation.

First of all, I would like to express my gratitude to my supervisor and doctor father Prof. Dr. Ingo Drexler for giving me the opportunity to carry out my PhD thesis in his lab. I really enjoyed working on that project, although I had to face a few hurdles at the beginning. I learned how to think and work independently, tried to solve problems without giving up, which would not have been possible without his support throughout these 3.5 years.

I am also very thankful to Prof. Dr. Willbold for directly accepting to be my mentor without hesitation, despite his very though time schedule, which is not a matter of course.

Thanks to my lab fellows Gregor, Sha and Ronny.

Special thanks to my friend Baila for the motivation, mental support and scientific as well as non-scientific discussions. The times would have been much more difficult, frustrating and less joyful without a good friend at my site.

Thanks to Dr. Inge Krümpelbeck for taking care of the administration and organisation within the MOI II graduate school. Thanks also for the numerous e-mail reminders, in case we would have missed any appointment or to write any report, which gave us the possibility to concentrate more on our research.

My last and biggest thank goes to my family, especially my parents for their support throughout my life, for believing in me and for helping me to achieve all my goals. There are no words to express my gratitude for them.

“Appreciation is a wonderful thing.

It makes what is excellent in others belong to us as well.”

Voltaire

Eidesstattliche Versicherung

Ich, Frau Houda Khatif, versichere an Eides Statt, dass die Dissertation von mir selbständig und ohne unzulässige fremde Hilfe unter Beachtung der „Grundsätze zur Sicherung guter wissenschaftlicher Praxis an der Heinrich-Heine-Universität Düsseldorf“ erstellt worden ist.

Kaarst, 29.11.2016 Houda Khatif